The Dissertation Committee for Adam Michael Strecker certifies that this is the approved version of the following dissertation:

Predicting Damage and Blast Load Propagation Due to Internal Detonations

Committee:

Eric B. Williamson, Supervisor

Michael D. Engelhardt

Todd A. Helwig

Oguzhan Bayrak

Ofodike A. Ezekoye

Predicting Damage and Blast Load Propagation Due to Internal Detonations

by

Adam Michael Strecker, B.S.; M.S.

Dissertation

Presented to the Faculty of the Graduate School of

The University of Texas at Austin

in Partial Fulfillment

of the Requirements

for the Degree of

Doctor of Philosophy

The University of Texas at Austin

August 2015

Dedication

To my wife and kids

Acknowledgements

First, I would like to thank Brigadier General Gregory Seely, USAF, Ret., and the Department of Civil and Environmental Engineering at the United States Air Force Academy for believing in me and investing in my education. I discovered a true passion teaching cadets, and am excited to continue my career back at the Academy.

I would also like to thank Al Ohrt with the Air Force Research Laboratory for all of his assistance as my unofficial sponsor. He not only helped me find a research topic, but took time out of his busy schedule to support my work throughout. He was instrumental to me finishing this dissertation in the time allotted.

Next, I would like to thank my advisor, Eric Williamson. He has been a mentor even before being my academic advisor. There is no way I could have accomplished this work without his guidance. He has always shown a genuine interest in my career and my family. I look forward to continuing our professional relationship and friendship for years to come.

Finally, I would like to thank all of my family and friends for their support over the past three years. Thanks for all the visits to Austin, the prayers, and the interest in my work. I also want to thank my kids for the happiness they bring me every day and the welcomed distractions from work. Mostly, I want to thank my wonderful wife, Darci. Her support and love has made this entire process possible and enjoyable. What an incredible opportunity we were given to begin our journey in parenthood in Austin, TX.

Predicting Damage and Blast Load Propagation Due to Internal Detonations

Adam Michael Strecker, Ph.D.

The University of Texas at Austin, 2015

Supervisor: Eric B. Williamson

In recent years, the world has seen an increase in international terrorism. Terrorist attacks often involve explosive devices, and they frequently target non-military buildings constructed with typical details. The way in which the U.S. military currently trains and fights has also shifted in recent years from a conventional warfare focus during the Cold War, to a focus on military operations in urban terrain (MOUT). In these urban operations, military targets may include buildings constructed with typical details, and the employment of munitions can potentially cause excessive collateral damage. Most of the past research involving blast effects on structures has involved external detonations or internal detonations on hardened facilities. The current terrorist threat and the increase in MOUT have created a need to analyze internal detonations in buildings constructed with typical details.

The goal of the research study is to develop an engineering-level model to predict the damage and blast load propagation through buildings constructed with typical details resulting from an internal detonation. The research focuses on full-height steel stud interior walls and develops a mechanics-based predictive model.

Experimental tests performed by the Defense Threat Reduction Agency as well as concepts from an existing empirically-derived model created by Weidlinger and

Associates, Inc., were used to develop the model for the research study. This model simulates blast loads in an interior detonation room and computes the structural response of the interior steel-stud walls by using an equivalent single-degree-of-freedom system to analyze each wall. The structural response is combined with air mass flow through openings to predict blast load propagation. Pressure and impulse histories are computed for each room within a building. The predictive capability of the model developed for the research study is validated using a different series of experimental tests conducted by the Air Force Research Laboratory.

The research presented in this dissertation has created a predictive blast load propagation model for internal detonations for one specific scenario involving full-height steel-stud walls. This model can continue to be improved to encompass a broader spectrum of scenarios and become an extremely useful engineering-level tool for protective design and munitions employment.

Table of Contents

List of Tables

List of Figures

Chapter 1

Introduction

Most of the past research involving blast effects on structures has been for external detonations. Research involving internal detonations has focused mainly on hardened military facilities and single-room buildings. A shift in military operations and an escalating threat of terrorist attacks have led to an increased desire for information regarding internal detonations in buildings constructed with typical details and the ability to predict damage and blast load propagation through multiple interior rooms of these buildings. This research aims to develop an engineering-level model to predict blast load propagation through a typical building structure as a result of an internal detonation.

1.1 MOTIVATION

Prior to the end of the Cold War era in 1989, a main geopolitical focus of many countries included potential large-scale conflict between conventional militaries. As such, much of the research involving blast analyses and protective design from blast threats was military-sponsored work on hardened structures. Since this time, however, international terrorism has escalated and become a substantial concern among many countries (Krauthammer, 2005). The terrorists' tactics and weapons, as well as the methods modern militaries use to combat terrorism, have created a requirement for engineers to understand and analyze the structural response of common buildings subjected to blast loads from explosive threats seen throughout the world today.

1.1.1 Terrorist Threats

Throughout recorded history, terrorism has existed across the globe. For most of that time, it was typically seen in internal disputes within a nation. Beginning in the early

1980s, however, terrorism began to be used increasingly as a global political tool (Krauthammer, 2005). The United States began to take particular interest in terrorist threats after several attacks occurred within its borders. The 1993 World Trade Center attack, the Alfred P. Murrah Federal Building bombing in Oklahoma City, and the attacks of September 11, 2001 caused U.S. government agencies to give much greater consideration to national security and protection from terrorist attacks (Krauthammer, 2005). Terrorism continues to be a serious threat worldwide, and in 2014, there were 13,463 terrorist attacks resulting in more than 32,700 deaths, 34,700 injuries, and 9,400 kidnappings (National Consortium for the Study of Terrorism and Responses to Terrorism, 2015).

Terrorism is a continually evolving threat. The locations, participants, objectives, causes, weapons and tactics, and targets frequently change. Terrorists are likely not a well-defined adversary, and they typically engage in smaller intensity conflict compared to conventional military conflict. In general, terrorist activity is difficult to predict and not well understood from a military standpoint (Krauthammer, 2008). Among all the various options, explosives have remained terrorists' primary weapon in recent years. In 2005, Krauthammer states that historical data indicated approximately 85% of past recorded terrorist attacks used explosive devices (Krauthammer, 2005). In the U.S. Department of State's *Country Reports on Terrorism 2014*, the Annex of Statistical Information reports 54% of all worldwide terrorist attacks in 2014 used explosive devices, and 57% of attacks used explosives in 2013 (National Consortium for the Study of Terrorism and Responses to Terrorism, 2015). Although statistical information is not available on the types of explosives used, suicide vests are described in several attacks included in the *Country Reports on Terrorism 2014* (DoS, 2015). Suicide vests, backpack

bombs, and other small explosives are all capable of being used by terrorists inside a building and pose a severe internal detonation threat.

Targets of terrorist attacks are often non-military and in locations not typically designed to resist attacks and explosions. Table 1.1 shows a list of all worldwide terrorist targets in 2014. Many of the facilities within those targets types would be constructed using common construction practices with no special consideration for blast-resistant design.

Table 1.1 Targets of Terrorist Attacks Worldwide, 2014 (adapted from National Consortium for the Study of Terrorism and Responses to Terrorism, 2015)

Target Type	**Number of Targets**	**% of Total Targets**
Private Citizens & Property	5016	36.1%
Police	2679	19.3%
Government (General)	1545	11.1%
Business	1127	8.1%
Military	805	5.8%
Religious Figures/Institutions	418	3.0%
Terrorists/Non-State Militia	400	2.9%
Educational Institutions	384	2.8%
Transportation	355	2.6%
Utilities	344	2.5%
Journalists & Media	231	1.7%
Government (Diplomatic)	155	1.1%
Violent Political Party	131	0.9%
Other	85	0.6%
NGO	82	0.6%
Airports & Airlines	58	0.4%
Telecommunications	50	0.4%
Food or Water Supply	21	0.2%
Maritime	16	0.1%
Total	13911	

Regarding protective design and physical security from terrorist attacks, "the study of heavily fortified military facilities may no longer be the main area of concern…Careful attention must be devoted to typical civilian facilities whose failure could severely disrupt the social and economic infrastructure of nations" (Krauthammer, 2005). The behavior of commonly constructed buildings subjected to blast loads must be better understood in order to evaluate these targets subjected to terrorist explosive attacks.

1.1.2 Military Operations in Urban Terrain

The way in which the U.S. military currently trains and fights also has shifted greatly since the end of the Cold War. Recent military conflicts have occurred primarily in urban settings, creating unique combat operations that are referred to as military operations in urban terrain (MOUT) (Ohrt et al., 2013). When these operations involve multiple military services, they are referred to as joint urban operations and defined as "operations planned and conducted on, or against objectives within, a topographical complex and its adjacent natural terrain, where man-made construction or the density of population are the dominant features" (JCS, 2013). Urban environments pose significant complexities to military commanders and their operations (JCS, 2013). For this reason, U.S. adversaries, such as terrorist organizations, utilize the urban environment to wage asymmetric warfare and to equalize the battlespace against a conventionally superior U.S. military force (Desch, 2001).

Of particular importance to this research, commanders utilizing MOUT must consider the infrastructure when employing weapons. Especially in air operations, a "propensity for collateral damage" (JCS, 2013) exists when using munitions in an urban environment. Excessive damage to buildings and/or destroying critical infrastructure can

cause catastrophic consequences or casualties to civilian populations near military targets within the urban environment. This consideration is extremely important as excessive collateral damage can potentially violate the law of war concerning the utilization of force (JCS, 2013). Military munitions are often used to defeat hardened targets. The majority of structures in an urban environment, however, are built using typical construction methods with relatively weak components when subjected to explosions compared to hardened targets. Attacks against such structures can lead to significant damage, and a need exists to adequately predict the potential damage to the target and associated collateral damage that may occur when these munitions are employed (Ohrt et al., 2013).

1.1.3 Internal Detonations

The focus of this research is aimed at understanding and predicting an internal detonation that occurs in a commonly constructed building. An internal detonation is when an explosion originates inside a building, and common construction includes several rooms with interior non-loadbearing walls with weak lateral resistance. In many instances, an internal detonation in these types of facilities causes many of the interior walls to fail, and blast loads propagate through the building. Understanding and predicting this scenario is important from both a protective design standpoint and a munitions employment standpoint.

From a protective design perspective, analyzing an internal detonation scenario can help determine the survivability of a building and the safety of its occupants from an internal explosion threat. In most modern situations, the internal explosion threat would be a terrorist attack utilizing a suicide vest, a backpack bomb, or another form of concealed small explosives. Using information about known terrorist attacks and current

intelligence, one can assess the potential risk and potential threat for a given building. The goal from a protective design perspective would be for an engineer to analyze a building's response to the potential explosive threat and identify the extent of possible damage. If the level of desired survivability of the building is not attained, a redesign of the building or possible retrofit options for strengthening interior walls and other components could be analyzed to assess if the required protection from the potential threat is achieved.

Many government agencies, as well as professional organizations, desire the ability to perform this type of protective design analysis for an internal detonation scenario. The Defense Threat Reduction Agency (DTRA) is one government agency that has invested significant resources on this topic, including the experimental tests used for the current research study (DTRA, 2010a; 2013a; 2013b). The American Society of Civil Engineers (ASCE) has also demonstrated interest in advancing the practice of protective design by establishing initiatives such as the ASCE Task Committee on Design for Physical Security (Krauthammer, 2005) and maintaining the Committee on Blast, Shock, and Impact (ASCE, 2015). Other professional organizations, such as the American Concrete Institute (ACI) and the Precast/Prestressed Concrete Institute (PCI), have committees that focus on the structural response to blast (ACI, 2015; PCI, 2015).

From a munitions employment perspective, analyzing the internal detonation scenario is essential for the selection of appropriate munitions to destroy targets and limit collateral damage. As mentioned previously, the extent of structural damage can be significant when munitions are detonated in an urban building due to the inability of typical light construction to resist lateral blast loads from an internal explosion. A key component of predicting the damage due to the employment of military munitions in MOUT is the ability to quantify the blast loads that propagate through failing walls in a

typical urban building (Ohrt et al., 2013). Military agencies, such as the Air Force Research Laboratory (AFRL) Munitions Directorate, have also spent significant time and resources studying the internal detonation scenario with the "goal of developing, improving, or validating modeling and simulation capabilities for estimating weapon effects against fixed targets that may be encountered in an urban operation" (Staubs et al., 2014a). Experimental tests performed by AFRL are also used for the current research study (Staubs et al., 2014a; 2014b).

1.2 RESEARCH APPROACH

As described in the previous section, a need exists from both a protective design perspective and weapons employment perspective to predict building damage and the overall blast environment in a building subjected to an internal detonation. Because interior walls in commonly constructed buildings often fail violently when subjected to blast loads, the damage prediction and response analysis must incorporate blast loads propagating through the building due to failing walls. In many cases, the engineers analyzing an internal detonation scenario, whether for protective design or munitions employment, need an efficient, engineering-level model to perform the prediction. Ideally, these predictions would run quickly on a personal computer. Several analysis iterations for the threat scenario of interest may be necessary to determine appropriate levels of building protection or appropriate selection of munitions, and high-fidelity models may take too much time and resources to employ in an efficient manner. As such, the goal of the research study described herein is to develop an engineering-level model to predict wall damage and blast load propagation through failing walls due to an internal detonation.

Limited research has been performed on the structural response of typical interior walls subjected to blast loads. Therefore, the research study described herein focuses on one specific type of interior wall: full-height, cold-formed steel-stud walls. By limiting this research to one type of wall, a thorough understanding of the wall behavior is realized and a thorough predictive model was developed. In future research efforts, the components of the model developed for this research study can be applied to different wall types.

Another goal of the research study described herein is to develop a predictive model that is mechanics-based versus empirically-based. Many existing blast load computational methods, design procedures, and analysis models rely on available test data. The model developed for this research study aims to analyze the structural response of interior walls and compute blast load propagation using actual wall properties and explosive charge characteristics.

Chapter 2 of this dissertation provides a review of available literature on explosions and blast wave phenomena, internal explosions, structural response to blast loads, cold-formed steel-stud wall response to blast loads, and existing engineering-level models for blast load propagation. A complete description of the internal detonation problem is presented in Chapter 3, followed by descriptions of several modeling approaches. The chapter continues with a detailed explanation of the proposed model developed for the research study described herein. Chapter 4 presents the experimental tests used to develop the model as well as the analysis results for those tests. Next, a separate experimental test series is presented and used to validate the predictive capability of the model. Finally, Chapter 5 includes a summary of the research contained in this dissertation and recommendations for future research.

DISCLAIMER CLAUSE: The views expressed in this dissertation are those of the authors and do not reflect the official policy or position of the United States Air Force, Department of Defense, or the U.S. Government.

Chapter 2

Literature Review

The research outlined in this dissertation focuses on developing an engineering-level model to predict blast load propagation through structures that have interior cold-formed steel-stud walls. To investigate the complex structural response from an internal detonation and predict loads propagating through failing walls, an understanding of explosions, blast loads, structural response, and internal detonations is necessary. Additionally, the specific behavior of steel-stud walls subjected to blast loads must also be understood. This chapter provides an overview on blast phenomena and explains the current state-of-the-practice for analyzing structures subjected to an internal blast. It also presents a brief synopsis on steel-stud wall behavior subjected to blast loads and provides a summary of existing engineering-level models

2.1 Explosions and Blast Wave Phenomena

An explosion is a large-scale, rapid and sudden release of energy (Ngo et al., 2007). "The release occurs so rapidly that there is a local accumulation of energy at the site of the explosion. The accumulated energy dissipates through blast waves, propulsion of fragments, and thermal radiation" (Williamson, 2014).

Explosives can be categorized by the speed at which the chemical reaction occurs. A high explosive is a material where the chemical reaction front travels through the material at a supersonic velocity, and the combustion process is defined as a detonation. When the chemical reaction front travels subsonically, the combustion process is referred to as a deflagration, and the explosive material may be termed a low explosive. A main difference between a detonation and a deflagration is the formation of a shock wave that occurs with a detonation. Figure 2.1 shows the characteristics of a blast wave caused by a

detonation and a deflagration. A detonation causes a shock wave characterized by its instantaneous rise in pressure to a peak value above ambient pressure, P_0, followed by a gradual decline and eventual return to ambient pressure. A deflagration may create a pressure wave characterized by a gradual increase in pressure to a peak value above ambient pressure, and a gradual decline to ambient pressure similar to that of the shock wave. The blast waves originate in the medium surrounding the explosive material and propagate outward from the center of the explosive.

B

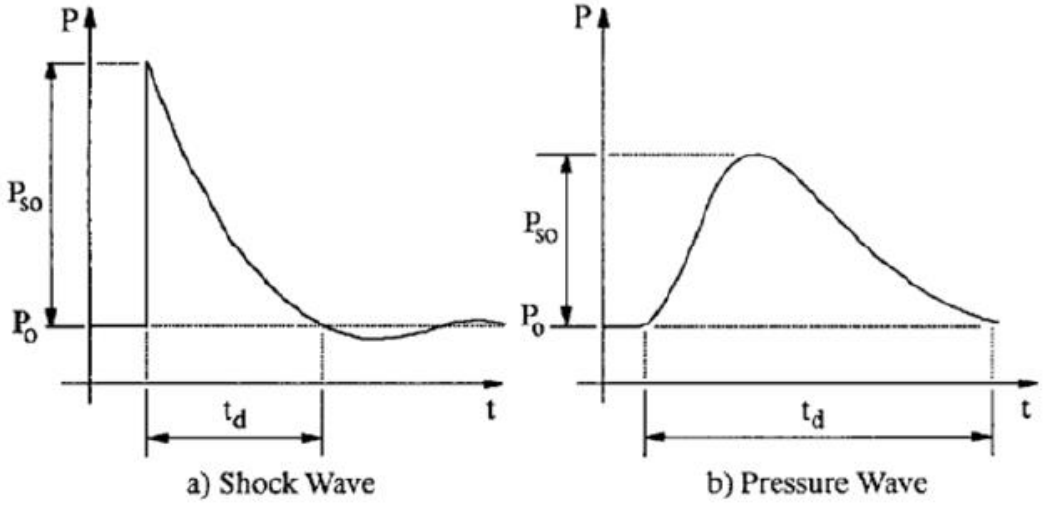

Figure 2.1 Characteristic Shapes of Blast Waves: (a) Typical Shock Wave from a Detonation, (b) Typical Pressure Wave from a Deflagration (ASCE, 2010)

This research focuses on internal detonations of high explosives; hence, deflagrations will not be addressed. Initially in this section, the general behavior of blast waves will be described in terms of a free-field detonation, and then a brief overview of

the blast wave's interaction with surfaces will be presented. The unique components of an internal detonation will be presented in the subsequent section.

When defining a blast load, the most important quantities that influence structural response are peak overpressure and impulse. Overpressure is the pressure above or below the ambient air pressure. The peak overpressure, often referred to as simply the peak pressure, is the maximum overpressure. The impulse is the area under the overpressure curve. A pressure-time curve is needed to quantify both. Figure 2.2 shows an idealized free-field pressure-time curve for any given point located an unobstructed distance from a detonation. The ambient air pressure is labeled as P_o. The peak overpressure, P_{so}, is also referred to as the peak incident pressure, or peak side-on pressure (DoD, 2008). The side-on pressure is what would be measured as the direction a shock wave travels parallel to a point or object. The term t_A is the arrival time, or the time it takes the shock wave to

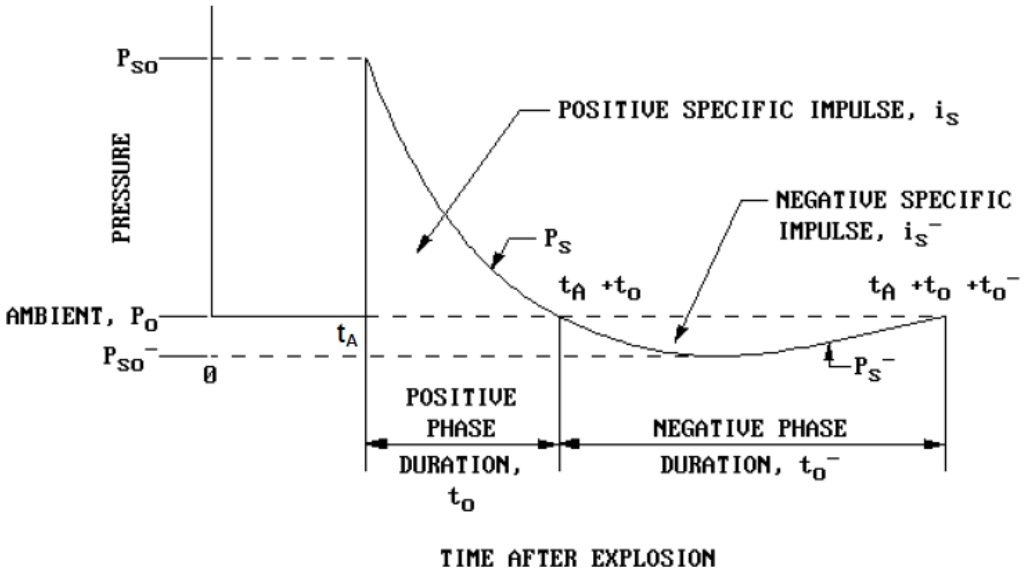

Figure 2.2 Free-Field Pressure-Time Variation (DoD, 2008)

travel from the explosive charge to the point of interest. The positive phase duration, t_o, describes how long the overpressure is positive. The positive specific impulse, i_s, is the area under the overpressure curve during the positive phase duration.

Shock waves from detonations also create a negative phase, or suction phase, where the pressure is below the ambient pressure, creating a negative overpressure. The minimum negative overpressure is labeled as P_{so}^-, and the negative phase duration is described as t_o^-. The area under the overpressure curve during the negative phase is referred to as the negative specific impulse, i_s^-.

The distance from the center of an explosion plays a large factor in the magnitude of a shock wave's peak incident pressure and impulse. This distance is referred to as standoff distance. As a shock wave travels away from the center of an explosion, the volume of medium it travels through continually increases. Consequently, as the standoff distance increases, not only does the arrival time of the shock wave increase, the peak incident pressures decrease and the phase durations increase (DoD, 2008).

Figure 2.2 shows a typical incident shock wave which propagates away from an explosion. This incident shock front will interact with objects in its path, and the wave will be reflected and reinforced (DoD, 2008). An idealized reflected shock wave off an infinite plane reflecting surface is shown in comparison to the incident shock wave in Figure 2.3. The magnitude of the reflected peak pressure, P_r, is greater than the incident peak pressure, P_{so}, but the positive phase duration remains essentially the same for both waves. Nearly identical results are observed for the negative phase, where the duration remains approximately the same, but the minimum reflected negative pressure, P_r^-, is lower than the incident negative pressure, P_{so}^-.

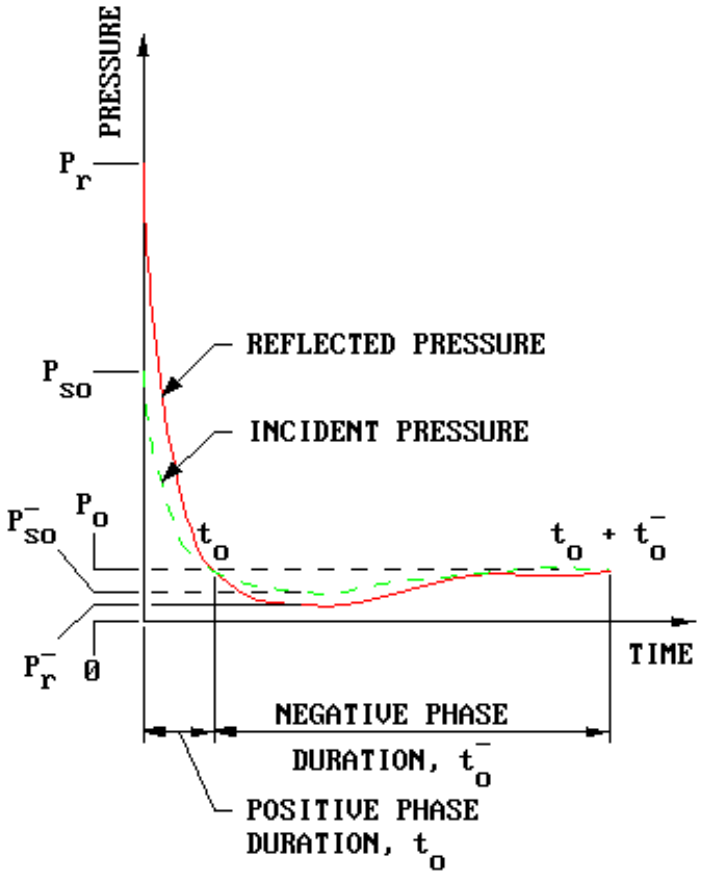

Figure 2.3 Idealized Incident Shock Wave and Reflected Shock Wave (DoD, 2008)

The angle at which the reflecting surface is oriented in comparison to the direction of travel of the incident wave is referred to as the angle of incidence, α, and is shown in Figure 2.4. The magnitude of the reflected shock wave is generally greatest when the angle of incidence is 0 degrees. If the angle of incidence is 90 degrees, the surface does not reflect the wave, and the peak pressure on the surface is the incident pressure.

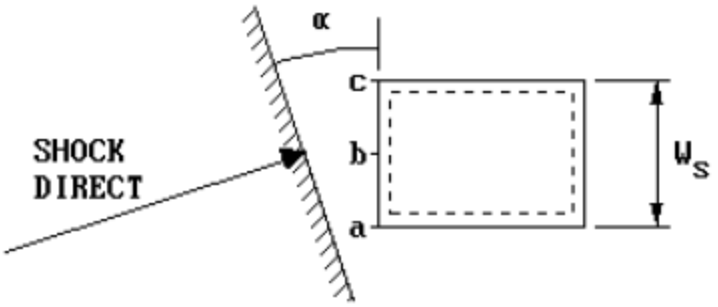

Figure 2.4 Angle of Incidence for a Reflecting Surface (DoD, 2008)

As a shock wave travels through the air, it changes the temperature and density of the air. Subsequently, the reflected shock wave does not travel through the same medium as the incident shock wave. This change in medium introduces several phenomena regarding reflected shock waves. First, the reflected angle is often not equal to the angle of incidence. Second, the reflected pressure can be increased significantly compared to the incident pressure. For a normal reflecting surface, this increase can be anywhere from a factor of 2 to over 12. Lastly, the formation of a Mach front occurs and is explained in more detail below.

The ratio of the peak reflected pressure to the peak incident pressure is called the reflected pressure coefficient, $C_{r\alpha}$, and is dependent on both the magnitude of the peak incident pressure and the angle of incidence. Much research has been devoted to better understanding shock wave reflections, and this research has been used in the development of the chart from the UFC 3-340-02 (DoD, 2008) shown in Figure 2.5. As shown in the figure, for extremely high incident pressures, the reflected pressure can increase by more than a factor of 12. The curves are highly irregular, and each curve for the different overpressure values contains a hump somewhere between an angle of incidence of 40 degrees to 80 degrees.

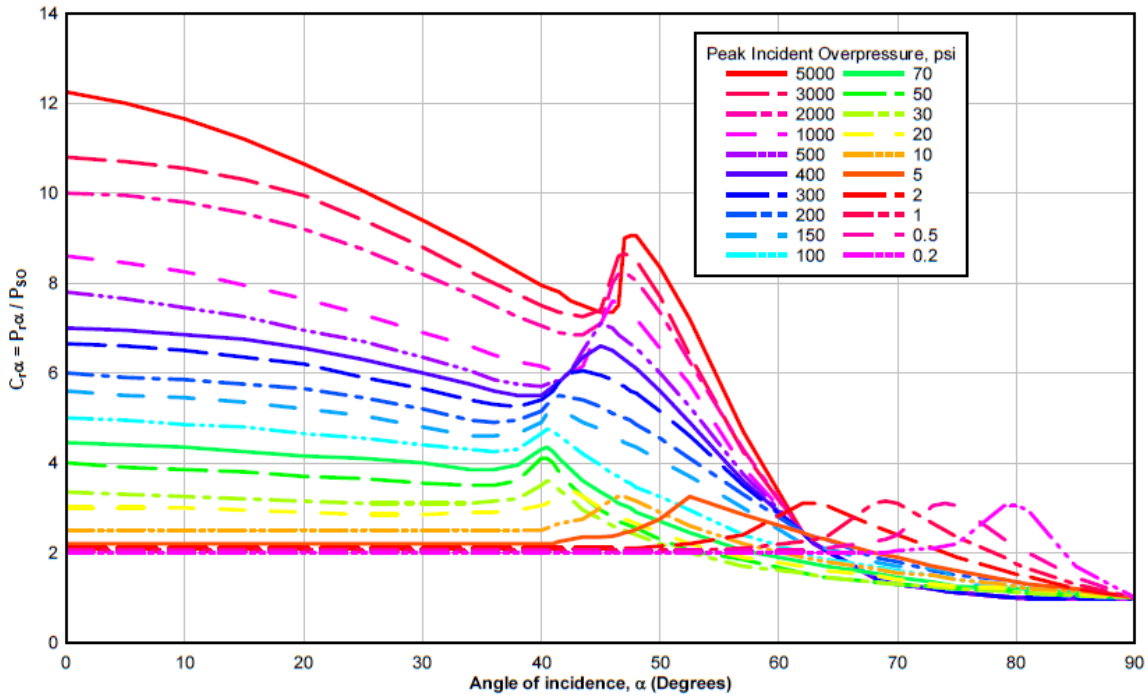

Figure 2.5 Reflected Pressure Coefficient versus Angle of Incidence (DoD, 2008)

The humps in Figure 2.5 are due to the formation of a Mach wave. A Mach wave is formed when an incident wave reflects off a surface (i.e., the ground), and the reflected wave eventually merges with the incident wave. This phenomenon occurs because the reflected wave travels through a medium that has been altered by the original incident wave. Accordingly, the reflected wave travels at a faster speed than the incident wave and merges with the original incident wave to form a Mach wave or Mach front. Figure 2.6 shows a free air burst where the incident wave reflects off the ground and forms a Mach front. The point where the incident wave and reflected wave meet is referred to as the triple point. Although some variation exists along the height, for design purposes, the Mach front is considered planar (DoD, 2008; Krauthammer, 2008). When a point of interest is located below the triple point, it experiences the pressure associated with the Mach front as shown in Figure 2.7(a). When a point of interest is located above

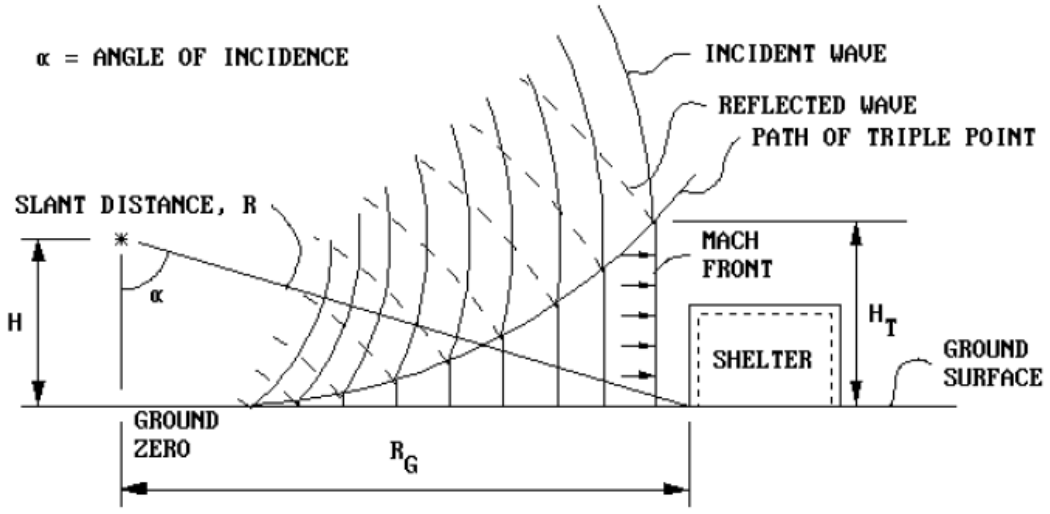

Figure 2.6 Formation of Mach Front (DoD, 2008)

the triple point, however, it experiences the pressure of the incident wave first, followed by the reflected wave from the ground as shown in Figure 2.7(b). This interaction of the incident and reflected waves vary with the height above the triple point (DoD, 2008).

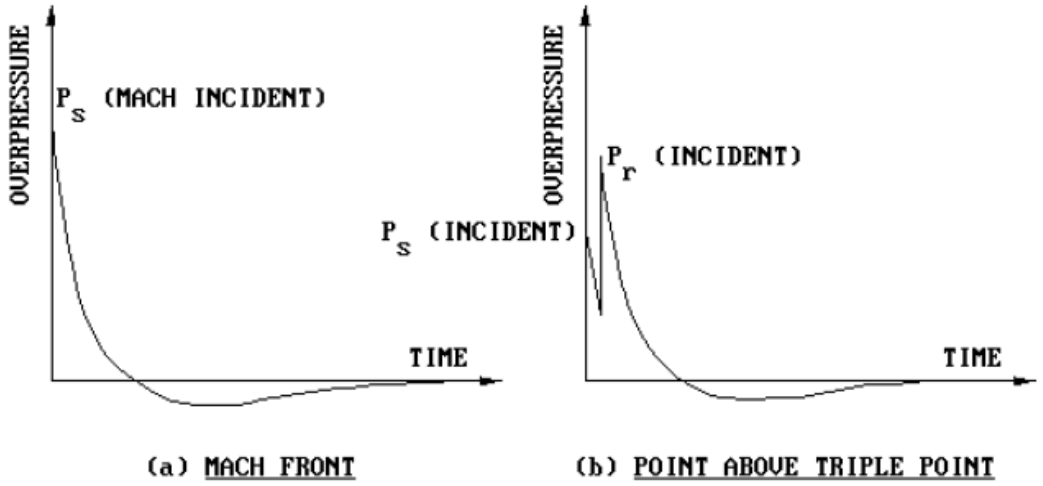

Figure 2.7 Pressure-Time Variation in Relation to Formation of Mach Front: (a) Location Below the Triple Point on the Mach Front, (b) Location Above the Triple Point Before the Formation of the Mach Front (DoD, 2008)

This section presented a description of shock wave behavior in general terms of a typical external detonation. A basic understanding of an external detonation is needed before examining the more complex scenario of an internal detonation. The following section provides an overview of internal explosions.

2.2 INTERNAL EXPLOSIONS

An internal explosion includes two complexities that are not typical in an external explosion. First, there are multiple reflecting surfaces, which results in a combined effect from the incident shock wave and multiple reflected shock waves. Second, the explosion occurs within an enclosed volume, which results in the development of gas pressure as a result of the chemical reaction that sustained the detonation.

2.2.1 Multiple Reflecting Surfaces

In general, the early-time initial shock phase of an internal detonation can be predicted similarly to an external detonation. The incident shock wave will travel from the explosive source, and the initial (sometimes referred to as first-order) reflections off all interior surfaces can be characterized in a similar manner to an external detonation described in the previous section (Krauthammer, 2008; DoD, 2002). This initial shock phase is distinguished as an initial instantaneous rise in pressure as shown in Figure 2.8, which shows a typical pressure history of a point on an interior surface of a room subjected to an internal detonation (DoD, 2008). After this initial shock phase, the multiple reflected waves begin to interact with each other and reflect off other surfaces in the room, creating additional reflected shock waves. This interaction can occur for a significant duration, resulting in a complicated pressure history as depicted in Figure 2.8. The distribution of the blast pressures is also highly non-uniform due to the small standoff distances that are typically associated with internal explosions and because the

positioning of reflecting surfaces and unique room features (such as corners) relative to the center of detonation.

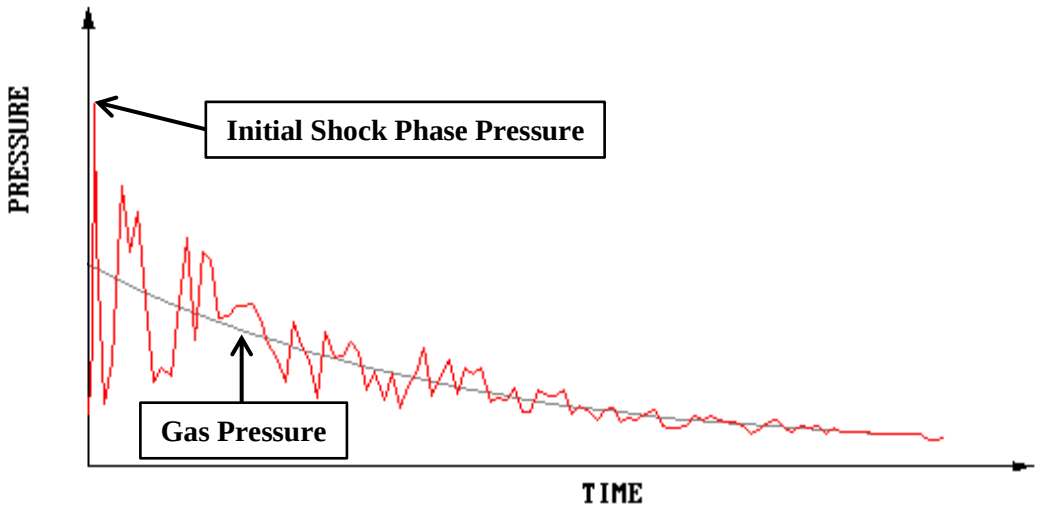

Figure 2.8 Pressure History of Internal Detonation with Partial Venting (adapted from DoD, 2008)

2.2.2 Gas Pressure and Venting

In addition to the shock wave reflections and interactions, an internal detonation also introduces gas pressures to the blast environment. The detonation process results in high pressure and high temperature gas products which expand into a confined volume (Krauthammer, 2008). The resulting pressure from these expanding gases is referred to as the gas pressure load, and this pressure is added to the shock pressure loads within a room. The peak gas pressure develops more slowly than the initial shock pressure, and the decay, in general, also occurs more slowly, but is dependent on the amount of venting present and the cooling rate of the gases (DoD, 2002; Krauthammer, 2008). The gases in the detonation room will vent through openings into adjacent rooms. Under these conditions, the gas pressure in the detonation room drops, and the pressure in the adjacent

room increases until equilibrium between the two rooms is achieved (DoD, 2002). Figure 2.8 shows the gas pressure as a function of time in a partially vented room. The gradual decay of the gas pressure can be seen as the gas pressure vents.

2.2.3 Predicting Internal Blast Loads

Predicting the loads on interior surfaces from an internal detonation is an important aspect of the research study described herein. Several methods are available, and three of the most common current state-of-the-practice methods are presented here.

2.2.3.1 UFC 3-340-02 Empirical Charts

UFC 3-340-02 (DoD, 2008) contains a method to predict blast loads from internal detonations using empirical charts. These charts are based on experimental test data from three-wall, fully-vented cubicles and four-wall, partially-vented cubicles. The predicted load is an idealized pressure history that includes the initial shock pressure and the gas

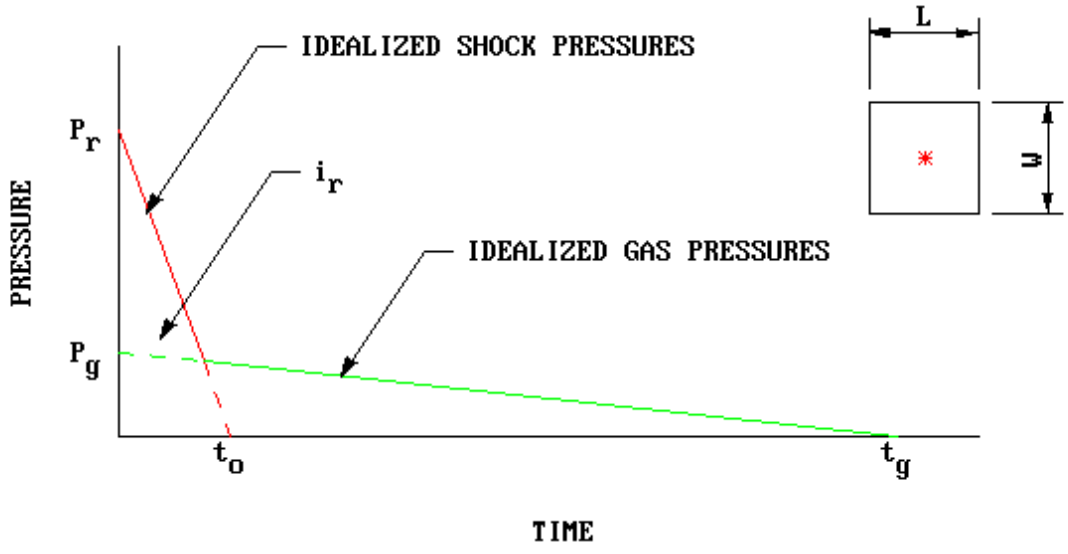

Figure 2.9 Idealized Blast Load From Internal Detonation (DoD, 2008)

pressure as shown in Figure 2.9. This load is assumed to be uniformly distributed on the interior surfaces (DoD, 2008). The accuracy of this method is limited because it ignores variations in the shock pressure resulting from the reflected shock waves. Additional limitations with this method are discussed further in Sections 3.1 and 3.2.1.

2.2.3.2 BlastX

The U.S. Army Corps of Engineers offers the computer program BlastX (USACE, 2011) to compute the combined effects of incident and reflected waves from multiple surfaces. This engineering-level program was developed by the U.S. Army Engineer Research and Development Center and the Air Force Research Laboratory. The distribution of this program is limited to U.S. Government agencies, their contractors, and NATO Government agencies. It is preferred to compute blast loads for internal explosions because it includes the shock pressure loads from multiple reflecting surfaces and the gas pressure loads.

The BlastX code uses a ray-tracing methodology to compute the blast load at a given point of interest, including first-order and higher-order reflections from walls within a room (DoD, 2002). In this method, the interior walls are considered to be rigid reflecting surfaces, and a set of physical ray paths is determined from an explosive source to a point of interest, including all paths reflecting off all surfaces (DoD, 2002; Sammarco, 2014). The ray path model assumes the angle of incidence is equal to the angle of reflection (Sammarco, 2014). Each reflected ray can be treated as a resulting shock wave from an "image source" located on the other side of the reflecting surface (DoD, 2002). The resulting pressure at the point of interest comes from the interaction of the free-air shock wave from the original explosive source and each "image source." This resulting pressure is computed by nonlinear superposition using the LAMB shock

addition rules (Britt, 2001; DoD, 2002). The BlastX code also accounts for gas pressure by calculating the associated gas pressures for given explosive components. The venting of gas pressures is handled as a time-dependent flow of gases through openings between rooms.

The BlastX code can accommodate many different room geometries and configurations. It also includes empirical data for a large variety of explosive types. These data are used to determine the free-air shock waves from the aforementioned explosive source and "image sources." The code has also been validated with experimental data from several internal and external detonations (Britt et al., 2001). For these reasons, the BlastX program is used in the research outlined in this dissertation to predict blast loads for internal detonations.

2.2.3.3 Finite Element Models

Computational fluid dynamics (CFD) software can also be used to predict internal blast loads. Examples of such software with this capability are CTH (Sandia National Laboratories, 2014), SHAMRC (Applied Research Associates Inc., 2014), LS-DYNA (LSTC, 2011), and Autodyn (ANSYS, 2015). These high-fidelity, physics-based models use fluid mechanics calculations and governing conservation equations to determine fluid flow and variations in fluid properties as a function of time and position. With appropriate boundary conditions, these numerical computations are able to account for multiple reflections, pressure magnification, turbulence, and pressure buildups to predict accurate blast loads from an internal detonation (Williams, 2009). Using such software to predict blast loads, however, is extremely computationally demanding compared to the methods previously described. Using CFD software also requires an experienced analyst with extensive knowledge in advanced modeling techniques and a thorough

understanding of blast phenomena to both input the analysis parameters and interpret the results (Williams, 2009). Example results from a numerical simulation using Autodyn (ANSYS, 2015) to simulate research conducted by Feldgun et al. (2012) are shown in Figure 2.10. The study examined the numerical analysis of an internal detonation in a partially vented room. The numerical prediction shows the multiple peak pressures due to the reflected shock waves can be simulated using the CFD software. Figure 2.10 also shows the idealized predicted load computed using the UFC 3-340-02 empirical charts, which can significantly overestimate pressures and does not capture any pressure variations due to reflected shock waves.

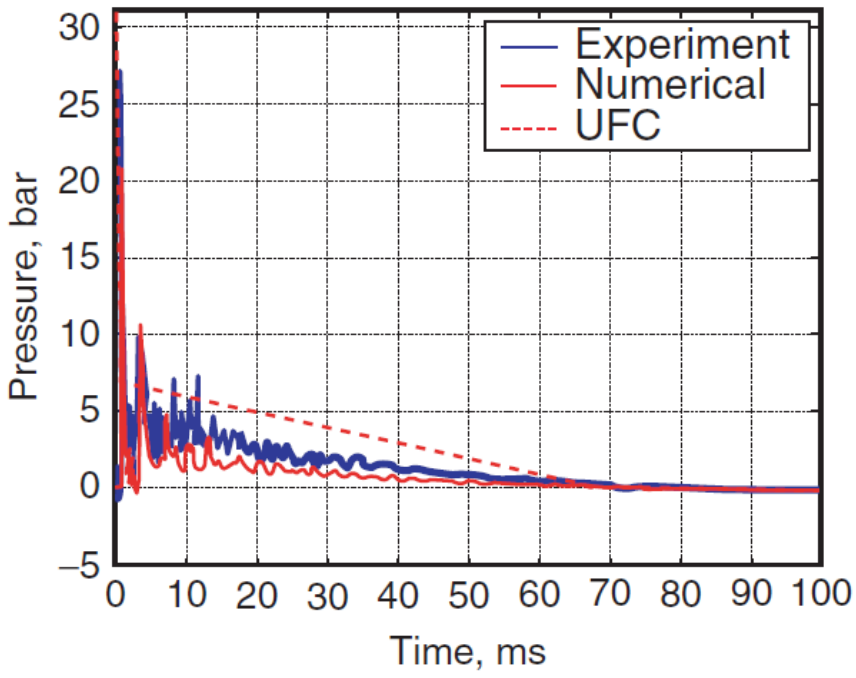

Figure 2.10 Example of CFD predicted Internal Blast Load versus Experimental Test and UFC 3-340-02 Idealized Prediction (Feldgun et al., 2012).

Using CFD software to predict internal blast loads can produce extremely accurate results. For many internal blast scenarios, however, the uncertainty of the threat and/or the room configuration does not warrant the use of such computationally demanding load prediction methods.

2.3 STRUCTURAL RESPONSE TO BLAST LOADS

An internal blast load produces a complex loading scenario on interior walls. The load can typically be described as a variable high-pressure short-duration dynamic lateral load. The duration of a blast load is typically on the order of milliseconds, and far less than the natural period of a typical structural member. Due to the dynamic nature of a blast load, the structural response is also considered dynamic.

The proximity of an explosion to an interior wall in an internal detonation may result in significantly different loads on each individual wall. Furthermore, individual members or components that make up a wall may also experience different loads depending on the detonation proximity. For this reason, the individual response of structural members is often considered in a blast load scenario rather than global response of the entire wall.

Blast threats are considered a rare occurrence for most structures. Typically, the results of a structural analysis are for determining life safety, and significant levels of damage are accepted. For these reasons, factors of safety are typically not used in blast analysis and design. Also, the actual material strengths are desired for analysis instead of using minimum design strengths. Additional information on these topics for steel-stud walls are presented in Section 2.3.2.3. Additionally, structural analysis for blast normally includes the plastic response of members. The inelastic response of members is necessary

to account for the energy dissipation associated with permanent deformations and in determining when a structural member completely fails.

2.3.1 Dynamic Analysis for Response to Blast Loads

Several analysis methods are available to compute the dynamic response of structural members subjected to blast loads. These methods are typically categorized as being either uncoupled or coupled. An uncoupled analysis first calculates the blast load as if the structure the blast acts against is rigid. This blast load is then applied to the structure, and a dynamic analysis is performed. For a coupled analysis, the interaction between the structural response and blast load is considered, and the blast load is computed simultaneously with the structural response. Coupled analyses are more realistic than uncoupled ones for internal detonations because the structural response will often result in venting and localized failure and cause a lower blast load than that computed using an uncoupled analysis (Williamson et al., 2010).

This section presents the two most common methods used in the current state of the practice. An uncoupled, approximate single-degree-of-freedom (SDOF) method is presented first. Subsequently, a description of uncoupled and coupled finite element analysis methods is provided.

2.3.1.1 Equivalent Single-Degree-of-Freedom

The most common analysis method used in current blast analysis and design is the equivalent SDOF method (ASCE, 2010; Krauthammer, 2008; DoD, 2008; Biggs, 1964). This method is primarily used because it provides reasonably accurate results and can be performed considerably more efficiently than other computationally demanding methods. Also, inherent uncertainties exist in most blast analysis scenarios that do not warrant a

highly detailed dynamic analysis. In his book *Introduction to Structural Dynamics*, Biggs explains that the SDOF approximate analysis method,

> should not be regarded as merely crude approximations, to be used for rough or preliminary analysis, nor should they be regarded as methods to be used only by engineers who lack the training or intellect to employ more sophisticated techniques. Problems in structural dynamics typically involve significant uncertainties, particularly with regard to loading characteristics. Such being the case, complex methods of analysis are often not justified (1964).

This statement was presented in 1964, and it still remains true in the current state of the practice.

In order to use a SDOF analysis approach on a continuous structural member, a transformation into an equivalent SDOF system is required. This transformation is explained in many structural dynamics references as well as many blast analysis references (Biggs, 1964; DoD, 2008; Krauthammer, 2008). To demonstrate this process, an example of a simply-supported beam transformed into an equivalent SDOF system is presented and is shown in Figure 2.11.

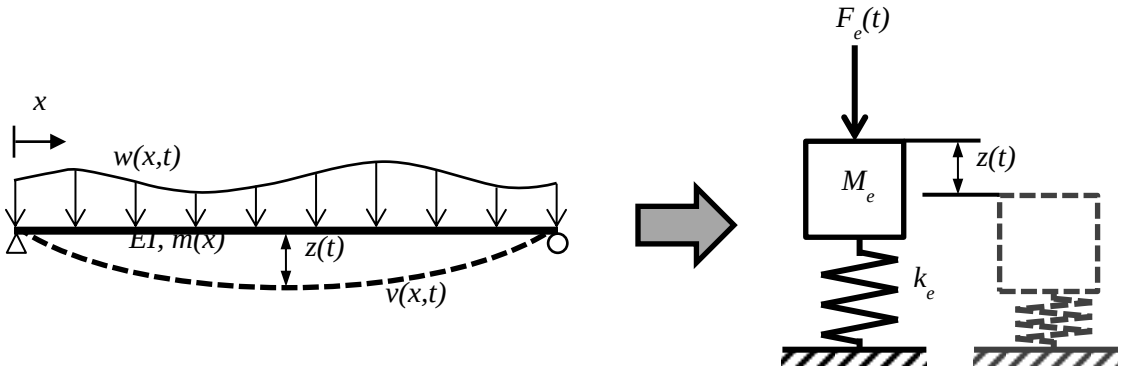

Figure 2.11 Simply-Supported Beam Equivalent SDOF Transformation (a) Real System, (b) Equivalent SDOF System

In the continuous system shown in Figure 2.11(a), the simply-supported beam has a constant modulus of elasticity and moment of inertia, *EI.* The mass of the beam, *m(x)*, is distributed along its length. The beam is subjected to a distributed load, *w(x,t)*, that varies with position and time. The displaced shape of the beam is defined as *v(x,t)*, which also varies with time and position along the length of the beam. The variable *z(t)* is the displacement at a particular point of interest on the beam. This may be the midspan, the point of maximum elastic displacement, or the point at which a plastic hinge forms. This displacement at the point of interest will be the displacement computed by the equivalent SDOF system. This equivalent SDOF system is shown in Figure 2.11(b). Here, M_e, represents the effective mass, $F_e(t)$ describes the effective load, and k_e, represents the effective stiffness.

The continuous system is transformed into the equivalent SDOF system by assuming a normalized shape function, $\varphi(x)$, for the displaced shape of the beam and using equivalent work and energy principles. The assumed mode shape should be the displaced shape of the beam under a static application of the applied distributed load. This method of using the static displaced shape opposed to the modal shapes associated with the natural frequencies of vibration is often used in blast analysis (Biggs, 1964; Williams, 2009). In general, this method is simpler, covers symmetric and asymmetric deformation, better handles inelastic response, and is more accurate than using vibration modes (Biggs, 1964; DoD, 2008; Williamson, 2014). This mode shape is then normalized by the displacement of the point of interest under the same static application of the load to obtain the shape function, $\varphi(x)$ (DoD, 2008; Williamson, 2014). The displaced shape of the beam can now be expressed by Equation (2-1).

$$v(x,t) = \varphi(x) \cdot z(t) \tag{2-1}$$

where $v(x,t) =$ displaced shape of beam

$\varphi(x) =$ shape function

$z(t) =$ displacement of point of interest

Equation (2-2) is used to determine the equivalent mass, M_e. This equation is derived by equating the kinetic energy of the continuous and equivalent systems (DoD, 2008; Williamson, 2014).

$$M_e = \int_0^l m(x)\left[\varphi(x)\right]^2 dx \tag{2-2}$$

where $M_e =$ equivalent mass

$l =$ length of beam

$m(x) =$ distributed mass of beam

The equivalent load, $F_e(t)$, is computed using Equation (2-3). This equation is derived by equating the external work of the continuous and equivalent systems (DoD, 2008; Williamson, 2014).

$$F_e(t) = \int_0^l w(x,t) \cdot \varphi(x) dx \tag{2-3}$$

where $F_e(t) =$ equivalent load

$w(x,t) =$ applied distributed load

The equivalent stiffness, k_e, is computed using Equation (2-4). This equation is derived by equating the internal strain energy of the continuous and equivalent systems (DoD, 2008; Williamson, 2014).

$$k_e = \int_0^l EI\left[\varphi''(x)\right]^2 dx \tag{2-4}$$

where $k_e =$ equivalent stiffness

$E =$ beam modulus of elasticity

$I =$ beam moment of inertia

$\varphi''(x) =$ second derivative with respect to x of shape function

As mentioned above, it is important in blast analysis to include the inelastic response of members. Thus, the formation of plastic hinges must be included in this equivalent system. Each stage of response will have a different mode shape, and in turn, result in a different equivalent SDOF system for each stage of response. To illustrate this process, Figure 2.12 shows the three stages of response and formation of plastic hinges for a fixed-fixed beam (Biggs, 1964). The dashed line for each response stage would be

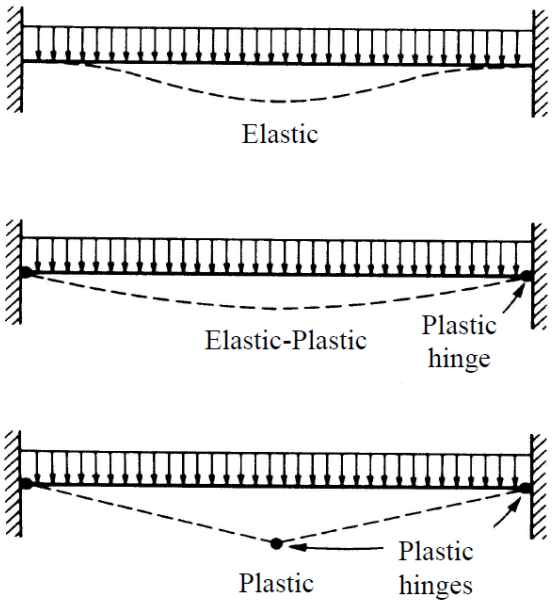

Figure 2.12 Stages of Response for Fixed-Fixed Beam (Biggs, 1964)

the mode shape, and it would be normalized by the midspan displacement for each stage, resulting in a unique shape function, $\varphi(x)$, for each stage. A unique equivalent SDOF system ensues for each stage of response.

Many times in blast analysis, it is convenient to describe the equivalent system in terms of equivalency factors. These factors are shown in Equations (2-5), (2-6) and (2-7).

$$K_M = \frac{M_e}{M} \tag{2-5}$$

where $K_m =$ mass factor

$M_e =$ equivalent mass

$M =$ actual total mass

$$K_L = \frac{F_e(t)}{F(t)} \tag{2-6}$$

where $K_L =$ load factor

$F_e(t) =$ equivalent load

$F(t) =$ actual total load

$$K_k = \frac{k_e}{k_{POI}} \tag{2-7}$$

where $K_k =$ stiffness factor

$k_e =$ equivalent stiffness

$k_{POI} =$ actual member stiffness for displacement at the point of interest

Equivalency factors for common boundary conditions and loading distributions have been developed and are widely published in blast analysis reference manuals (DoD,

2008; Krauthammer, 2008; Biggs, 1964). Using equivalency factors, the governing equation of motion for the equivalent SDOF system is shown in Equation (2-8).

$$\left(K_M M\right)\ddot{u} + c\dot{u} + \left(K_k k_{POI}\right)u = \left[K_L F(t)\right] \tag{2-8}$$

where $K_m =$ mass factor

$M =$ actual total mass

$\ddot{u} =$ acceleration of point of interest

$c =$ damping coefficient

$\dot{u} =$ velocity of point of interest

$K_k =$ stiffness factor

$k_{POI} =$ actual member stiffness for displacement at the point of interest

$u =$ displacement of point of interest

$K_L =$ load factor

$F(t) =$ actual total load

Damping is typically ignored in blast analysis because it generally has little effect on the maximum displacement of a structural component. Also, energy dissipation due to plastic deformation is much greater than that due to structural damping in a blast analysis scenario, and accounting for the energy dissipation of viscous damping during plastic response is also questionable (DoD, 2008; ASCE, 2010).

Conveniently, the load factor, K_L, and the stiffness factor, K_k, are mathematically equal. This is because the shape function is normalized and based on the static application of the load. The stiffness at the point of interest is equal to the internal force required to return the member to its original position, so the stiffness is equal to the applied static load (Biggs, 1964; DoD, 2008). By ignoring damping and substituting K_L

for K_k, then dividing all terms in Equation (2-8) by K_L, the equation of motion for the equivalent SDOF system becomes Equation (2-9).

$$\left(\frac{K_M}{K_L}M\right)\ddot{u} + k_{POI}u = F(t) \tag{2-9}$$

Now the equation of motion for the equivalent system can be described using only one equivalency factor called the load-mass factor, K_{LM}. The load-mass factor is defined by Equation (2-10). Load-mass factors for common boundary conditions and load distributions are also widely published like the other equivalency factors.

$$K_{LM} = \frac{K_M}{K_L} \tag{2-10}$$

The load-mass factor, K_{LM}, and the stiffness at the point of interest, k_{POI}, change with each stage of response. It is common in structural dynamics to replace the stiffness and displacement term with an equivalent resistance function, *R(u)*, to describe the member's internal force, or resistance, throughout the stages of response. An example resistance function for the fixed-fixed beam in Figure 2.12 is shown in Figure 2.13.

Equation (2-10)**Error! Reference source not found.** shows the final resulting equation of motion used in the equivalent SDOF system for blast analysis. The dynamic analysis can now be performed using only one equivalency factor for each stage of response, the actual mass and actual loading of the system, and a single resistance function that encompasses all stages of response.

$$\left(K_{LM}M\right)\ddot{u} + R(u) = F(t) \tag{2-10}$$

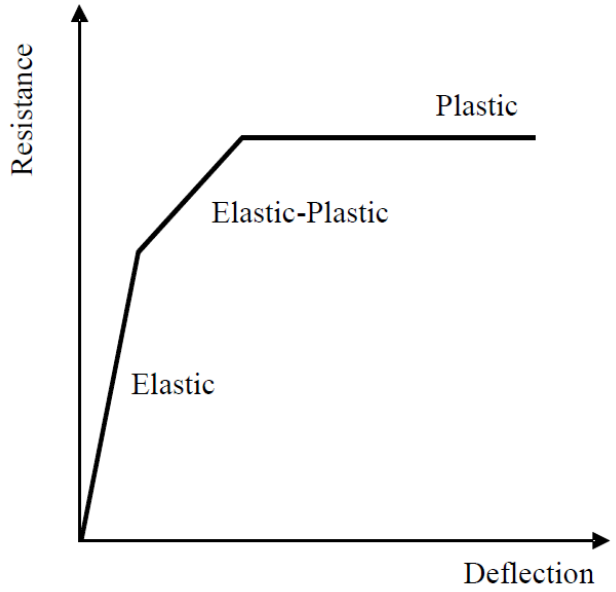

Figure 2.13 Typical Resistance Function for Fixed-Fixed Beam (Williams, 2009)

As stated previously, blast analysis is often performed at the individual member level. The interaction between structural members can also be considered by using a series of equivalent SDOF systems. An example of this is a beam framing into two girders as shown in Figure 2.14. By examining the load path of the structure, the beam is loaded by the uniformly distributed load, and the girders are loaded by the ends of the beam as point loads. An equivalent SDOF system is established for both the beam and the girder. The beam is treated as described in the section above. The equivalent system for the girder includes the addition of mass from the beam, and the force on the girder SDOF system is the reaction force determined from the beam SDOF system. The amount of mass added to the second SDOF system, referred to a mass participation, is often left to

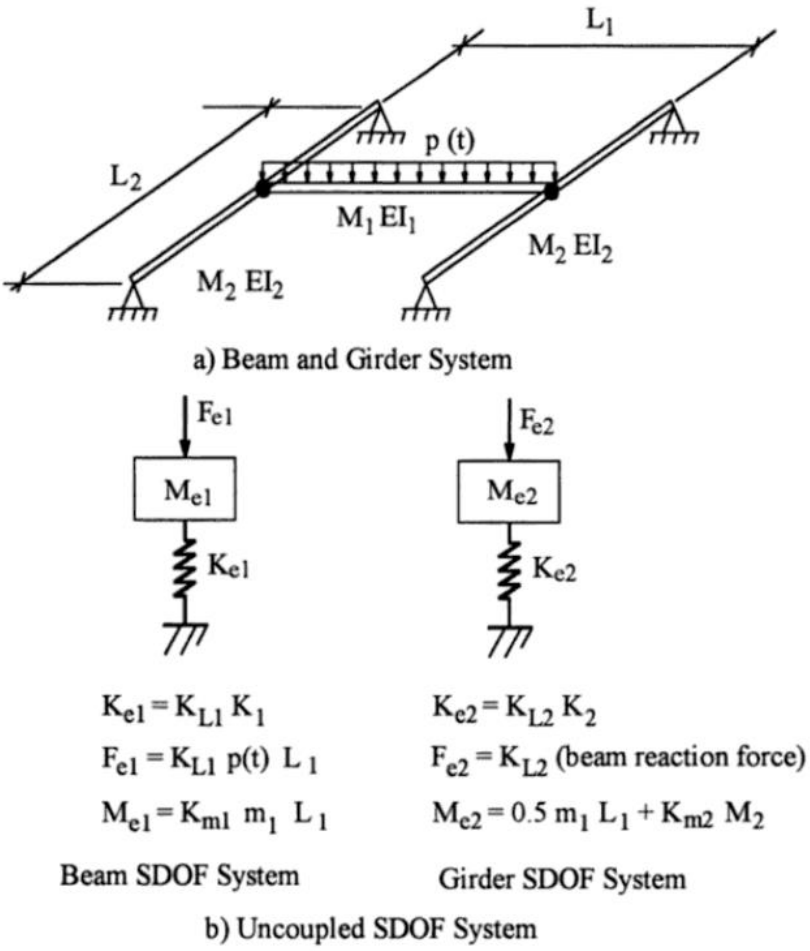

Figure 2.14 Typical Series of SDOF systems for Multi-Member System: (a) Uniformly-Loaded Beam Framing into Two Girders, (b) Individual Equivalent SDOF System for Beam and Girder (ASCE, 2010)

engineering judgement (ASCE, 2010). For the example shown in Figure 2.14, 1/2 of the beam's mass is added to each girder as a point mass. For typical structural systems, 1/5 to 1/4 of the mass is commonly added to each girder (Williamson, 2014). This analysis method has been shown to provide acceptable results when the ratio of the natural period of the larger member to the smaller member is greater than or equal to 2.0 (Williamson, 2014).

2.3.1.2 Finite Element Method Analysis

Some blast analysis scenarios may need a higher-level of analysis than can be achieved using an approximate SDOF analysis. Williamson et al. (2010) describe in detail these possible scenarios. The ones most relevant to an interior wall include:

- Scenarios involving localized failure: Close-in or contact charges where the detonation occurs next to or at an interior wall may cause localized failure. The most common failure mode for this scenario is a breach failure.
- Scenarios where the failure mode is uncertain: The mathematical resistance function for a beam is developed based on flexural response, but some loading scenarios may result in shear (or other limit state) dominating the failure mode.
- Scenarios where the P-Δ effect may contribute to failure: If an interior wall is also a load-bearing wall, the axial force will contribute to the wall's structural resistance. This behavior can be accounted for with axial-flexural interaction, but typical SDOF analysis does not account for the resulting P-Δ effect.
- Scenarios where the blast load cannot be approximated over the entire length of a member as a function of time: In an internal detonation, the variation of load can be substantial. For example, peak pressures can occur at the midspan of a beam at much different times than they occur at the beam ends due to the inherent close proximity of internal detonations and reflections off of adjacent surfaces.
- Scenarios where several members contribute to the overall structural response: Equivalent SDOF systems are best suited for individual member response. Using load path analysis and a series of equivalent SDOF systems can be used as described in the previous section, but these methods have limitations. Complex interactions, extent of mass participation, and connected members with similar

natural periods may require a rigorous analysis approach that exceeds the capabilities available using SDOF analysis methods.

- Scenarios where the load cannot be treated as uncoupled: Typical SDOF analyses are uncoupled, where the blast load is computed independently and does not change with the computed structural response. Interior walls may fail early in time with respect to the blast load duration. This early-time failure can create vent openings and alter reflecting surfaces, which may significantly alter the blast load. A coupled analysis may be required to account for this interaction.

When an equivalent SDOF analysis is not sufficient, a multiple-degree-of-freedom (MDOF) analysis must be performed. The most common MDOF analysis method utilizes the finite element method (FEM) (DoD, 2002). The analysis can be either uncoupled or coupled. For an uncoupled analysis, the structural system can be modeled using a variety of available FEM analysis software packages. This approach requires a knowledgeable user to properly represent the structural members with appropriate element types, boundary conditions, and material models with the appropriate detail to capture the desired structural behavior. The load in an uncoupled analysis is computed in a manner described in Section 2.2.3, then applied to the structural model. When performing an uncoupled FEM analysis, it is important to remember the accuracy of the structural response is also related to the accuracy of the predicted load. Therefore, increasing the detail of the structural model does not always result in a more accurate analysis results than a model with less detail. The UFC 3-340-01 (DoD, 2002) recommends users start with the simplest structural model and then progress to a more detailed model until the desired important behavior is captured. Typically, an experienced

specialist is required to be able to create a structural model that captures appropriate nonlinear dynamic behavior associated with blast events (Williamson et al., 2010).

The most accurate structural response analysis method for blast scenarios is a coupled 3D nonlinear FEM analysis. This method is the highest resolution procedure currently available (Williamson et al., 2010). For this type of analysis, a blast load prediction using CFD is solved simultaneously with the structural response using computational solid mechanics (CSM) (Ngo et al., 2007). Examples of software with this capability are LS-DYNA (LSTC, 2011) and Autodyn (ANSYS, 2015). Due to the number of inputs and the complexity of the fluid-structure interaction, this method requires extensive experience and time to develop a model, run the analysis, achieve correct failure modes, and interpret results (Williams, 2009). Ngo et al. states, "successful computational modeling of specific blast scenarios by engineers unfamiliar with these programs is difficult, if not impossible" (2007). In most cases, the internal detonation scenario's inherent uncertainties, combined with the extensive analyst experience needed and the computational cost for a coupled FEM analysis, do not warrant this highest level of analysis.

2.3.2 Steel-Stud Wall Structural Response

The focus of the research study outlined in this dissertation involves the response of interior steel-stud walls. A brief overview of steel-stud wall construction and behavior is presented in this section, as well as descriptions of structural response characteristics unique to these walls when subjected to blast loads.

2.3.2.1 Steel-Stud Wall Design and Behavior

Cold-formed steel (CFS) stud walls, commonly referred to as steel-stud walls or metal stud walls, have been constructed with increasingly popularity in recent years as an

alternative to wood-stud walls. Compared to wood, CFS provides increased ductility, has a higher strength-to-weight ratio, and offers resistance to fire, insects, mold, and rot (Salim et al, 2005; Bewick et al., 2011; Yu and LaBoube, 2010). A typical steel-stud wall detail is shown in Figure 2.15. Studs are evenly spaced and connected at the top and bottom to a track using self-drilling sheet metal screws. The tracks are connected to the floor and ceiling (not shown in Figure 2.15) using various types of fasteners. Most studs have utility holes to allow electrical wiring and other utilities to be run through a wall. Bracing is commonly provided by installing bridging through the utility holes, as shown

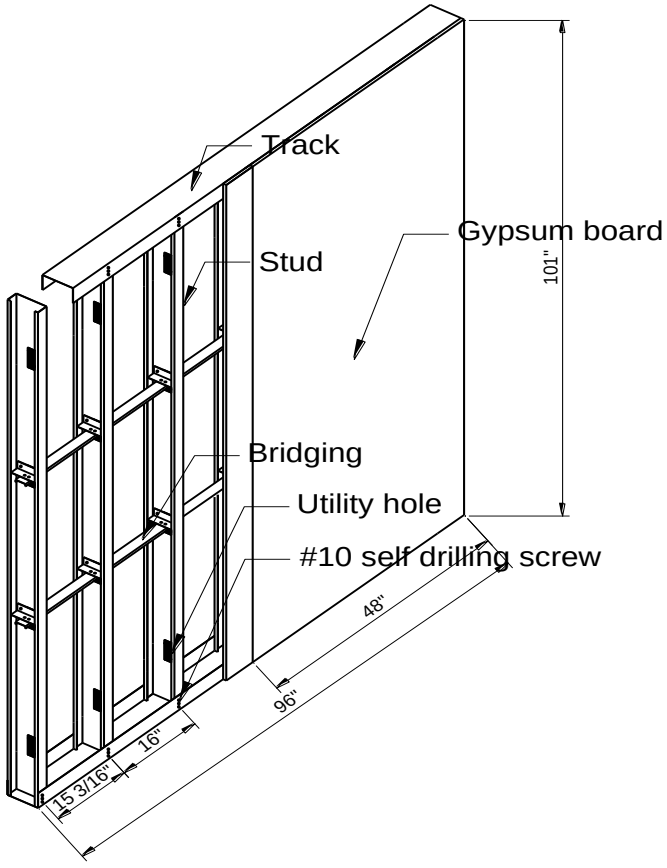

Figure 2.15 Typical Interior Steel-Stud Wall Details (Li et al., 2014)

in Figure 2.15, or by continuous metal straps installed on the stud flanges. This bracing method is shown later in Chapter 4 in Figure 4.7. Gypsum board is typically installed on both faces of an interior wall using self-drilling drywall screws.

CFS differs from hot-rolled steel in two main ways. First, the manner in which member shapes are formed result in different material properties. The cold working process to form CFS sections results in an increased material strength, especially in the corners of a section. This increase in strength is mainly due to strain hardening and strain aging. It is important to note that while the strength increases due to cold working, the ductility also decreases compared to virgin steel (Yu and LaBoube, 2010).

The second main difference between CFS and hot-rolled steel is the significantly higher width-to-thickness ratios found in CFS sections, which tends to give rise to limit states controlled by local buckling because of the thin plate behavior found in CFS sections. Local buckling can occur in both stiffened and unstiffened elements subjected to compression. The local buckling capacity of stiffened elements is considerably higher than that of unstiffened elements, which is why many CFS sections possess stiffener lips. When the stiffener lip does not sufficiently provide stability to a compression flange and web, another buckling mode shape, referred to as distortional buckling, is possible (CFSEI, 2008). Figure 2.16 shows the possible buckling modes of a CFS stud subjected to applied flexural stresses. A typical hot-rolled steel section analysis considers lateral-torsional buckling, and local buckling is only considered for sections defined by AISC (2010) as being non-compact. All analyses of CFS sections, however, consider local buckling, distortional buckling, and lateral-torsional buckling.

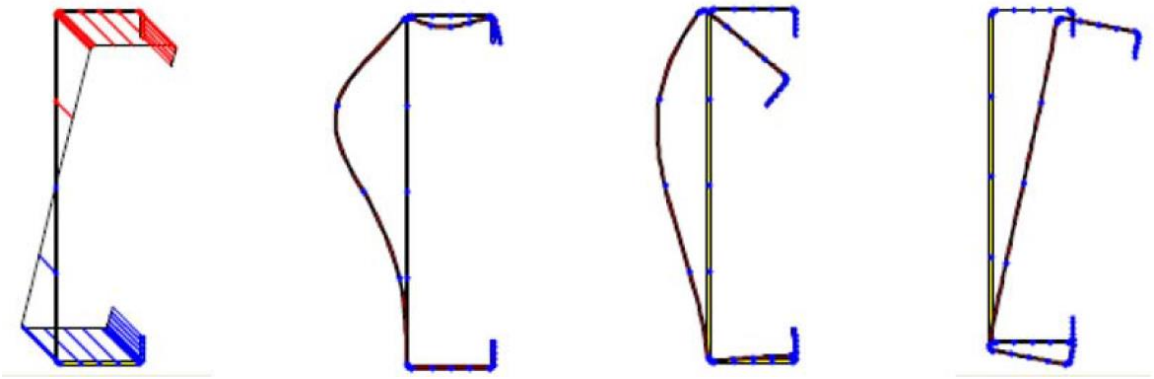

(a) (b) (c) (d)

Figure 2.16 Buckling Modes of a Typical CFS Stud: (a) Applied Stress, (b) Local Buckling, (c) Distortional Buckling, (d) Lateral-Torsional Buckling (CFSEI, 2008)

The American Iron and Steel Institute (AISI) design specification (2007) handles the effects of local buckling through an effective width method. Effective widths are calculated for flange and web elements, and then used in design strength computations. Effective section properties are also computed, such as the effective section modulus, S_e, used to compute flexural strength. The effective moment of inertia, I_e, is used to compute flexural displacements. Directions for computing distortional buckling capacity are presented in the AISI Specification (2007), and design aids and examples for distortional buckling computations are provided is the Cold-Formed Steel Engineers Institute Technical Note G100-08 (2008). Additionally, the effective section properties, as well as allowable design moments for local and distortional buckling for CFS studs, are published in the Steel Stud Manufactures Association (SSMA) Product Technical Guide (2013). Additional details on the design and analysis of CFS members can be found in the AISI Specification (2007).

Complete plastic design is not typically considered in CFS design because local and distortional buckling instabilities prevent the formation of plastic hinges (Yu and

LaBoube, 2010). For this reason, the design moment of a CFS section is based on the yield moment, not the plastic moment as it is in hot-rolled steel design. However, beginning in 1980, the AISI specification has included provisions to include reserve capacity from inelastic flexural behavior (Yu and LaBoube, 2010).

2.3.2.2 Connection Details

Connection design and analysis in CFS is handled similarly to hot-rolled steel. All applicable failure limit states for a given connection must be checked. For a screw connection in shear, the limit states include screw shear failure, bearing failure, and tilting. For a screw connection in tension, the limit states include screw tension failure, pull-out, and pull-over. These limit states and provisions can be found in the AISI specification (2007). The connection strength of a screw connection between a stud and tracks will be important when examining the response of interior steel-stud walls subjected to blast loads.

Another specific connection with importance in the response of steel-stud walls subjected to blast loads is the track-to-floor and track-to-ceiling connections. Different fastener types to attach a track may be used, and one of the commonly used fastener types for attaching tracks to both concrete slabs and hot-rolled structural steel members is powder-actuated fasteners (LGSEA, 2001). Both the shear and tensile strength of these connections are needed to analyze a wall's overall lateral force resistance. Powder-actuated fastener manufactures publish design strengths for their fasteners embedded into both concrete and structural steel (RAMSET 2011). The Light Gauge Steel Engineers Association (LGSEA) also provides Technical Note 562 (2001), which describes the design and analysis of powder-actuated fasteners connections. The shear strength of a powder-actuated fastener connecting a track to concrete is dependent on the shear

capacity of the fastener, the embedment length, the strength of the concrete, and the bearing capacity of the track. The tensile strength of the connection is dependent on the pull-out strength of the fastener and the pull-over capacity of the track (LGSEA, 2001).

2.3.2.3 Increase Factors for Blast Analysis

As stated earlier, in blast analysis and design, actual material strengths are used instead of minimum design strengths. A strength increase factor (SIF) is commonly used to increase the material yield strength over the expected minimum value. This factor provides an average increase value for a given material. CFS sections are formed from sheet steel that conforms to ASTM A653/653M (2013). The most common grades are Grade 33 and Grade 50, which have minimum yield strengths of 33 ksi and 50 ksi, respectfully. CFS sections made from this material generally have an actual yield strength that significantly exceeds the specified yield strength, and the recommended SIF for this material from the UFC 3-340-02 is 1.21 (DoD, 2008). ASCE 59-11 (2011) recommends a SIF of 1.1 for CFS. Current research on cold-formed rectangular hollow sections performed by Sun and Packer used 20 tensile coupon tests from four CFS rectangular sections to determine an average SIF. The resulting average SIF was 1.16 for the flat or unbent portions of the cross-sections and 1.59 for the corner portions of the cross-sections (2014). Their results not only confirm there is an increase in strength in the cold-worked portions of a CFS member, but also suggest the ASCE 59-11 recommended SIF of 1.1 underestimates the actual material strength. It should also be noted that the strength increase factors are applied to the yield strength of materials, but they are not typically applied to the ultimate strength (DoD, 2008). As mentioned previously, factors of safety are typically not included in blast analysis or design, so from a design perspective, not using a SIF for the ultimate strength provides a slightly conservative design and may

prevent a potential catastrophic failure from an over-prediction of a material's ultimate strength.

Structural members subjected to blast loads also exhibit additional increases in strength compared to statically loaded members due to rapid strain rates that occur from dynamic loading (DoD, 2002). Most research conducted on high strain-rate properties of steel have used hot-rolled sections, reinforcing bars, and plates (Sun and Packer, 2014). In general, uniaxial tensile stress tests under rapidly applied loads have shown the effects of high strain-rates on the mechanical properties of steel. Compared to material properties under statically applied loads, a high strain-rate substantially increases the yield strength, slightly increases the ultimate strength, and does not affect the modulus of elasticity (DoD, 2008). In blast analysis, the high strain-rate effects are accounted for by multiplying the material strength by an increase factor called the dynamic increase factor (DIF). The DIF is dependent on the strain rate, and the UFC-3-340-02 (DoD, 2008) provides charts where the DIF can be computed based on a known strain-rate for structural steel. Alternatively, different DIFs are tabulated for various behaviors (i.e., bending versus tension or compression) of structural steel for a low-pressure strain rate of 0.1 in./in./s (for flexure) and a high pressure strain rate of 0.3 in./in./s (for flexure). However, because of the limited test data available for CFS, both the UFC 3-340-02 (2008) and ASCE 59-11 (2011) recommend a single DIF of 1.1 for the yield strength corresponding with all behaviors and all high-strain rates of CFS. Both references also do not consider any increase in the ultimate strength and specify a DIF of 1.0 for this value.

The research performed by Sun and Packer (2014) looked closely at the DIF of CFS. They performed 166 Split Hopkinson Pressure bar tests to determine the dynamic properties of CFS and compared the results to static properties. The conclusions were that the DIF for yield stress did substantially increase as the strain-rate increased, and the DIF

was lower for portions of the corners of the cross-section compared to the flat portions of the cross-section. Example results from the tensile tests of one specimen are shown in Figure 2.17. The DIF_y ranged from 1.18 to 1.78 for strain-rates from 181 to 1028 s^{-1}.

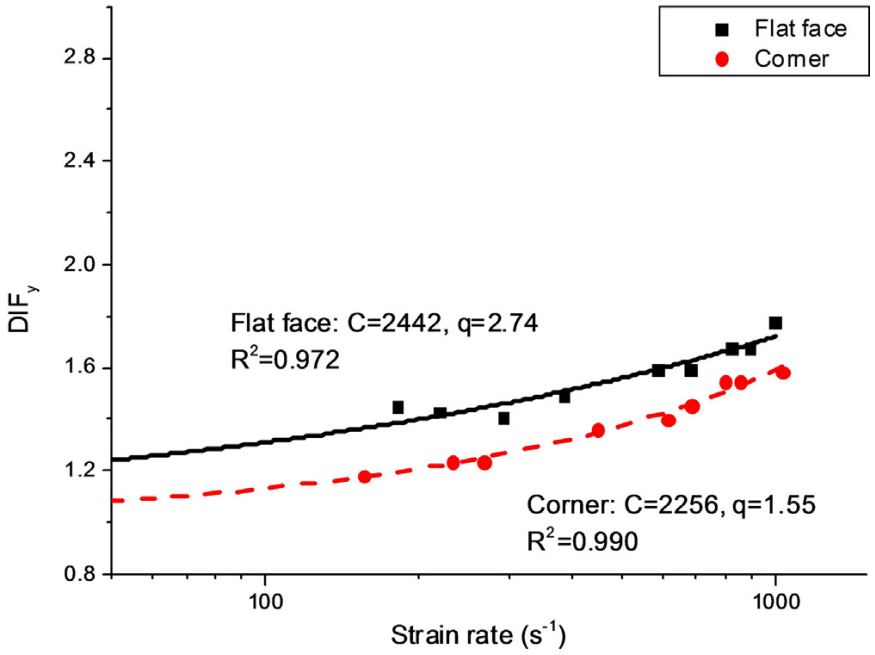

Figure 2.17 Tensile Yield Strength Dynamic Increase Factors for Cold-Formed Steel Rectangular Hollow Section (Sun and Packer, 2014)

The test did not include any strain rates close to the low-pressure explosive range of 0.1 in./in./sec, or any data on the ultimate strength. With the absence of this data, the UFC 3-340-02 and ASCE 59-11 recommended all-inclusive yield strength DIF of 1.1 for CFS remains the best approach for estimating the strength increase due to high strain-rates in blast analysis of steel-stud walls.

2.3.2.4 Blast Resistance of Steel-Stud Walls

In the past, the inertial resistance provided by mass has been the primary method to absorb energy in blast-resistant design (Bewick et al., 2013). In recent years, however,

research has shown that lightweight steel-stud walls can be successfully used in blast mitigation by taking advantage of the energy absorption capability due to the wall's ductility (Salim et al., 2005a; Salim et al., 2005b; Bewick et al., 2011; Bewick et al., 2013; Bondok and Salim, 2014; Bondok et al., 2015). Much effort has gone into developing resistance functions to capture the elastic and inelastic response of these walls.

With adequate connection strength, the full inelastic capacity of steel studs can be realized through tensile membrane action. After plastic hinges form in the studs, a mechanism is formed as shown in the plastic response stage of Figure 2.12. The studs continue to resist load during this stage as a tension membrane. The resistance actually increases during this phase, resulting in significant energy absorption capability. Early experimental testing using static load tree tests on individual studs and a static uniform resistance chamber on full wall sections demonstrated the full capacity of the tensile member action (Salim et al., 2005a). The resulting static resistance functions are shown in Figure 2.18.

While achieving full tensile membrane capacity is desirable, it may require a specialized clip connection not commonly used in typical construction practices. Conversely, conventional construction of steel-stud walls may only provide enough connection strength to achieve an elastic response (Bewick et al., 2013). Figure 2.19 shows a typical resistance function for a steel stud with different stud-to-track connection details. Bewick et al. examined simplified methods to improve the resistance of steel-stud walls. They found that using deep tracks with long flange widths and increasing the number of screws in the stud-to-track connection will significantly enhance the resistance of a steel-stud wall and allow it achieve tensile membrane response (2013). The research

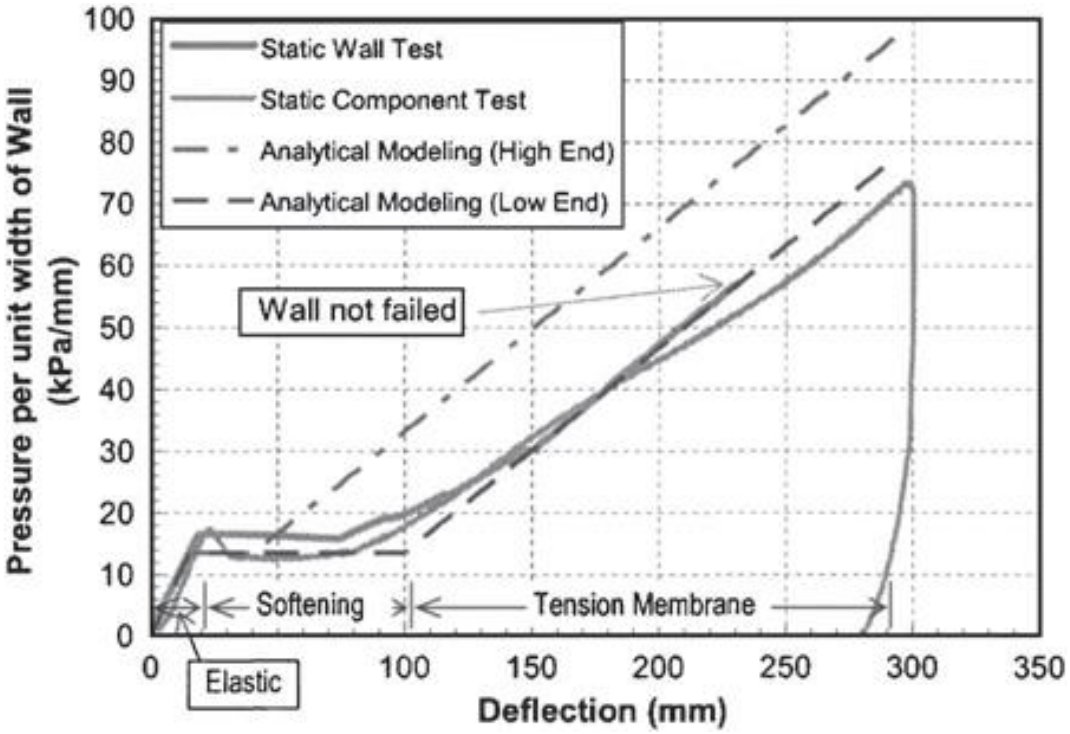

Figure 2.18 Static Resistance Function of Steel-Stud Wall (Salim et al., 2005a)

specifically examined stud-to-track connections and did not test the track-to-floor or track-to-ceiling connections. No known research has fully examined the track-to-floor or track-to-ceiling connections in conventional construction. Their response and interaction with other failure modes and the effect on the steel-stud wall resistance is not fully understood at this time.

Another important finding of the research performed by Bewick et al. (2013) was the effect of sheathing. A static load tree test apparatus was used to determine the resistance of steel-stud wall sections with and without sheathing. The load tree, shown in Figure 2.20, simulates a uniform load on the wall section. Through these load tree tests, it was determined that sheathing significantly increased the resistance of steel studs by providing lateral bracing. Load-deflection results from the static load tree tests involving

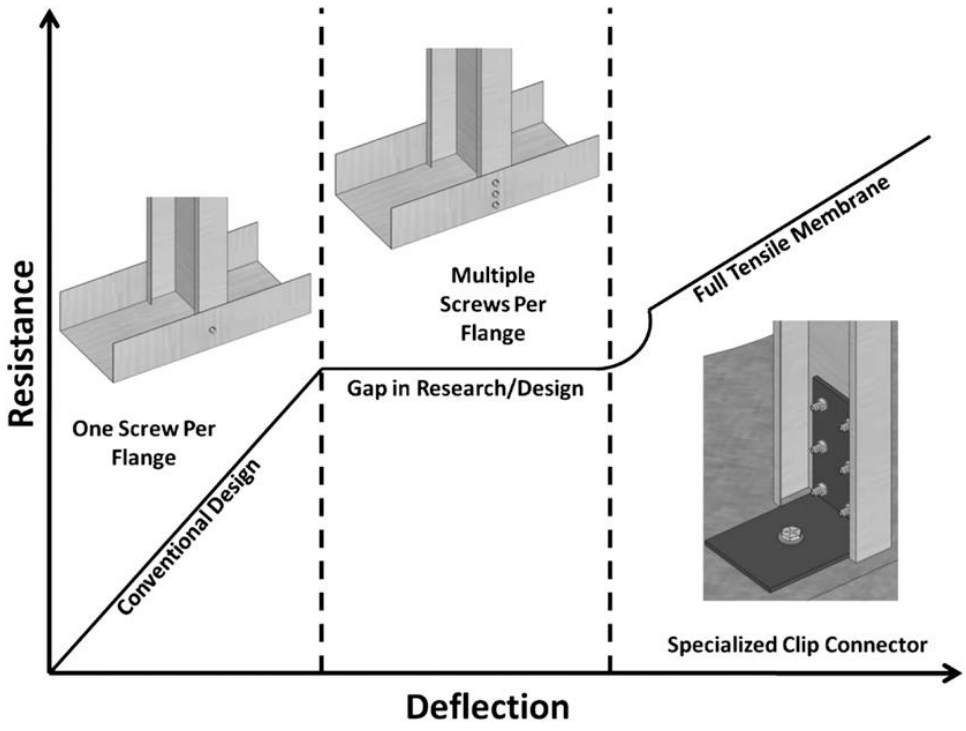

Figure 2.19 Typical Steel Stud Resistance Function Resulting from Different Stud-to-Track Connections (Bewick et al., 2013)

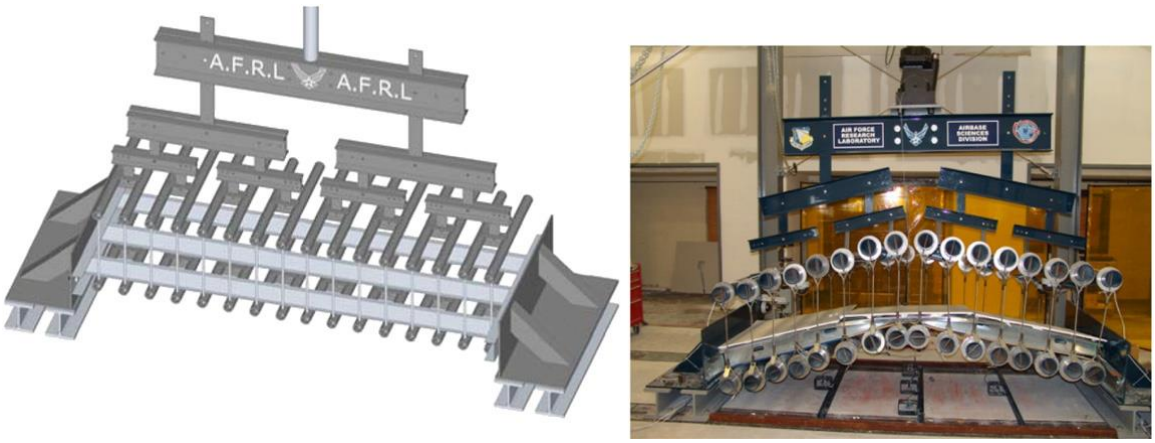

(a) (b)

Figure 2.20 Static Load Tree Test Configuration: (a) Undeformed Starting Position, (b) Deformed Position (Bewick et al., 2011)

unsheathed and sheathed steel studs are shown in Figure 2.21. The results of the sheathing tests also suggested composite action of a stud and sheathing material has little influence on the overall resistance. If the studs had acted compositely with the sheathing, a variation in the elastic stiffness would have been observed for different types of sheathing, and this was not the case. Therefore, the added resistance from sheathing is attributed to providing lateral bracing (Bewick et al, 2013).

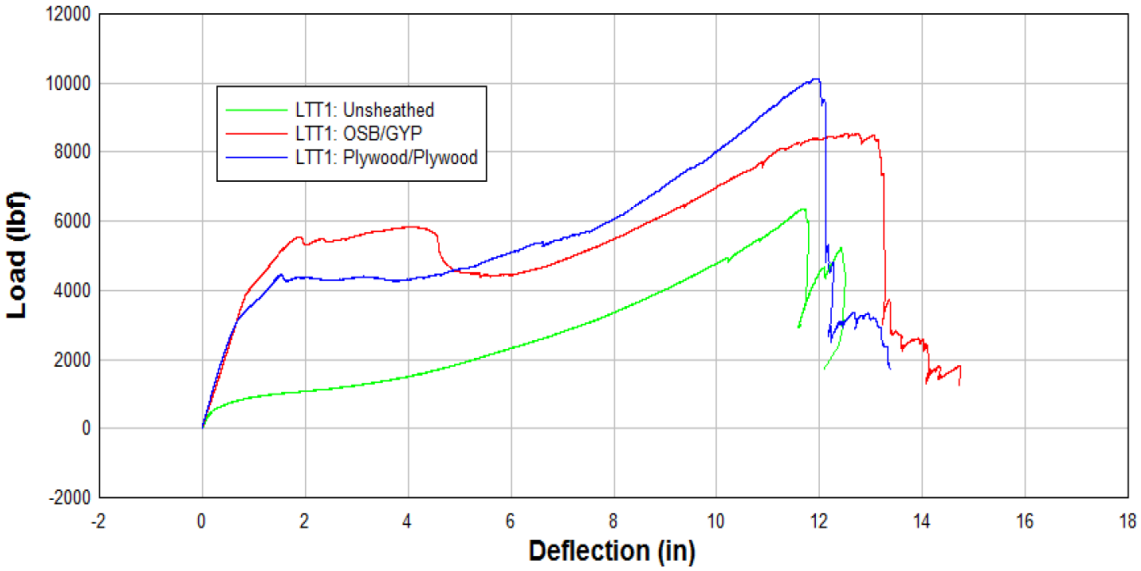

Figure 2.21 Effect of Sheathing on Resistance of Steel-Stud Walls (Bewick et al., 2011)

Static resistance functions have been shown to produce accurate results in blast analysis (Salim et al., 2005a). Even though static resistance functions may not capture all dynamic failure modes, their use has been validated, and the current state of the practice is to use static resistance curves for computing the dynamic response of steel-stud walls. The current research suggests three main methods to determine realistic static resistance functions to capture the entire range of response for steel-stud walls.

First, analytical methods can be used to determine the resistance function. If tensile membrane action is ignored, the method described in Section 2.3.1.1 for determining an equivalent SDOF resistance function can be used. Salim et al., also provides an analytical method to compute the resistance due to full tensile membrane action (2005a). The results of this analytical method can be seen with the High End and Low End predictions shown previously in Figure 2.18. The analytical method is limited when full tensile membrane action cannot be achieved, and it does not consider multiple failure modes.

The second resistance function method, demonstrated by Bewick et al. (2013), is the static load tree test. The static load tree test can develop an experimentally derived resistance function for a steel-stud wall. A benefit of the load tree test is the ability to capture the interaction of different failure modes. Example resistance functions from a static load tree test can be seen in Figure 2.21. This method is limited by the availability of experimental test results.

The final method of resistance function development is numerical modeling. Numerical modeling has the potential to capture inelastic behavior, geometric nonlinearities, and failure mode interaction. Bondok and Salim (2014) demonstrated the ability to develop a resistance function using nonlinear finite element analysis. Figure 2.22 shows the results of a finite element analysis of a two-stud section of a wall. The resulting resistance function is compared to experimental data. Numerical modeling can produce accurate static resistance functions, but it also requires experience and time to develop.

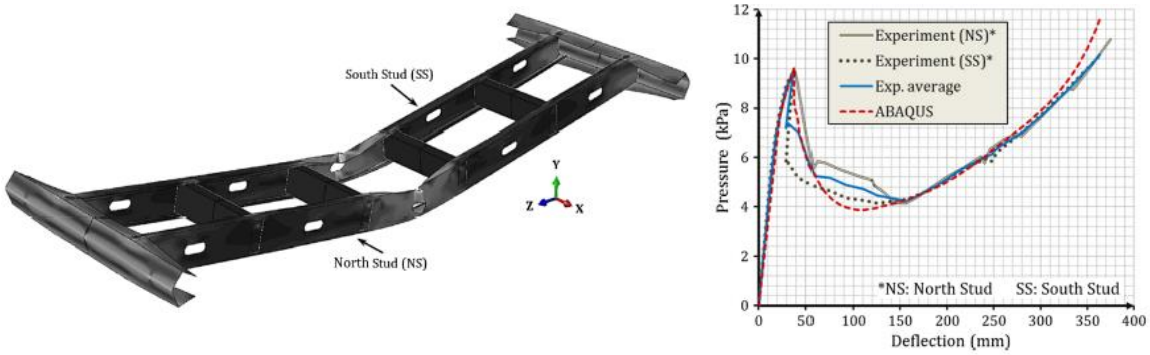

(a) (b)

Figure 2.22 Finite Element Analysis of Steel-Stud Wall Section: (a) Finite Element Analysis Deflected Shape, (b) Resistance Function Results (Bondok and Salim, 2014)

The resistance function developed for a steel-stud wall using any of the three methods presented can readily be applied to an equivalent SDOF system. The recent research conducted concerning the blast resistance of steel-stud walls has provided a greater understanding of behavior and failure modes, and has produced comprehensive resistance functions which accurately capture the structural response of steel-stud walls subjected to blast loads.

2.4 ENGINEERING-LEVEL MODELS TO PREDICT BLAST LOAD PROPAGATION DUE TO INTERNAL DETONATIONS

Before attempting to develop a mechanics-based engineering-level model to predict blast load propagation through failing interior steel-stud walls, a thorough understanding of existing models with this capability is needed. This section provides an overview of two existing models.

2.4.1 BlastX

The computer program BlastX (USACE, 2011), described in Section 2.2.3.2 as a blast load prediction tool, also has the ability to predict blast load propagation through failing surfaces. BlastX has the capability to model an internal detonation in a multi-room

structure with existing openings between rooms. The default wall in any room is a rigid, non-responding wall. As described in Section 2.2.3.2, the BlastX code predicts shock waves reflecting off all interior surfaces and propagating through existing openings. It also predicts gas pressure and venting through the openings between rooms.

Additionally, BlastX has the ability to model a failing wall as an opening. Using this method, the user can define an interior wall as an opening with specific failure criteria. The opening is initially considered "closed", and the wall is treated as a rigid reflecting surface until the failure criteria are met. At this time, the opening is instantly "opened", and the defined wall area now becomes an opening. Authorized personnel can obtain additional information about the failure criteria in the BlastX User's Manual (Britt et al., 2001). In general, this BlastX model for blast load propagation has some limitations in addressing the structural response of walls and their associated openings.

2.4.2 Weidlinger Associates, Inc. Model Using a Series of SDOF Systems

Weidlinger Associates, Inc. (WAI) developed a fast-running engineering-level model to predict blast load propagation for interior detonations using a series of SDOF systems to represent the interior walls (Vaughan et al., 2013). This model is referred to henceforth as the "WAI model". The WAI model is used as the baseline for the model developed in the research study outlined in this dissertation; thus, a general overview is presented in this section. Some details of the WAI model are omitted as the research was performed for a U.S. Department of Defense agency, and portions of the research are considered limited distribution.

The WAI research began with a series of shock tube tests to observe the behavior of interior steel-stud walls and the environment of an adjacent room subjected to a shock wave load (Vaughan et al., 2013). Observations from these tests led to the initial

development of the WAI model that couples air flow and wall response (Vaughan et al., 2013). Volume elements are used to represent the air in each room as an ideal gas. Each responding wall is modeled as a nonlinear SDOF system. Opening conditions in each wall are also established to allow air flow between rooms to model gas pressure venting (Vaughan et al., 2013). The individual volume elements, the SDOF non-linear springs and masses, and the openings can be seen in the one-dimensional diagram of the WAI model shown in Figure 2.23.

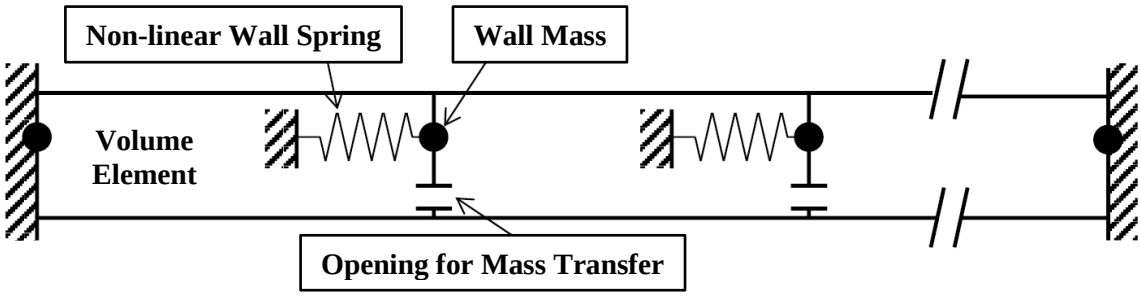

Figure 2.23 WAI Model Diagram (adapted from Vaughan et al., 2013)

For a given internal detonation scenario, the WAI model predicts the pressure and impulse histories in each room and estimates the amount of damage and deflection for each responding wall (Vaughan et al., 2013). The model uses the program NLFlex (WAI, 2011) for the numerical calculation of the air volume equation of state, SDOF response, and air mass flow. NLFlex is a finite-element modeling software of structural response to blast and impact load (WAI, 2011). Although FEM software is used for their model, it is possible to perform the numerical computations using simpler methods.

The resistance function for a wall spring in the SDOF system uses an elastic-plastic model and is used to determine wall displacements and when a wall fails. The

values defining the resistance function are empirically derived from shock tube tests performed by WAI and other internal detonation experimental tests performed by DTRA (Vaughan et al., 2013).

The gas pressure venting between rooms is captured by determining the air mass flow through openings between rooms. A wall break-up model controls the break-up and debris formation of the failing walls until a wall reaches complete destruction. Similarly to the resistance function, all parameters defining the wall break-up model are empirically derived using test data.

The detonation room loading in the WAI model is computed in one of two ways. First, a back wall in the detonation room acts as a plunger wall and displaces to produce a pressure wave. This wall displacement is calibrated to achieve a similar pressure history observed in experimental tests. Second, an initial air energy is defined in the detonation room to match the peak pressure and impulse from the detonation room of an existing experimental test (Vaughan et al., 2013). Both loading methods in the WAI model involve matching existing detonation room pressure histories. The model does not possess an ability to produce a predictive blast load that differs from known experimental data.

Although initially developed based on one-dimensional shock tube tests of steel-stud walls, the model was applied to CMU walls and two-dimensional applications. Resistance functions and wall break-up model parameters for each wall type were empirically developed based on shock tube tests and DTRA tests (Vaughan et al., 2013). For each different test setup analyzed, these empirical parameters were adjusted to match one of the experimental results from the test setup. The loading was also calibrated for each test setup to match the known detonation room pressure history.

The WAI model demonstrates an engineering-level model to predict blast load propagation using a series of SDOF systems can produce accurate results for an internal detonation. This model, however, is limited in its predictive capabilities when a scenario does not closely match already available experimental data. Even though the model is empirically based and limited, the assumptions and principles can provide the framework for a mechanics-based engineering-level model.

2.5 SUMMARY

Before explaining the model developed in the research study outlined in this dissertation, a basic overview of relevant topics was provided in this chapter. First, an overview of explosions and blast wave phenomena was presented. This information was then expanded to explain the characteristics of an internal detonation and the resulting higher-order reflected shock waves, gas pressure, and venting that occur in such cases. Because the model developed for the research study is strictly for internal detonations, a thorough understanding of the internal blast environment is needed before quantifying blast load propagation. Next, methods to predict internal blast loads were presented and summarized. An important goal of the research study described herein is to predict blast load propagation, so the ability to predict internal blast loads is an important component of this research study.

After blast loads are quantified, the structural response of walls subjected to blast loads must be analyzed. Two dynamic structural analysis methods were presented. The approximate equivalent SDOF system method has been commonly used and produces accurate results given the inherent uncertainties of the internal blast scenario. FEM analyses can produce the most accurate results, but such analyses require an experienced user and a significant amount of time.

After the analysis methods were presented, the specific behavior of steel-stud walls was described. Recent research regarding the blast resistance of steel-stud walls has provided a good understanding of steel-stud wall response to blast loads, which is another important component of the research study outlined in this dissertation. Finally, this chapter presented the current state-of-the-practice engineering-level models to predict blast load propagation through steel-stud walls subjected to an internal detonation, and the WAI model forms the foundation of the model developed in the research study outlined in this dissertation.

Chapter 3

Development of Steel-Stud Wall Damage and Blast Load Propagation Model

Considering existing terrorist threats and increasing military operations in urban terrain (MOUT) there is a need for improved modeling and simulation of high explosive detonations inside buildings constructed using typical construction practices. Predicting damage and blast load propagation through failing walls is important from both a protective design and a munitions employment point of view. Chapter 2 provided a brief overview of internal detonations and the current state of the practice for modeling and predicting an internal blast scenario involving steel-stud walls. This chapter explains the mechanics-based model for predicting blast load propagation developed for the research study outlined in this dissertation.

3.1 Problem Description

The goal of this research is to create an engineering-level model to predict blast loads propagating through failed surfaces. Such a model can be beneficial for two reasons. First, from a protective design perspective, the model can predict damage and lethality in an existing building from a given internal threat. If a given threat is known, damage levels can be predicted and adjusted by improving the construction details. Second, from a munitions employment perspective, the model assists in the ability to predict damage and lethality throughout a target building. If typical construction details of a target building are known, damage levels can be predicted and adjusted by changing the munition.

Internal detonations in an urban construction scenario can be extremely complex. First, the loading from an internal detonation can be much more difficult to predict than

an external detonation. An internal detonation creates shock waves that reflect off multiple surfaces, including the walls, the floor, and the ceiling. The initial incident shock wave and the multiple reflected shock waves interact with each other and become difficult to quantify as shock wave velocities, temperatures, and air densities all change. Just as standoff distance and height of burst are critical variables in determining loads resulting from an external detonation, the location of the explosive within an enclosed room is also crucial in determining loading for an internal detonation. The distance from the explosive to each reflecting surface must be known to determine when and how the reflected shock waves interact with each other. Distribution of blast loads is highly non-uniform because of the multiple reflections and time phasing (DoD, 2008). Complex room geometries such as hallways, L-shaped rooms, doorways, and existing openings contribute even more complexities to the behavior of the shock waves by adding rarefaction waves and shock wave vortices. Figure 3.1 shows a simulation of the behavior of a blast wave as it encounters a convex corner of a structure. In addition to the reflected wave off the surface of the structure, a clearing effect causes a rarefaction wave to form

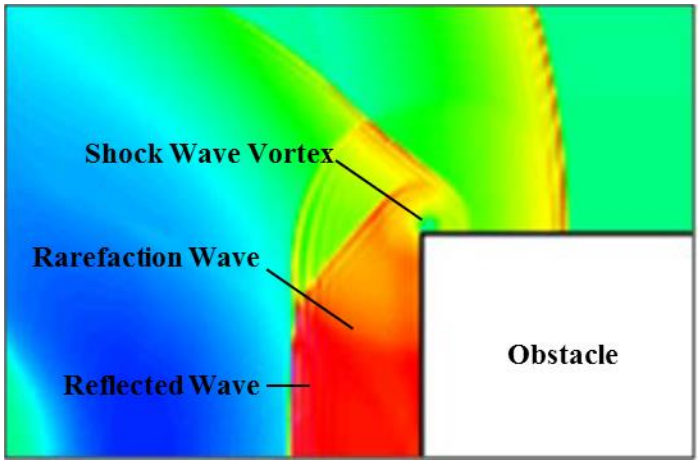

Figure 3.1 Rarefaction Wave and Vortex Formation (adapted from Britt et al., 2010)

at the free edge of the surface, and a highly turbulent vortex region results at the corner of the structure.

An additional challenge in quantifying internal detonations versus external detonations is the accumulation of gas pressure and the resulting venting effect. A detonation within an enclosed space generates gaseous products that remain trapped within the space unless the room is fully vented. These trapped gasses and increased temperatures from the chemical reaction result in additional overpressure (DoD, 2008; ASCE 2011). In general, the overpressures are less than the shock wave overpressures, but the duration can be significantly longer (ASCE, 2011). These gas pressures also vent through existing openings or through openings created from failing components. The magnitude of the gas pressure and the duration are directly related to the size of the vent opening (DoD, 2008). Gas pressures are considered uniform if contained within a small or square room. However, in a long room, the magnitude and duration of the gas pressure vary along the length of the room (DoD 2008). Figure 3.2 shows an example of the pressure history of a detonation in a partially vented room. The high and low peaks are due to the multiple shock wave reflections, as explained in Section 2.2.1. The gas pressure, P_g, is a function of the charge weight and the contained room volume (DoD, 2008). The duration of the gas pressure is a function of the vent area. Whenever venting is present, the overpressure eventually reaches zero as the gas pressure is all vented to the outside atmosphere.

The aforementioned complexities of an internal detonation can be accounted for and blast loads estimated using current state-of-the-practice methods described in Chapter 2. The UFC 3-340-02 (DoD, 2008) has equations and charts from empirical data to estimate internal blast loads, and the computer program BlastX (USACE, 2011) provides

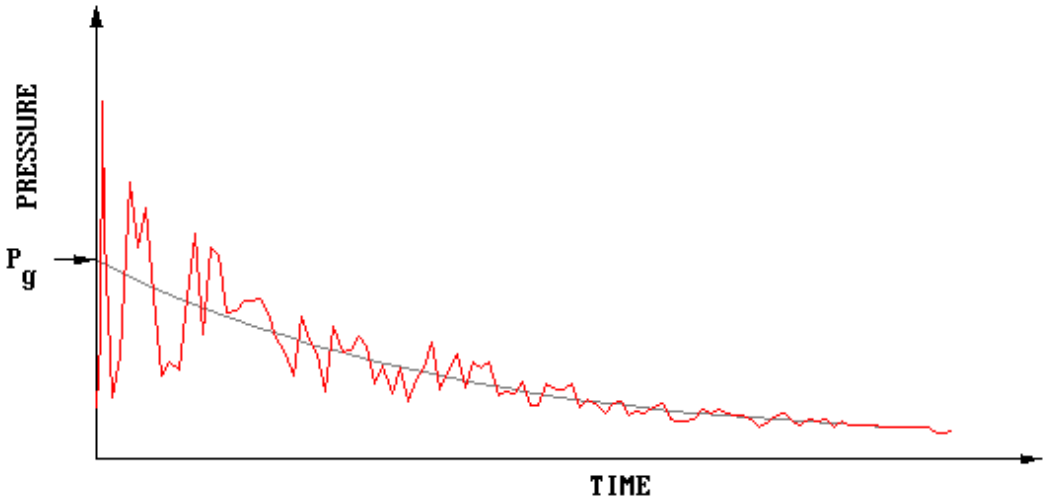

Figure 3.2 Pressure History of Internal Detonation with Partial Venting (DoD, 2008)

numerical simulations of an internal blast environment using ray tracing methods, as described in Section 2.2.3.2, to determine internal blast loads. These methods only work well, however, when the detonation room has non-responding surfaces. Urban construction scenarios often contain surfaces that respond significantly when subjected to a blast load. Some typical interior wall construction materials include steel-stud walls with gypsum board, wood-stud walls with gypsum board or plywood, and unreinforced concrete masonry unit (CMU) walls. Some interior walls may be load-bearing walls, while many other interior walls are non-load-bearing partition walls. These interior walls have limited lateral force resistance as even the load-bearing interior walls are designed to support mainly gravity loads. However, there is some lateral force resistance to the overpressures of an internal blast. The walls, floor, and ceiling all have a mass and a structural resistance. The UFC 3-340-02 states, "the combined effects of the inertial force and the resistance can be accounted for by performing a dynamic analysis and determining the time to reach failure" (DoD, 2008). A dynamic analysis to predict the structural response of the walls is required, but this can also pose many difficulties.

Section 2.3.1.1 presents the equivalent SDOF method of dynamic analysis. Although this method is the most commonly used simplified analysis method and can provide accurate results, it has its difficulties and limitations. It is difficult to capture the nonlinear dynamic behavior of a wall and the interaction of multiple failure modes in a single resistance function. Due to the limited research involving the dynamic response of typical interior walls, this research study focuses on one specific type, steel-stud walls. Section 2.3.2.4 describes the existing research and methods to develop resistance functions for steel-stud walls.

As interior walls dynamically respond to blast overpressures, they displace, which changes the volume of the room. Because of the low lateral force resistance, many of these interior walls will fail when subjected to an internal blast load. When a wall fails, it no longer has any structural resistance, though it still has inertial resistance as a moving mass. As a wall fails, it may also create openings that will vent gas overpressure. These vent openings due to wall failure did not exist initially, and the opening area typically will not remain constant as the wall continues to fail or break up. The varying size of the vent opening creates difficulty in predicting the gas pressure venting.

The loading on interior walls can also be highly non-uniform. A detonation that occurs near a wall can potentially cause a different structural response and failure mode than a detonation located in the center of a room or far from a wall of interest. A close-in charge can produce intense pressures on the nearest wall, resulting in a localized failure or a breach. A charge located in the center of a room or on the far side of the room from an interior wall of interest may produce a more uniform load and produce a global response and failure of that wall. These different failure modes can alter the evolution of how openings develop and change size in a failing wall, and they can also change the timing of the vent openings.

So far, the discussed complexities of the internal detonation problem have all dealt with the detonation room. One must account for multiple reflections, rarefaction waves, vortices, gas pressure and venting, failing surfaces with some lateral resistance, and time-varying vent openings. A major goal of this research, however, is to predict the loads propagating into adjacent rooms.

To predict the load propagating into adjacent rooms, the shock wave overpressure and gas overpressure that travel into an adjacent room during and after a wall failure must be determined. The propagating shock wave through an opening is referred to as "leakage pressure" in the UFC 3-340-02 (DoD, 2008). As the shock wave travels through the opening, "shock pressures spill around the edges of the structure and form highly turbulent vortices" (DoD, 2008). These complex shock waves travel through openings at the same time gas pressures are vented through openings. The UFC 3-340-02 only discusses this leakage pressure propagation and gas pressure venting from a room into the open atmosphere. It does not discuss these pressures traveling and venting into another enclosed volume. These propagating and venting pressures become the loading on the surfaces of an adjacent room.

If an opening exists prior to detonation, the shock waves could travel through the opening, and gas pressures would vent through the opening. If no openings exist before detonation and the opening is created by a wall failing, the magnitude of shock pressure and gas pressure propagating into an adjacent room must be determined. Some combination of the initial shock wave, reflected shock waves, and gas pressure will cause a wall to fail. The strength and ductility of a wall will determine when it fails and how it fails. The shock wave propagation would be a determination of how much shock is reflected off the wall before failure and how much shock travels through the openings created by the wall failure. This determination is highly dependent on time, such as when

the wall fails and how long it takes the wall to fail, the size of the opening as the wall is failing, and the direction and speed the shock waves are traveling.

The gas pressure venting through a failed wall into an adjacent room must also be captured. The difficulty of determining the gas pressure venting through a varying opening was discussed when determining the detonation room pressure. The same difficulties occur when determining the loading in an adjacent room. The higher gas pressure in the detonation room will vent into an adjacent room. An adjacent room has a finite volume, but as the walls of the room respond to loads and begin to displace, the volume changes. Thus, this venting through the time-varying opening will pressurize an adjacent room with a time-varying volume. This time variance can cause the gas pressure loading computation to be particularly difficult. How the volume of an adjacent room changes also depends on how the wall fails or breaks up. If a wall fails as a rigid body, it can travel into an adjacent room and significantly decrease the volume of the room. If the wall breaks apart into small pieces, wall fragments can also potentially compress the air, but quantifying a volume would be difficult.

It addition to the propagating shock wave, gas pressure venting, and changing volume of an adjacent room, a debris load is highly likely. Debris from the failing wall can be accelerated into an adjacent room. This debris can impact surfaces in an adjacent room causing an additional load besides overpressure. This additional load must also be included when determining the total load acting on a wall in an adjacent room.

Clearly, the task of accurately capturing all components of an internal blast scenario and predicting blast load propagation is complex. The current state of the practice does not include an engineering-level model that includes this capability. In the next section, several different modeling approaches are briefly examined before thoroughly explaining the model developed for this research.

3.2 MODELING APPROACHES

The problem of interest is truly multi-disciplinary. As stated by Ohrt and Ehlers,

> Airblast propagation through failing structural surfaces inherently involves the 'coupled' behavior of airblast loading and structural response. Engineering-level predictive tools usually treat the problem as "un-coupled", often limiting the treatment to allowing quasi-static gas pressure to propagate through an imposed opening in the failed surface. Even numerical simulations are highly challenged by the coupled fluid and structural dynamics, and the requirement to predict failures/fractures in structural panels. Thus, the scientific and engineering understanding of airblast propagation through failing structural surfaces is seen as immature, and in need of investigation (2010).

To accurately predict the load propagating through a building, one must understand both the loading from an internal detonation and the associated dynamic structural response. The loading is typically studied and thoroughly understood by engineers having a strong fluid mechanics background, whereas the structural response is studied and understood by a structural engineer. This research requires a unique understanding of both the load side and the response side.

In some attempts at creating a simplified engineering-level model, one side of the problem is either ignored or significantly simplified. On the other extreme, detailed finite element analyses including fluid-structure interaction can be modeled and analyzed. This modeling may produce accurate results, but are extremely difficult and time-consuming. This detailed approach was not taken for the current study because the goal of the research was to develop a fast-running model that can be run on a typical personal computer. Given the uncertainties associated with internal detonation scenarios, including explosive magnitude and placement, an engineering-level model is seen as being highly valuable because it can provide acceptably accurate solutions within a fraction of the time needed to conduct more rigorous finite element analyses. Several engineering-level modeling approaches are described in the next sections.

3.2.1 UFC 3-340-02

In the UFC 3-340-02 (DoD, 2008), the current state of the practice for determining the loading of an adjacent room due to blast load propagation is an attempt to determine the "leakage pressure." Again, the "leakage pressure" quantifies the shock pressure that travels out of the detonation room and into an adjacent room. The data and charts used to calculate this loading are based on studies of fully vented three-wall rooms and partially vented four-wall rooms with a vent opening in the roof. All of the vent areas studied were existing openings; no frangible panels were tested for the vents. All walls of the rooms were non-responding walls, even the wall with an existing vent opening. The studies did not examine a frangible panel which has a resistance that is considered by the UFC 3-340-02 to be negligible, which is any panel with a resistance less than 25 psf. The presence of a frangible panel covering an opening is assumed to increase the gas pressure in the detonation room and reduce the leakage pressure entering the adjacent room when compared to the same scenario with no panel covering the opening. These effects, however, are ignored, and the leakage pressure determined is over-estimated (DoD, 2008). When determining the shock pressure inside the detonation room, there is mention that the frangible panels do have mass and an inertial resistance. For panels with a resistance above 25 psf, a dynamic analysis can be performed to account for the inertial force and structural resistance of the panel. This dynamic analysis, however, is not included in the data or the procedures outlined for determining the leakage pressures. In fact, for a partially-vented four-wall room with a vent opening through a wall, as shown in Figure 3.3, the UFC 3-340-02 states, "Leakage pressures resulting from an explosion in a partially-vented four-wall cubicle where the vent opening is located in a wall have not been documented" (DoD, 2008). The data for this

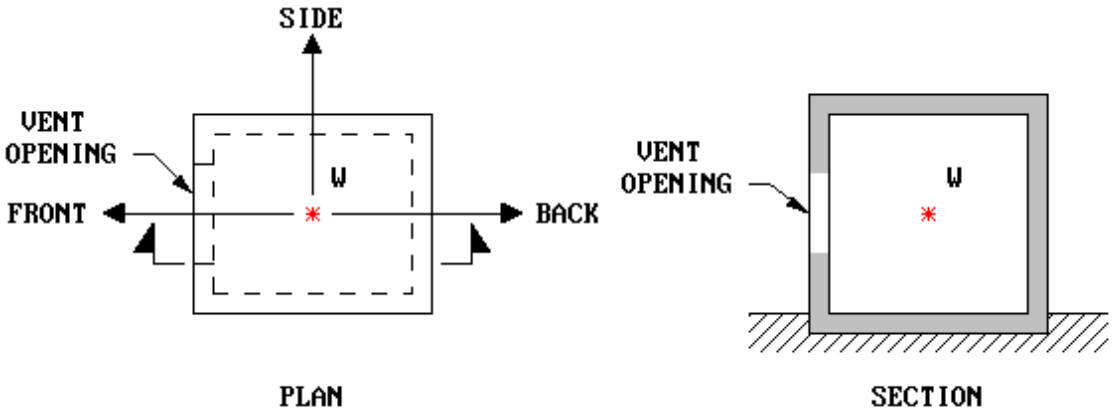

Figure 3.3 Four-Wall Room with Venting in Wall (DoD, 2008)

scenario are interpolated from a three-wall fully-vented room and a four-wall room vented through the roof. As seen in Figure 3.3, this scenario of a four-wall room with venting through a wall accurately depicts a detonation room within an internal blast problem. In addition to the limited method to determine the propagating shock wave or "leakage pressure," the UFC 3-340-02 does not address calculating gas pressure venting into another enclosed volume like an adjacent room. The only data provided is for venting to the outside atmosphere. When the gas pressure vents into an adjacent room, the pressure of the adjacent room will increase because of its finite volume, and the rate of the gas pressure venting will be affected. Ultimately, the UFC 3-340-02 does not include a method to properly estimate the blast load propagation into an adjacent room.

3.2.2 Models Neglecting the Presence of Interior Walls

One simplified method to predict the internal blast load in an urban construction environment is to ignore the presence of internal walls. Many internal walls are non-load-bearing walls with limited lateral capacity to resist internal blasts. This is especially true when considering steel stud or wood-stud walls. Because these types of walls will fail at

relatively small loads, and their mass is small compared to CMU walls, one simplified approach for computing internal blast loads ignores the presence of the internal stud walls and treats the building as one enclosed volume. The blast loads for the entire internal volume can be calculated using empirical charts and tables such as in UFC 3-340-02 (DoD, 2008), or by using software to calculate internal blast loads such as BlastX. These calculated loads would provide a rough estimate of the loading expected in the interior rooms of a building. Given a particular load threshold, such as a peak pressure or peak impulse for lethality or wall failure, this method could also calculate a volume required to produce a loading below the threshold. Then, knowing the building dimensions, a required safe distance can be calculated where loading would be below the threshold, and rooms outside of that safe distance would be considered safe.

This method would only be intended to provide a rough estimate of damage or lethality. It could be useful based on the complexity and uncertainty of the problem. The combination of unknown variables and properties with the complexity of correctly capturing all fluid-structure interaction within a single room lends itself to promote an exceedingly simplified model. This model, however, relies on one crucial assumption; the stud walls provide negligible structural resistance. Although the structural resistance of a stud wall is typically much smaller than a CMU wall, and the stud walls fail in all experimental tests examined in the current research, this assumption of negligible resistance is not reasonable because the steel-stud walls actually dissipate a considerable amount of blast energy before failing.

3.2.3 Models Treating Interior Walls as Variable Openings

Another simplified approach to predicting blast load propagation is to ignore the structural response of a wall, and treat failing walls as openings. The BlastX prediction

model uses this method and is described in detail in Section 2.4.1. Blast loads and behavior are predicted with the wall present as a rigid surface until failure criteria are met. Then, the wall is instantly opened, and blast loads are calculated with the created opening present.

A significant problem with this method is that determining when a wall fails requires a structural analysis. The failure criteria may encompass some wall types and failures, but variations in wall construction and geometry are not able to be analyzed. The predicted results include no consideration as to how the structural response of a given wall contributes to the blast load propagation.

Although this method does include the presence of the interior walls, it oversimplifies the problem by neglecting the structural response of those walls. The resistance of steel-stud walls varies significantly depending on the construction details as shown in Section 2.3.2.4. A structural analysis is needed, and most often it requires a displacement-dependent resistance function.

3.2.4 Models using Equivalent SDOF Systems

A current engineering-level, blast propagation model that includes the structural response of steel-stud walls is the WAI model described in Section 2.4.2. This model uses a series of equivalent SDOF systems for the response of interior walls, and it computes the gas pressure venting through openings between rooms. A detailed explanation of the model is provided in Section 2.4.2.

The WAI model shows this modeling method is effective and can produce accurate results without using high-fidelity FEM analyses (Vaughan et al., 2013). The WAI model is limited, however, because it is entirely empirically based. The loading, wall resistance, and wall break-up model parameters are all derived from existing blast

and shock tube experimental tests. Scenarios that vary from the existing test setups are unable to be predicted with accuracy using this model.

3.2.5 FEM Analysis

As described in Section 2.3.1.2, the most accurate representation of blast propagation from and internal detonation would be a fully-coupled FEM analysis that models the fluid-structure interaction of the air and interior walls of all rooms within a structure. This modeling approach is not considered an engineering-level model as it requires an extensive amount of time and experience to input, run, and interpret results. It is possible, however, to run a significant number of simulations for various scenarios and generate a set of simulated test data. Then, an empirically-based model like the WAI model can use the simulated test data to determine the empirically-based components of that model. This methodology has the potential to produce an engineering-level model, but it still requires a relatively large amount of time and expertise to run numerous coupled FEM simulations. The resulting model is also still limited by the simulated data. Predicting scenarios that vary significantly from the simulated test setups would not be possible.

3.3 PROPOSED MODEL FOR CURRENT RESEARCH STUDY

The model developed for this research study utilizes engineering mechanics and a few key assumptions to calculate blast load propagation in a typical internal detonation scenario. The engineering-level model is able to run a simulation within minutes on a PC and predict blast loads and wall damage throughout multiple rooms within a building. Ideally, the engineering-level model would be able to consider all aspects and variables of this complex problem. The current state of the practice, however, has not yet advanced to this level. The model developed for this research study considers in depth one specific

part of the internal detonation problem that has not been fully investigated—the steel-stud wall. In previous research, steel-stud walls have been viewed as insignificant because of the relatively small lateral structural resistance provided by a conventionally constructed steel-stud wall. The focus of load propagation in internal detonation scenarios in past research has been mostly on CMU-type walls. The resistance of a steel-stud wall, however, does affect the load propagation and is an important aspect of the internal blast problem. Also, with just slight structural improvements to conventional construction, such as additional screws at the stud-to-track connection, the resistance of a steel-stud wall can be significantly increased (Bewick et al., 2013). With these improvements to the resistance, the model can predict and analyze the added protection steel-stud walls can provide in an internal blast environment.

This research is also valuable because it combines both the structural response of the walls and the opening associated with failing walls. As discussed previously, other simplified models do not consider the combined interaction of both these components. This combination allows for the model to capture the quantity of the load being transferred between rooms and to more accurately capture the timing of when the load is transferred between rooms.

A diagram of the model is shown in Figure 3.4. An overview of the model is provided in the subsequent section, followed by detailed descriptions of all the model's components.

3.3.1 Overview

This model uses the framework of the WAI model as a baseline. A description of the WAI model can be found in Section 2.4.2. Some details of the WAI model in that section were omitted due to the limited distribution of the research. As such, these same

details are omitted from the description of the model developed for the research study outlined in this dissertation. The model developed herein utilizes the main concepts used by WAI that couple air flow and wall response.

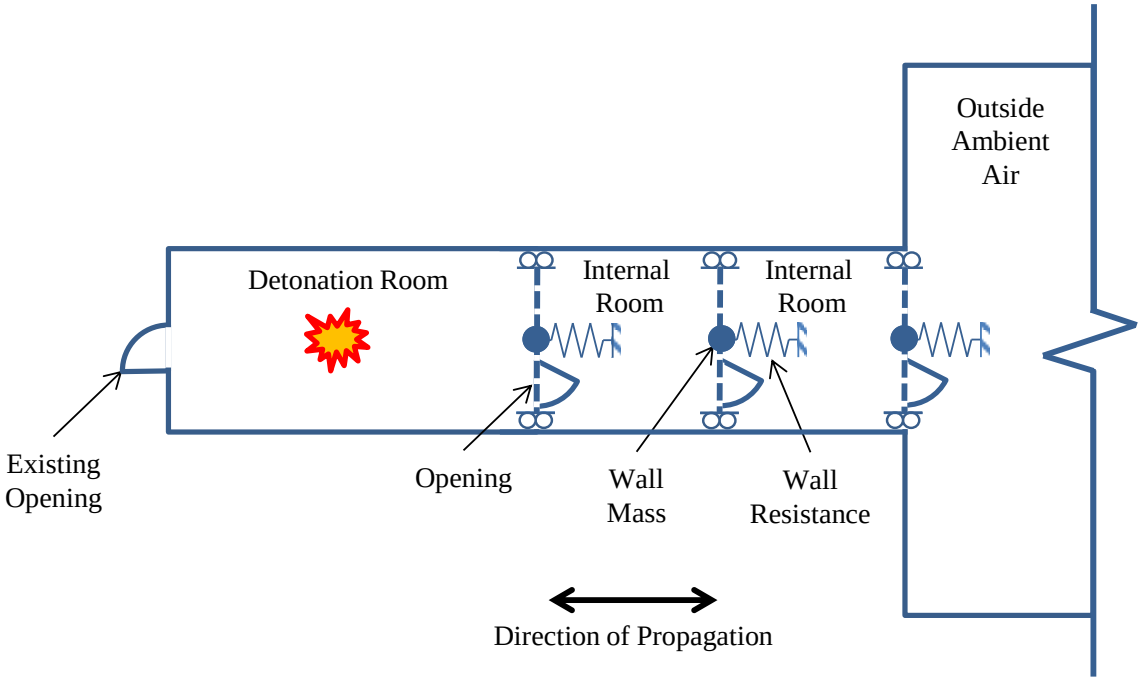

Figure 3.4 Internal Detonation Model

3.3.1.1 Assumptions and Simplifications

Many simplifying assumptions were made in developing the model for this research. Often, the use of simplified methods is justified because typical blast scenarios have considerable uncertainty. Rigorous analyses using detailed finite element modeling, multiple degrees of freedom, or multiple iterations may often times be unnecessary and take up valuable time and resources. In a typical internal blast scenario, many unknown variables exist. In a protective design scenario, often the charge weight, charge type, and location in the detonation room are unknown. The wall construction details are known, but the structural interaction with such an unknown load is difficult to predict. A rigorous

structural analysis and wall break-up model is not justified because of the uncertainty of the loading. In an offensive weapon scenario, the charge type and weight are known, but the charge location would have some variability, and the wall construction details are likely unknown. A rigorous analysis of the loading and its structural interaction with the walls is not justified because of the uncertainty of the wall structural resistance and wall break-up. Some of the key assumptions and simplifications used in the analysis model for this research study are provided in Table 3.1. Additional assumptions and simplifications were used, but not included because of the limited distribution content.

Table 3.1 Key Assumptions and Simplifications of Model for Current Research Study

Assumption / Simplification	**Benefits / Justifications**	**Limitations**
No debris or fragment load: Additional impulse due to debris and fragments impacting walls is ignored.	- In observed tests used for this research, a steel-stud wall would fail from propagating overpressure before debris and fragments from previous failed walls impacted it.	- Steel-stud walls built stronger than standard construction may provide resistance to overpressure long enough to receive a significant impact load from debris and fragments.
Non-responding floor and ceiling: The floor and ceiling are considered rigid.	- Reasonable assumption for tests included in current research study. - Ability to isolate response of steel-stud walls.	- Acoustic ceilings, roofs, and floors of multi-story buildings are not rigid. Structural analysis of floors and ceilings is needed, and multi-directional propagation would occur.
One-dimensional: Current model is one-dimensional. Side walls in each room are rigid and non-responding	- Reasonable assumption for tests included in current research study. - Ability to isolate response of steel-stud walls along a single direction of propagation.	- Realistic building configurations contain rooms with up to four responding walls, and multi-directional propagation is probable.

3.3.1.2 Description

Each internal blast problem is modeled with a series of rectangular rooms. For each problem there must be a detonation room, a number of internal rooms of interest, and an outside ambient air room. Figure 3.4 shows the one-dimensional model of a three-room building subjected to an internal blast.

Each room of the model is separated by internal responding walls in the direction of propagation as shown in Figure 3.4. Each responding wall is modeled as an SDOF system. Each wall is considered a single lumped mass with a nonlinear spring resistance. The walls can displace in the direction of propagation, as depicted with the roller supports along the sides of the walls. The displacement of each wall is governed by the generalized equation of motion shown in Equation (3-1).

$$M\ddot{u} + R(u) = F(t) \tag{3-1}$$

where $M =$ lumped mass of wall

$\ddot{u} =$ wall acceleration

$R(u) =$ nonlinear resistance function

$F(t) =$ loading

The structural resistance is described in more detail in Section 3.3.3.3. The floor (not shown in Figure 3.4), ceiling (not shown in Figure 3.4), and side walls are rigid, non-responding walls.

The outside ambient air room should be an extremely large room compared to the size of the rooms in the building. The dimensions of a typical outside ambient air room should be approximately 100 times larger than the largest internal room dimensions. This will provide an outside air volume 10^6 times larger than the largest internal room, which

will allow the model to simulate an outside air environment of essentially unchanging ambient pressure for the last internal room to vent into. This method of modeling a large outside air room is similar to how BlastX simulates outside ambient air (Britt 2001).

The loading on the responding wall in the detonation room is calculated for a given detonation scenario. The detonation room geometry, charge weight and location, and target wall location are all input into a BlastX simulation to produce a pressure-time curve, which is used as the loading, *F(t)*, in Equation (3-1) for the first responding wall. The loading is described further in Section 3.3.2. The model does not attempt to accurately predict the actual pressure history in the detonation room. It only uses the detonation room as an initial loading to predict the blast load propagation throughout the other rooms in the building being analyzed. There are known differences between the detonation room initial loading produced using this model and the actual blast environment in the detonation room. These differences are discussed in detail in Sections 3.3.2 and 4.4.1.

The air in each room is considered to be an ideal gas. Air mass can also flow through the openings between rooms. The model uses a time-stepped calculation to compute the pressure of this ideal gas in each room as well as the wall motion. The analysis of the SDOF wall system is governed by the equation of motion given by Equation (3-1), and the displacement is computed using the central difference method of numerical integration. The nonlinear resistance of the wall is considered in the analysis until the wall structurally fails. After failure, the dynamic motion of the is computed using Equation (3-1) with a structural resistance, *R(u)*, equal to zero. The wall displaces until it reaches a defined maximum displacement. An important point to understand for this overview is the wall continues to interact with the air of the rooms even after structural failure.

In summary, the model uses a simplified method to simulate blast propagation throughout a building due to an internal detonation. It calculates the pressure history in all rooms except the detonation room. A pressure history from the detonation room is generated from a BlastX simulation of the charge exploding in the detonation room. This loading acts on the first responding wall that separates the detonation room from the first room in the direction of propagation. The pressure in each additional room can change at each time step due to the coupled structural response and flow of air mass through openings. Each wall is modeled by two phases that occur in series. The first phase is the structural response, which is modeled as an SDOF system with a nonlinear resistance, and the dynamic response is computed numerically. After the wall structurally fails, the second phase of the wall breaking up is defined by the break-up model. The wall continues to move dynamically with no resistance until it reaches a specified maximum displacement, and the wall no longer interacts with the air. When a wall reaches its maximum displacement, the wall no longer exists, and the pressures of the two rooms equalize.

3.3.1.3 Improvements/Importance

The greatest contribution of this new model is its ability to be used in a predictive sense. The WAI model demonstrates that a simplified engineering-level model can be used to calculate blast propagation associated with an internal detonation. Their model, however, has several components that are empirically derived. To use the model predictively, the scenario must have a similar loading and wall properties as an existing test for which they have sufficient data. The new model developed for this research is able to develop mechanics-based calculations to determine these variables, which allows

the model to be used in a predictive sense. The major areas of improvement are in the loading, the structural resistance, and the wall break-up model.

The initial test wall loading from the WAI model is accomplished by using a plunger wall, which models a shock tube test well, but not necessarily a detonation. Alternatively, the WAI model also uses an initial energy in the detonation room to model the initial test wall loading. Both of these loading methods require the model to be calibrated to achieve a pressure history approximately equivalent to existing test data for a given detonation. The new model introduced for this research uses BlastX to predict the initial wall loading for many different detonation room geometries, charge types, charge weights, and charge locations. This improved loading method is discussed further in Section 3.3.2.

The structural resistance in the WAI model is computed by determining an elastic-plastic nonlinear resistance and modifying it based on test data. The structural resistance model developed for the research study described herein uses structural analysis with actual wall properties to calculate a static resistance curve. The method to develop the resistance curve can be used for any size steel-stud wall with any known connection details. This feature is particularly useful in protective design applications because specific improvements to the structural resistance can be modeled and evaluated. This structural resistance development is discussed further in Section 3.3.3.

Finally, the new model improves the wall break-up model. Again, the WAI model uses an empirical approach to determine the wall break-up model for a given wall size and construction. The new model uses the WAI wall break-up model as a starting point, but the model is adjusted to use physical properties of the wall and applied load quantities to determine the components of the model. The wall break-up model can now be applied

to all steel-stud wall sizes and applied blast loads. The wall break-up model development is further discussed in Section 3.3.4.

3.3.2 Detonation Room Loading

In the detonation room, the loading is calculated using BlastX. In the WAI model, the loading in the detonation room was calculated first using a plunger wall. The wall would be calibrated to move with such velocity to create a pressure history that empirically matched loading from their shock tube tests. The WAI model utilized a second loading approach, which used an initial energy in the detonation room to empirically match the pressure history from known test data (Vaughan et al., 2013). By using BlastX to calculate the loading in the detonation room, the current model can be used in a predictive scenario for any given explosive within the BlastX database. The entire list of explosives can be found in the BlastX software, Version 4.2, User's Manual (Britt 2001).

The detonation room loading is determined by modeling the detonation room in BlastX with all non-responding walls. The geometry of the room should be accurately modeled within BlastX. BlastX can model rectangular rooms, L-shaped rooms, or cylinders. Any existing openings vented to the outside should also be included. When venting the detonation room to the outside, an outside room volume of 1000 units cubed should be used in BlastX (Britt 2001).

The explosive charge type and location can be specified in BlastX. To determine the loading on the wall of interest, a set of targets is placed on the wall, and the pressure-time curve is computed from all the target data. This computed pressure-time curve of the wall of interest is the estimated load on the responding wall in the detonation room. To accurately capture the loading on the entire wall, many targets should be used. It was

determined that placing targets along the entire surface of the wall at a spacing of 0.05 times the wall dimension provides an estimated load of sufficient accuracy. Figure 3.5 shows a typical detonation room modeled in BlastX. All six surfaces (i.e., four walls, ceiling, and floor) of the parallelepiped are non-responding walls. An existing opening (not shown in Figure 3.5) can exist between any wall and an outside room as described above. The red circle in Figure 3.5 represents the charge location. For the scenario shown, the charge is located in the center of the room at a height of 0.25 times the room height. The many blue boxes represent the targets on the wall of interest.

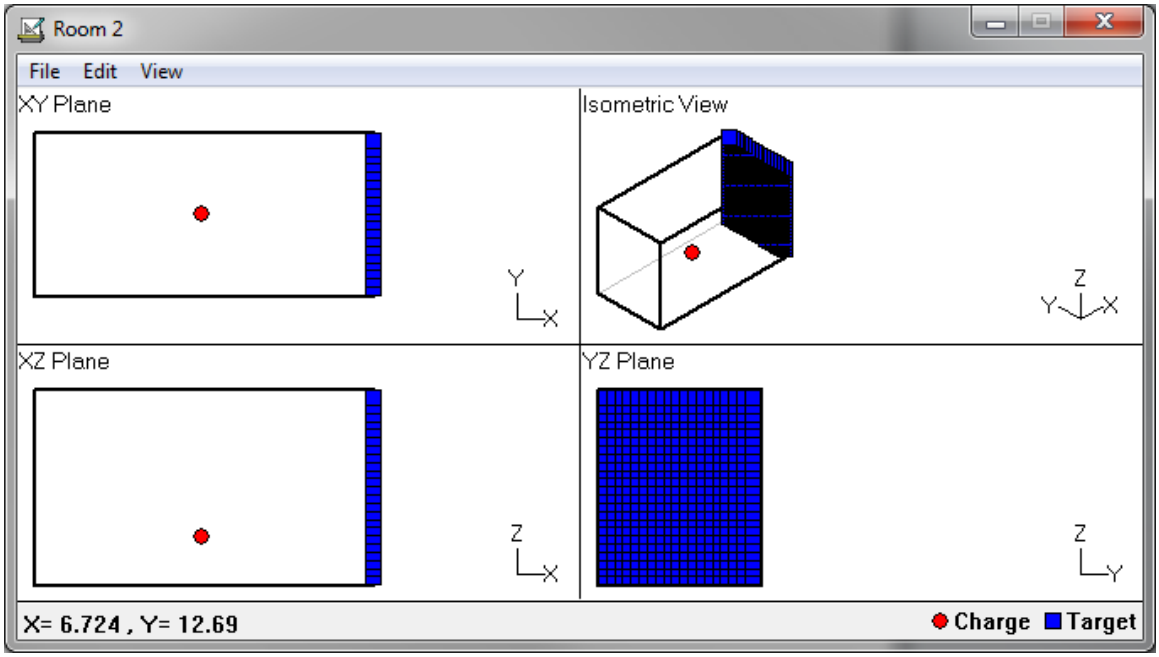

Figure 3.5 Example Detonation Room Modeled in BlastX

To use the data as the detonation room load in the Mathcad sheet developed for this research, the pressure-time curve must be computed as an equal interval plot, with the time interval being the same as the time step specified in the Mathcad sheet. Typically, the time interval of the BlastX loading output files are larger than the time step

used in the model developed for the research study described herein. Equal interval data points should be created using linear interpolation between the BlastX data points.

Using BlastX for the detonation room loading allows for a relatively quick prediction of the loading in most all internal blast environments using existing, readily available software that can be run efficiently on a PC. The ability to compute a complete loading history on the first responding wall provides the model with a non-iterative initial loading to begin the numerical computations.

3.3.3 Structural Response

The structural response in the model developed for the research study described herein uses a series of equivalent SDOF systems for each responding wall. This portion of the model is described in this section, along with the mechanics-based method of developing the resistance function.

3.3.3.1 Equivalent SDOF System

The structural response of each responding wall is performed using an equivalent SDOF analysis. Figure 3.6 shows a diagram of an SDOF system. Equation (3-1) presented in Section 3.3.1.2 is the generalized equation of motion that governs an SDOF system.

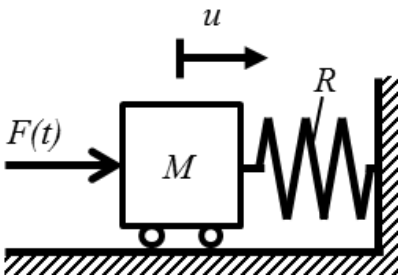

Figure 3.6 SDOF system

For an equivalent SDOF system, the loading and the mass are equivalent values as described in Section 2.3.1.1. Using the load-mass factor described in the same section, the equation of motion for the equivalent system can be expressed using Equation (3-2) with the actual wall mass and loading.

$$\left(K_{LM}M\right)\ddot{u} + R(u) = F(t) \tag{3-2}$$

where K_{LM} = load-mass factor

M = total mass of wall

$\ddot{u}$ = wall acceleration

$R(u)$ = nonlinear resistance function

$F(t)$ = loading

This form of the equation of motion utilizes one single variable, K_{LM}, to describe the equivalent SDOF system. The load-mass factor can be calculated as described in Chapter 2, or tables of load-mass factors for common beam loading situations and end fixities are readily available in documents such as UFC 3-340-02 (DoD, 2008). For steel-stud walls constructed using standard industry practices, the top and bottom connections fail under lateral loads before the studs can fully respond in flexure. Figure 3.7 shows the typical displaced shape of a steel-stud wall with a connection failure. The displacement due to the connection failures is greater than the displacement due to flexure. The overall behavior of the steel stud acts more like a rigid body than a flexural member. When this behavior occurs and the connection failure controls the static lateral resistance of a steel-stud wall, the load-mass factor, K_{LM}, is assumed to be equal to 1.0. In reality, there is a small amount of flexural response as depicted in Figure 3.7, which would result in a load-

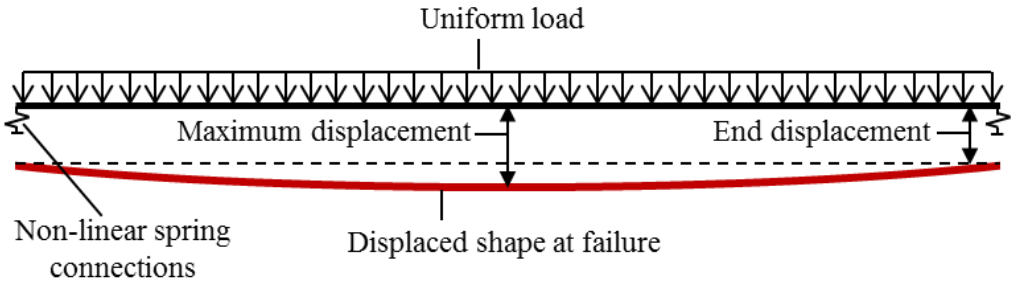

Figure 3.7 Displaced shape of typical steel stud with connection failure

mass factor less than 1.0, but for this simplified model, the flexural response can be ignored for the equivalent SDOF system. The connections control the failure of all the steel-stud walls examined in this research, so a load mass-factor of 1.0 is used. Further examination of the load-mass factor for steel studs wall controlled by flexure is discussed in Section 4.4.3.

There is no damping term in Equation (3-2). As stated in Section 2.3.1.1, damping is typically ignored in blast analysis because it generally has little effect on the maximum displacement of a structural component. Also, energy dissipation due to plastic deformation is much greater than that due to structural damping (DoD, 2008; ASCE, 2010), so for steel-stud walls, structural damping is ignored. The forcing function, *F(t)*, in Equation (3-2) is the total loading on each wall. The other two terms in Equation (3-2) that must be determined are the mass, *M*, and the resistance, *R*.

3.3.3.2 Mass

The mass, *M*, in Equation (3-2) is the total mass of the wall being evaluated. It is important to capture this quantity accurately as it will affect the displacement of the wall during both the structural response phase and the wall break-up phase. If the mass of the walls is not accurately captured, it can affect both the timing and magnitude of the peak pressures in a simulation.

3.3.3.3 Resistance Function: Static Pushover Analysis

A major goal of this research is to develop a mechanics-based model of structural resistance rather than one that is empirically based. Accordingly, the resistance function in the equivalent SDOF system should be determined through structural analysis using actual wall dimensions and material properties. For this research, the SAP2000 (CSI, 2011b) software is used to conduct a static pushover analysis to determine the resistance function.

A static pushover analysis is typically used in earthquake engineering applications. The SAP2000 Reference Manual states "the nonlinear static pushover analysis is a specialized procedure used in performance-based design for seismic loading" (CSI, 2011a). With proper adaptation, however, this method of analysis can be used to create a nonlinear resistance curve for a steel-stud wall subjected to blast loads.

In a static pushover analysis, a load is applied and increased through the elastic and inelastic ranges of response for a structure until the structure reaches an ultimate deflection. The output of this analysis is a force versus deflection curve. In SAP2000, the structure's nonlinearity is represented through nonlinear hinges, nonlinear links, and geometric nonlinearity. When modeled correctly, this analysis will capture the static failure for a given steel-stud wall and will provide the static resistance curve for the wall.

A single stud of the wall should be used to develop the resistance function. The overall resistance of the wall will be the resistance of the single stud multiplied by the total number of studs. The stud should be modeled as a beam with its actual length, and the beam should be equally subdivided into several elements. To determine an appropriate number of elements, the total number of degrees of freedom should be incrementally increased by adding additional beam elements, and each increase in the total number of elements should be analyzed separately. The maximum displacement

results for the increased subdivided beam should be compared against the previous results. When the difference in maximum displacement is less than 0.01 in., the beam is considered sufficiently subdivided. The walls modeled within this research required five elements.

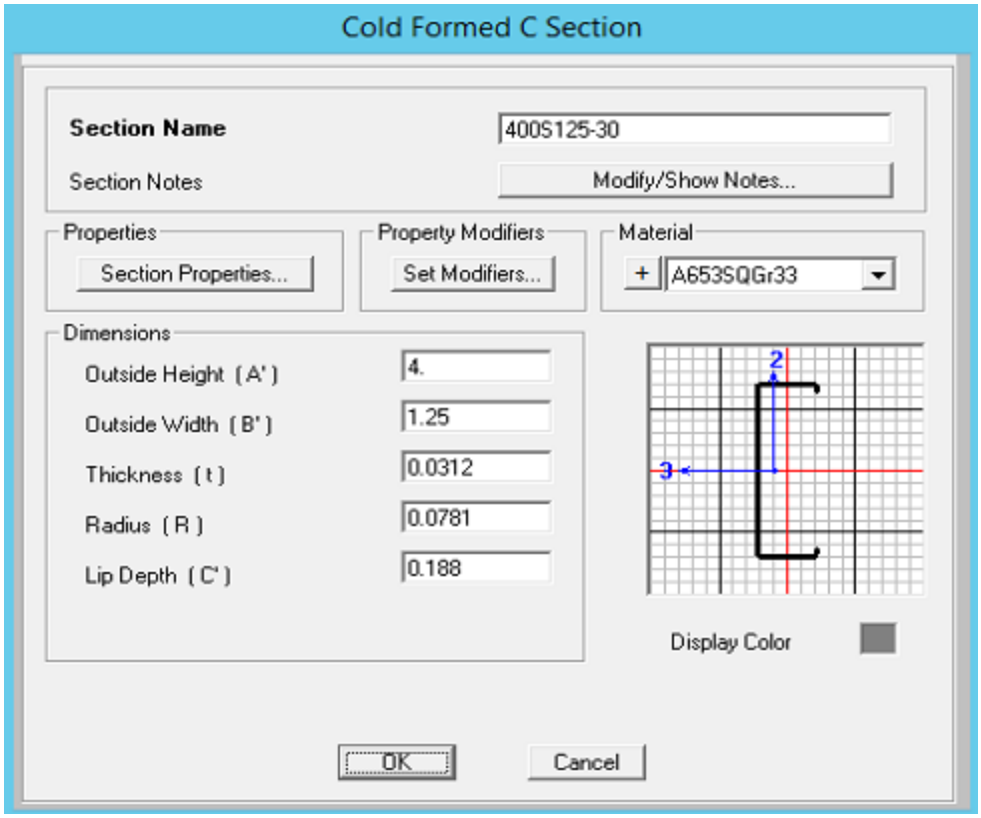

Figure 3.8 SAP2000 v15 Cold Formed Steel Stud Section Properties

The beam section properties should be entered into SAP2000 using the Cold Formed Steel C-Section option. For common steel stud shapes, these section properties are published in the Steel Stud Manufacturers Association (SSMA) Product Technical Guide (SSMA, 2013). Figure 3.8 shows a typical section input in SAP2000. The material properties of the steel stud are also input into SAP2000. The program includes default

ASTM A653 cold-formed steel material properties for both Grade 33 and Grade 50 steel. These material properties should be used with some modifications. Figure 3.9 shows the material property input from SAP2000. For a common steel stud, the default values for the weight, mass, and isotropic properties should be used. However, the yield stress should be increased by the strength increase factor, SIF, and dynamic increase factor, DIF. The UFC 3-340-02 recommends an SIF of 1.21 and a DIF of 1.1 for the yield stress for bending, shear, tension, and compression of cold-formed steel sections (DoD, 2008). Discussion of SIFs and DIFs can be found in Section 2.3.2.3. The constant DIF and SIF values for all structural behavior are convenient because the increase can be included in the overall material properties for all analyses within SAP2000. Equation (3-2) shows the equation for the increased design stress.

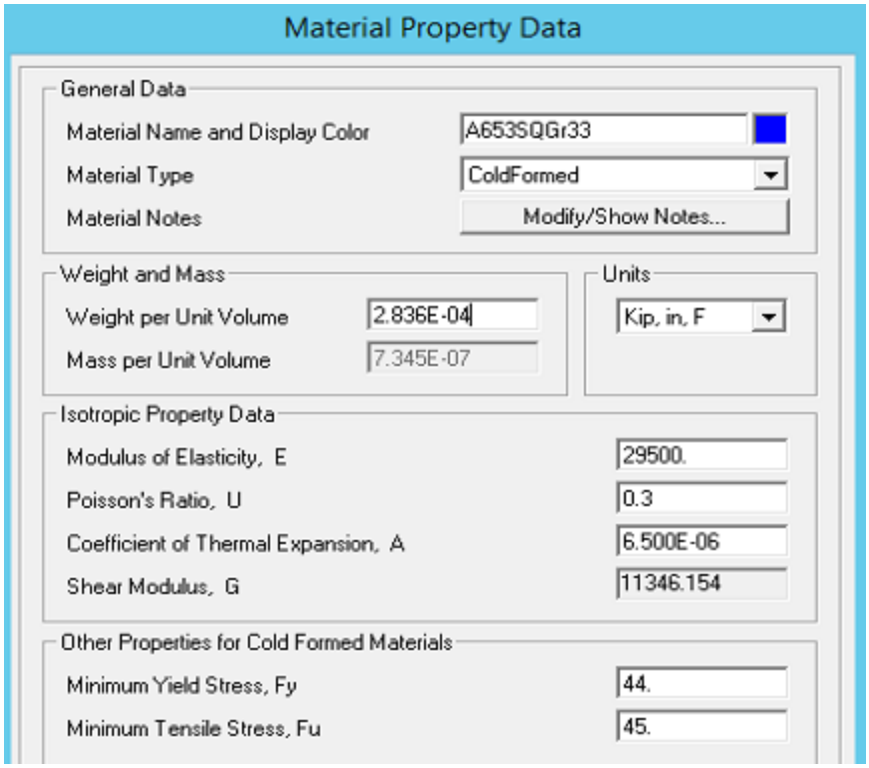

Figure 3.9 SAP2000 v15 Material Property Input

$$f_{dy} = (SIF)(DIF) f_y = (1.21)(1.1) f_y = 1.33 f_y \quad (3\text{-}2)$$

where f_{dy} = the design yield stress

f_y = minimum yield stress

For the ultimate stress, the DIF is 1.0 (ASCE 2010). The SIF is also not included in the design ultimate stress (DoD, 2008) as there is typically a smaller margin of increase in actual ultimate stress of a material compared to the increase observed in the yield stress. Therefore the ultimate stress for the material is not changed. If actual tested material properties for a given steel stud are known, they should be used. Figure 3.9 shows the SAP2000 material property input for ASTM 653 Gr 33.

To evaluate the flexural nonlinear behavior of a stud through a static pushover analysis, moment hinges must be defined at the locations of plastic hinges. For the research study described herein, the walls are assumed to be simply-supported at the floor and ceiling, so flexural hinges are only used at midspan. It is advisable to place multiple hinges within a distance equal to the depth, *d*, of the stud on each side of the midspan of the beam. Multiple hinges help spread the plasticity of the beam in the vicinity of the midspan location and capture a more realistic formation of a plastic hinge than using a single hinge at midspan. For this research, the studs are analyzed using five equally spaced hinges. One hinge was located directly at midspan, and two hinges were located on each side of midspan at a distance of *d/2* and *d* from the midspan. Using more than five hinges within this distance did not converge to a solution. The hinges should begin as the default steel hinges and be deformation-controlled hinges. Figure 3.10 shows a typical SAP2000 hinge property input for this model. It is important to note SAP2000 will not calculate the yield moment and yield rotation for a cold-formed steel section or for

ASTM 653 steel. Therefore, in the hinge properties, the “Use Yield Moment” and “Use Yield Rotation” options must not be selected. Those values must be manually calculated and input.

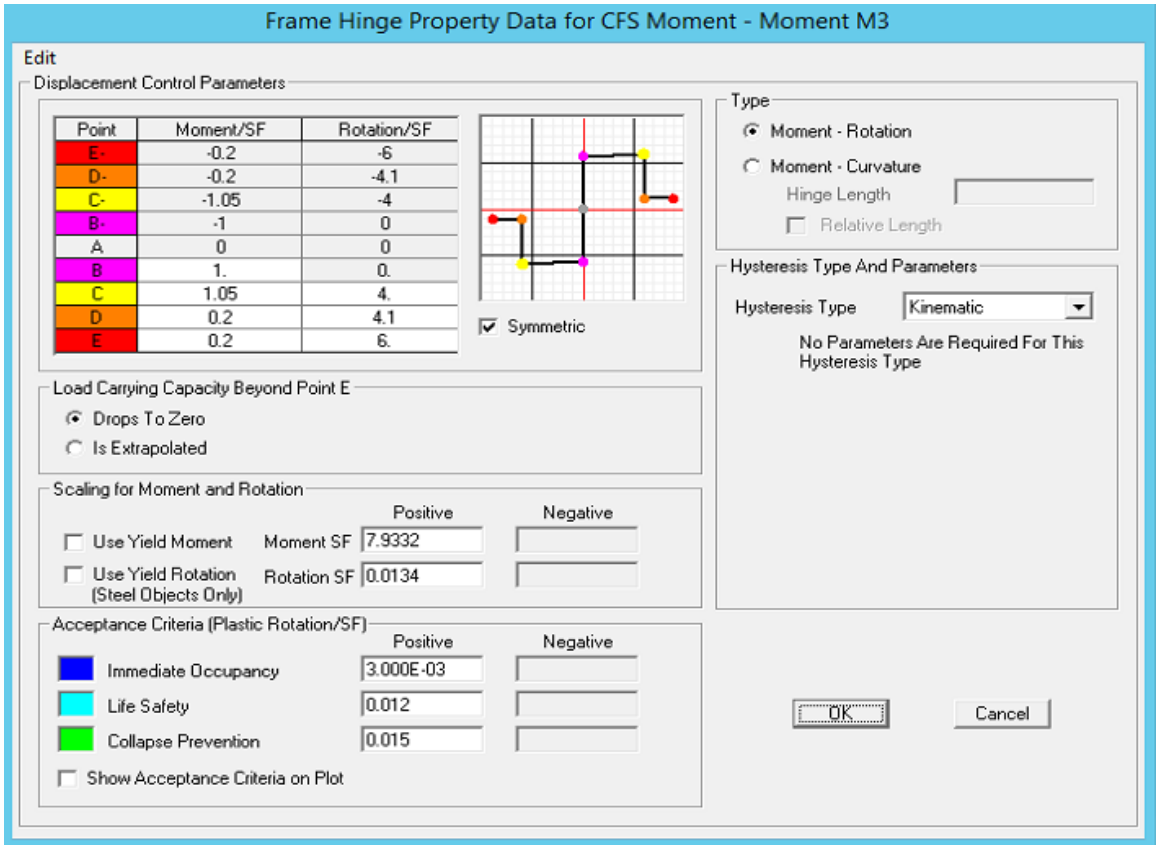

Figure 3.10 SAP2000 v15 Moment Hinge Property Input

Yield Moment: In cold-formed steel, the moment capacity of a stud is typically controlled by local buckling, distortional buckling, or lateral-torsional buckling. The AISI design specification (2007) contains several equations to calculate the yield moment of a cold-formed steel section. More conveniently, the SSMA Product Technical Guide (2013) publishes the allowable moment based on local buckling and the allowable moment based on distortional buckling, ignoring rotational stiffness provided by any

sheathing that may be present. These limit state capacities depend on the section. For some sections, the local buckling capacity and distortional buckling capacity are nearly the same, but for other sections, these capacities vary by as much as 17%. In all observed tests from the current research, and in an abundance of situations with interior steel-stud walls, distortional buckling does not control. Also, the gypsum board provides additional rotational stiffness to prevent distortional buckling that is ignored by the SSMA (2013) published allowable moments. Furthermore, observed flexural failure of steel-stud walls subjected to blast loads seen in the current research appears to be caused by local buckling. Therefore, it is recommended to use the local buckling flexural limit when determining the yield moment. When using the published allowable moment based on local buckling for a stud listed in the SSMA Product Technical Guide (2013), it is important to realize the moment is according to Allowable Stress Design and includes a factor of safety of 1.67. When analyzing structures subjected to blast, factors of safety are typically ignored, and increase factors are applied to better represent the actual strength of the material. As such, the yield moment input into SAP2000 is the SSMA (2013) published allowable moment based on local buckling multiplied by 1.67 for the factor of safety and by 1.33 for the SIF and DIF. If limited details are known about the steel stud, the yield moment can also be calculated according to Equation (3-4).

$$M_y = S_e \cdot f_{dy} \tag{3-3}$$

where $M_y =$ yield moment

$S_e =$ effective section modulus

$f_{dy} =$ design yield stress

The effective section modulus, S_e, accounts for local buckling of the section and is either published by the manufacturer or can be calculated according to the effective width method provided in the AISI design specification (2007). For most all interior walls, the studs will have sheathing on one or both sides. In the case of this research, all walls have gypsum board on both sides. The gypsum board provides sufficient bracing to prevent lateral-torsional buckling of the steel studs (Bewick et al., 2013), and many steel-stud walls contain additional steel straps or bridging to provide additional bracing. Therefore, lateral-torsional buckling of the studs does not generally need to be considered for sheathed interior walls.

Yield Rotation: To properly define the moment hinge for the pushover analysis, a yield rotation must be defined. In SAP 2000, "the hinge properties were created with pushover analysis in mind. Default hinge properties are provided based on FEMA-356 criteria" (CSI, 2011a). FEMA-356 (FEMA, 2000) is superseded by ASCE/SEI 41-13 (ASCE, 2014), and both standards provide the same equation to determine the yield rotation for a hinge used in a static pushover analysis, as shown in Equation (3-3).

$$\theta_y = \frac{M_p \cdot L}{6EI} \tag{3-3}$$

where $\theta_y =$ yield rotation

$M_p =$ plastic moment capacity = M_y for steel stud hinge

$L =$ beam length

$E =$ modulus of elasticity

$I =$ moment of inertia

It is assumed the yield rotation can be computed using the amplified moment capacity that already includes an SIF and a DIF, so no additional increase factors are included in

the yield rotation. In the absence of detailed test data, this approach was assumed to be reasonable, but the application of increase factors to the yield rotation of steel studs is potentially an area for future research.

The ductility of the moment hinge must also be defined. ASCE/SEI 41-13 (2014) provides many force-deformation relationships to be used for modeling hinges in a pushover analysis, and Figure 3.11 shows the generalized shape of this force-deformation ratio. ASCE 41-13 (2014), however, does not provide explicit recommendations for CFS sections (Ayhan and Schafer, 2012). Research is currently being performed, and proposed moment-rotation curves for CFS are being developed for future incorporation in the ASCE 41 standard (Ayhan and Schafer, 2012). The proposed curves from Ayhan and Schafer do not consider the effect of sheathing, and the overall ductility from these proposed curves is considerably lower than the ductility presented in the static resistance function research on steel-stud walls subjected to blast loads presented in Section 2.3.2.4 (Salim et al., 2005a; Salim et al., 2005b; Bewick et al., 2011; Bewick et al., 2013; Bondok and Salim, 2014; Bondok et al., 2015). Therefore, the lower limit for hot-rolled steel from ASCE/SEI 41-13 is used to define the moment hinges as it better matches ductility found in the current steel-stud wall blast research. The moment-rotation curve for the moment hinge follows the shape shown in Figure 3.11, and the values defining this curve are shown in Table 3.2.

These moment-rotation values for the lower limit of hot-rolled steel also correspond well to the recommended ductility parameters in The Single Degree of Freedom Structural Response Limits for Antiterrorism Design (USACE, 2008). In this report, the recommended ductility value is 5.0 and maximum rotation is 5º for complete failure of metal-stud walls with top and bottom connections to develop full tensile membrane capacity of the stud.

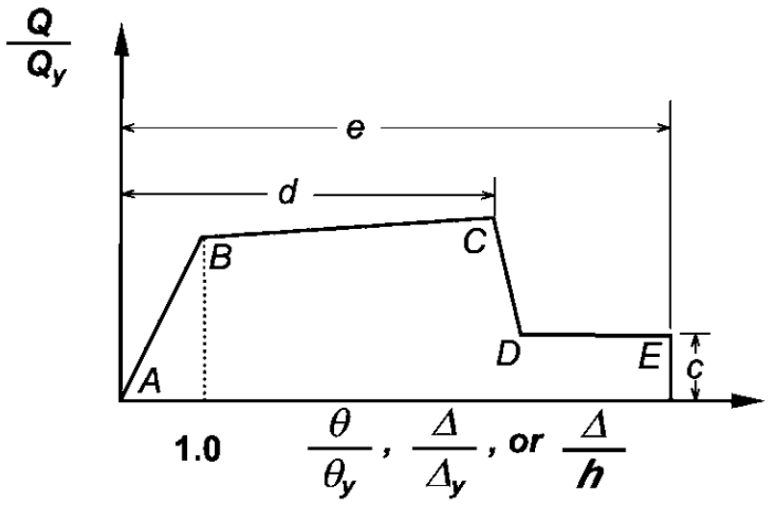

Figure 3.11 Generalized Component Force-Displacement Ratio for Modeling (ASCE, 2014)

Table 3.2 Moment-Rotation Values for Moment Hinge Definition

Point	Moment/M_y	θ/θ_y
B	1	0
C	1.05	4
D	0.2	4.1
E	0.2	6

The connection strength of the top and bottom of the wall should be modeled with a nonlinear link in SAP2000. The ability of SAP2000 to model the complete behavior of the connection is limited, so the controlling limit states of the connection must be determined first, then the controlling capacities of those limit states computed and defined in the nonlinear link properties. The controlling static connection limit state for a shear failure and a tension failure are determined as described in Section 2.3.2.2. The shear and tension strength of the stud-to-track, track-to-floor, and track-to-ceiling connections should be evaluated using the AISI specification (2007) and LGSEA

Technical Note 562 (2001). The computed strengths of the controlling shear limit state and tension limit state are used to define a link at the each end of the stud being analyzed in the pushover analysis. A link used to represent a connection at the end of a stud is considered a single-joint support, and modeled as a zero-length element in SAP2000. For zero-length elements, the U1 direction corresponds to the global Z axis (CSI, 2011a). Therefore, when a stud is modeled in an orientation as shown in Figure 3.12, the U1 direction of the link corresponds with the shear strength, and the U2 direction corresponds with the tensile strength. An example of the link properties input for the shear (U1) direction is shown in Figure 3.13. Any plastic behavior of the controlling connection limit state should be included, if applicable, such as a track bearing failure. Some connection failures, such as a tension pull-out, may not have any plastic behavior, and this should be represented in the link properties. Plastic behavior of a particular connection limit state may not commonly be computed, but this behavior is important to capture as it enhances a wall's ability to dissipate energy from a blast load. Therefore, an attempt to compute the plastic deformation should be made by the user and included in the link properties.

A nonlinear link is used instead of a shear or tension hinge because a link maintains its orientation with the global axis and does not rotate with the member as a hinge does. This represents the track-to-floor and track-to-ceiling connections well as there is typically limited rotation in the failure of these connections. Depending on the total connection details, a strong track-to-floor and track-to-ceiling connection may result

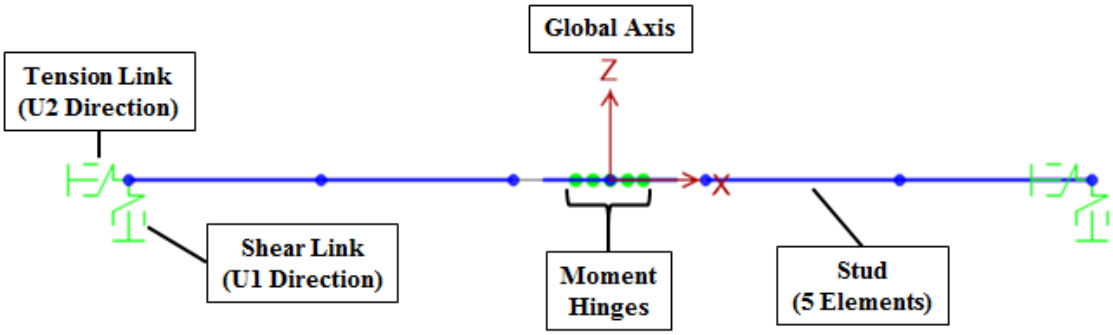

Figure 3.12 Typical Steel Stud Model for SAP2000 v15 Static Pushover Analysis

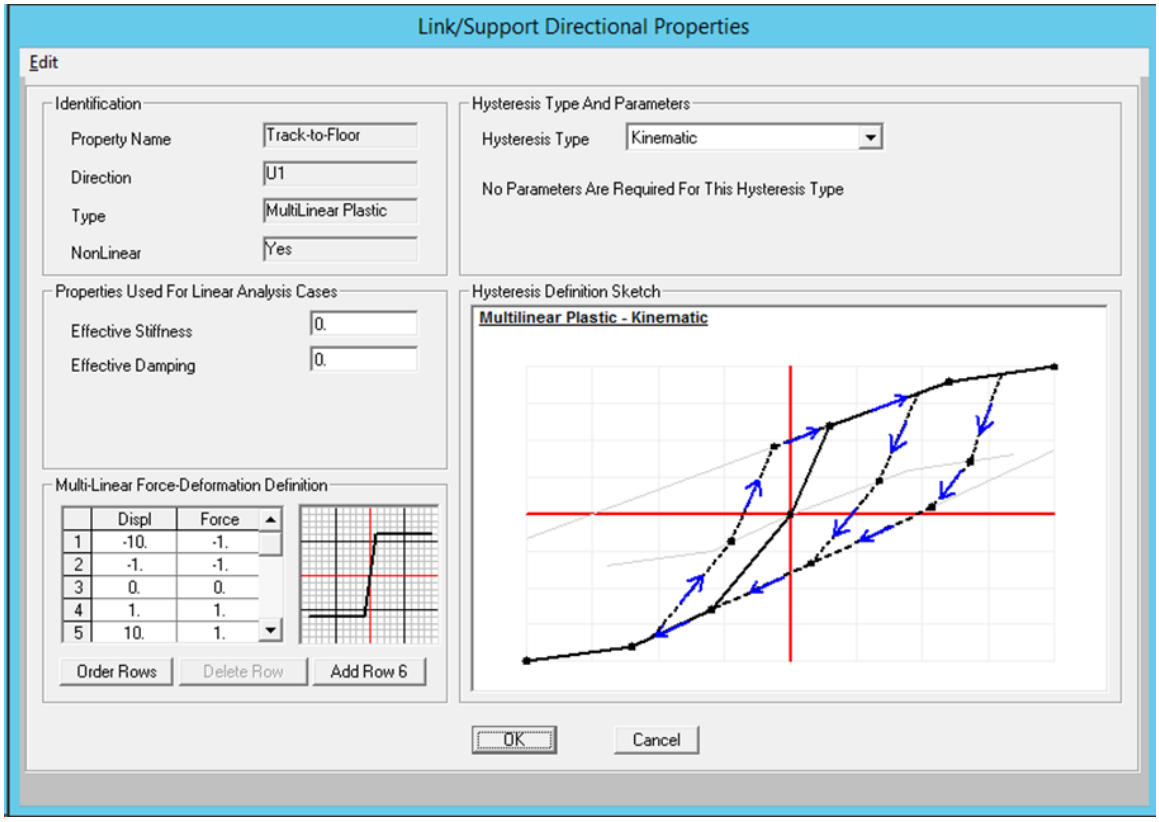

Figure 3.13 SAP2000 v15 Link/Support Property Input

in a stud-to-track connection limit state. This connection can rotate with the stud, and may be better represented with a shear and tension hinge. Engineering judgement should be used to determine the appropriate connection model; however, if a hinge is used to allow for connection rotation with the member, the flexural resistance of the track flange may also need to be considered. Based on all cases encountered in the current research, the nonlinear link is recommended for modeling the connection behavior at the ends of a stud.

No SIF or DIF is included for the connection strengths. The UFC 3-340-02 recommends using a DIF for connections (2008). Connection failure, however, involves the ultimate strength, and the recommended DIF for the ultimate strength of CFS is 1.0. No information is available on SIF for CFS connections, so no SIF if used. Actual material strengths should be used to the maximum extent available instead of using minimum design strengths. For example, the published design strength for the RAMSET powder-actuated fasteners includes a factor of safety of five (RAMSET, 2011). The strength used to model that connection in SAP2000 should be the published design strength multiplied by five.

The loading used in a static pushover analysis must be applied under a displacement-controlled load case (CSI, 2011a). First, a distributed load pattern is created and applied to a stud to simulate a blast load. This loading should have a maximum magnitude of 1 kip/in. acting along the entire length of the stud. Next, a blast load case is defined as a nonlinear static load case in which the distributed load pattern is applied. Finally, a pushover load case is defined as another nonlinear static load case that will be used in the pushover analysis. The distributed load pattern is again applied in this load case, but it is applied as a displacement-controlled load. The inputs for the pushover load case are shown in Figure 3.14. Within this input screen, under the “Other Parameters”

option, the load application must be entered as “Displ Control”, and the monitored displacement specified as the vertical translation of the joint at the midspan of the stud. This will ensure the pushover analysis force-displacement results will correspond to the midspan displacement of the stud. Also under the “Other Parameters” option, the results saved should be changed to “Multiple States” so that multiple data points will be saved in the force-displacement output. Under the “Geometric Nonlinearity Parameters” option, the “P-Delta plus Large Displacements” option should also be selected. This will enable the pushover analysis to capture the potential tension membrane action of a stud.

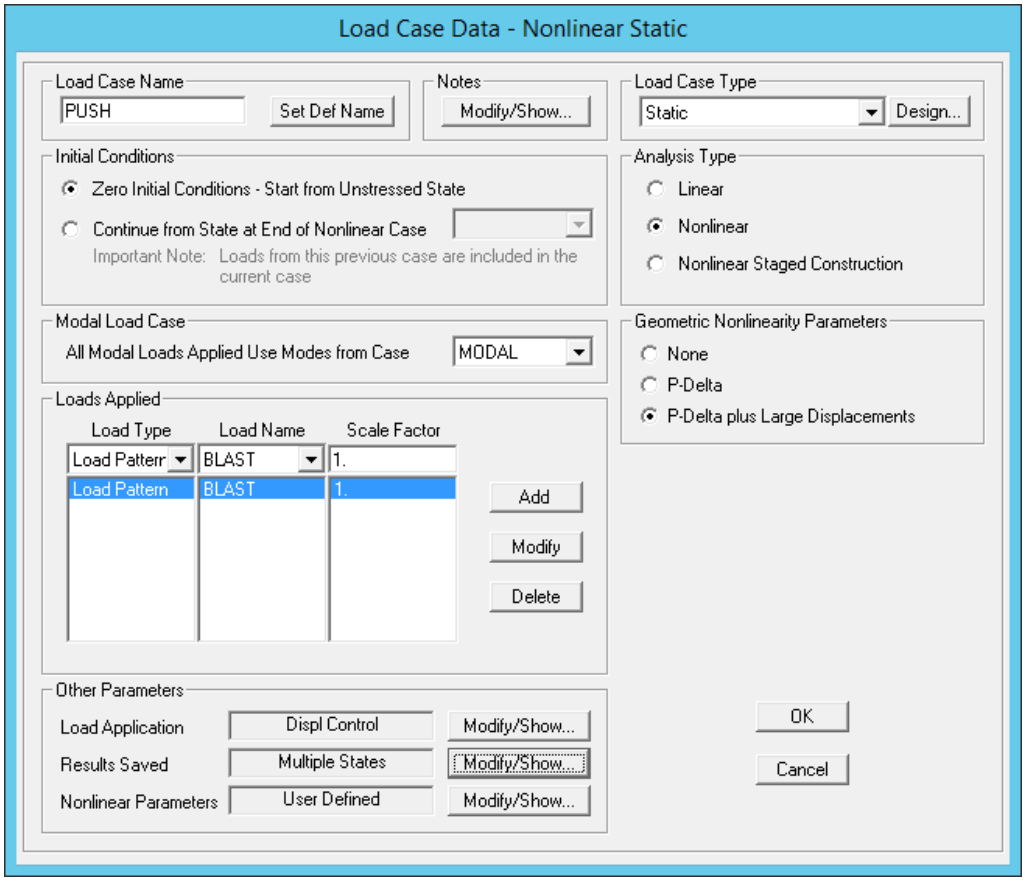

Figure 3.14 SAP 2000 v15 Pushover Load Case Input

To run the static pushover analysis, the blast load case and pushover load are selected to be run. The results of the analysis are a static pushover curve. The output plot in SAP2000 is titled "Resultant Base Shear vs Monitored Displacement." The resultant base shear in this case is the total resultant load on the stud, or the resistance. The monitored displacement is the specified midspan displacement of the stud. Therefore, the resulting force-displacement plot from the static pushover analysis is the static resistance function of the stud. The total resistance for an entire steel-stud wall is the resistance of a single stud multiplied by the total number of studs.

Even though the SAP2000 pushover analysis provides a mechanics-based method to determine the resistance function, it is important to also realize its limitations. The pushover analysis relies on nonlinear springs and hinges to capture the behavior of the steel studs. The parameters of these nonlinear springs and hinges are empirically based and do not capture all behavior of the steel studs. Behavior, such as buckling, must be accounted for through these nonlinear parameters. Anticipated behavior and associated limits must be known in advance to define appropriate parameters in the SAP2000 model.

Despite its limitations, the SAP2000 pushover analysis allows for a mechanics-based method to be used to compute a resistance function for a steel-stud wall for use in an equivalent SDOF system. When modeled correctly, it captures several possible modes of static failure, accounts for material and geometric nonlinearities, and can account for potential tension membrane action. Similarly to the other methods of developing resistance functions described in Section 2.3.2.4, the static pushover analysis does not capture any potential dynamic modes of failure. As previously stated in that section, though, the use of static resistance functions has been validated and represents the current state of the practice.

3.3.3.4 Effect of Gypsum Board

The structural capacity of a steel-stud wall is determined solely by the strength of the steel studs. The structural response of the gypsum board sheathing is not considered, as it is a brittle material and relatively weak compared to the steel studs. Other than the mass provided to the wall, the gypsum board is simply a tributary area that transfers load to the studs. It is assumed to transfer the total amount of the applied blast load to the studs before the gypsum board breaks apart.

In other applications of determining wall resistance to blast loading, the resistance of the sheathing has been considered in a series of uncoupled SDOF component responses as described in Section 2.3.1.1. Essentially, a section of sheathing material between the steel studs is treated as an equivalent SDOF system. A dynamic analysis of this sheathing section subjected to a blast load produces a reaction force history for the ends of the section, and this reaction force history is considered the loading on the steel studs. Then, a separate equivalent SDOF analysis is performed on the studs with this loading to determine the wall displacement history. The successful applications of this method have been for sheathing material such as OSB or sheet steel (Williamson, 2014). Incorporating the structural resistance of gypsum board has not been successfully implemented. Using published material properties from the Gypsum Association (2010), an attempt to incorporate the resistance of gypsum board in an uncoupled SDOF series analysis was performed on an interior steel-stud wall with gypsum board sheathing subjected to shock tube loading (Li et al., 2014). This method was shown to not accurately capture the behavior of the wall with gypsum board. Ultimately, using this method results in the gypsum board failing early in time before enough load is successfully transferred to the steel studs. Even though the time of failure of the gypsum board can be closely matched, the failing gypsum board transfers much more load to the

steel studs than the uncoupled SDOF method predicts. Treating the gypsum board as a non-structural component that transfers the full load over the tributary area of the studs provided a much better representation of the actual behavior in the shock tube tests than the uncoupled SDOF series (Li et al., 2014). Hence, the gypsum board is treated as a non-structural component for the model developed for the research study outlined in this dissertation.

3.3.4 Wall Break-up

The wall break-up model must capture all break-up modes. The term "break-up" is used when describing the wall opening behavior to distinguish it from wall "failure". Wall failure, as described in the previous section, refers to the loss of structural resistance. After wall failure, the resistance is zero, but the wall continues to move according to Equation (3-5).

$$M\ddot{y} = F(t) \tag{3-4}$$

The wall will either displace as a rigid body, or wall fragments and debris will displace. It is assumed that with no further structural resistance, all the mass of the wall will displace uniformly, so no load-mass factor is used in the equation of motion after wall failure occurs.

After a wall fails, it is assumed the wall will open and allow air mass to travel between rooms. The objective of the wall break-up model is to capture all possible break-up modes, which is a difficult task. To better understand the wall break-up model and its development, relevant wall break-up modes are presented in the following section.

3.3.4.1 Break-up Modes

First, a wall can fail and open as a rigid body. In this scenario, none or very little of the sheathing will break away from the studs. A wall will typically either tip over and open completely, or it will move as a rigid body, partially rotate, and get wedged between the floor, ceiling, and other walls.

Another possible break-up mode is the gypsum board breaking apart or disintegrating. Typically, the gypsum board on the front wall face will fracture between the studs first, and then along the line of the studs. The rear face of the gypsum board may fracture in a similar manner, or it may experience a pull through failure at the screws. Figure 3.15 shows a rear face gypsum panel that has pulled through at the screw holes. After the gypsum board initially fractures or pulls through, it may travel as a large piece as shown in Figure 3.15. It may remain that size and travel across the adjacent room until it impacts another surface or object. As the load increases, however, the gypsum board will continue to break apart after the initial fracture and pull through. Under these conditions, the gypsum board is essentially pulverized.

In all cases except for pulverization, the wall continues to interact with the air after wall failure. The entire wall or large pieces of gypsum board debris travel into an adjacent room. At the same time the wall is breaking-up, air mass is traveling between rooms through openings. The wall break-up model captures this behavior. Details of the wall break-up model are not included due to the limited distribution of the research.

3.3.4.2 Wall Break-up Model

The parameters defining WAI break-up model are empirically determined for a given wall size and strength in a given test series. The research study described herein aimed to develop a mechanics-based break-up model. Intuitively, the wall break-up should be a function of both the wall properties, including the strength and size, and the

loading. A strong wall could fail or open more slowly than a weaker wall. A shorter span wall would open at a different rate than a longer span. Also, higher magnitude loads would cause a wall to fail or open more quickly than lower loads, so it is important to also include the loading in the overall wall break-up model. The research study described herein developed a break-up model with components based on the wall physical properties and the loading. Again, details of the break-up model cannot be provided due to the limited distribution material used for its development.

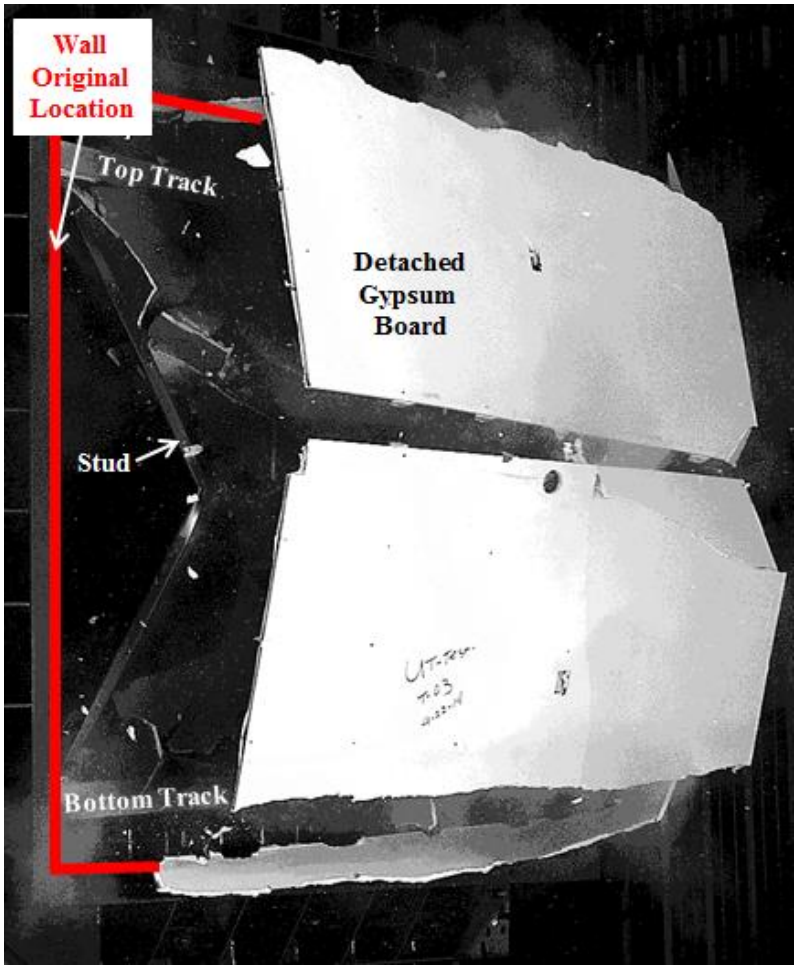

3.3.5 Figure 3.15 Gypsum Board Break-Up with Screw Pull Through (adapted from ABS Consulting, 2014)Numerical Analysis

The numerical analysis for the model developed in the research study described herein is performed using a routine programmed in Mathcad (PTC, 2012). The ultimate goal of the numerical computation is to produce pressure and impulse histories for all rooms in the simulation. This is done by computing the interaction of wall displacements and air mass flow through openings between rooms at every time step. The wall displacements are computed using the central difference method of numerical integration, and the air mass flow uses the wall break-up model described in Section 3.3.4.

A user must input a number of parameters in the Mathcad sheet to begin the numerical analysis. These parameters include the number of rooms, duration, time step, ambient air pressure and density, room dimensions, existing wall openings, wall mass, wall resistance function parameters, and the loading pressure-time curve with the same constant time step as specified in the input. Correct units must also be used in these inputs. The input units are consistent with BlastX to help make the loading computation work smoothly with the Mathcad routine. Inputs are generally lbs. for force, and ft. for length. The BlastX output for loading, however, is provided in psi, so the loading input in the Mathcad sheet is kept in psi to avoid an extra step of manually converting the BlastX loading output into psf. The Mathcad sheet converts the load to psf internally for unit consistency. The inputs used in SAP2000 for the pushover analysis are typically lbs. and in. for consistency with the SAP2000 default material properties. The resulting resistance function is provided in lbs. versus in. This input must be converted to psf versus in. for the input into the Mathcad sheet.

3.4 SUMMARY

First, a detailed description of the internal detonation problem was presented in this chapter. Several modeling approaches to predict damage and blast load propagation in these internal detonation scenarios were described. Ultimately, the model developed for the research study outlined in this dissertation was described in detail, including the major improvements. These three improvements included the detonation room loading simulation using BlastX, the resistance function development using a SAP2000 static pushover analysis, and a wall break-up model based on wall physical properties and the loading. The following chapter describes the model and its predictive results as it is applied to two separate experimental test series.

Chapter 4

Blast Load Propagation Model Validation and Application

The simplified engineering-level model to predict internal blast load propagation presented in Chapter 3 was developed and validated using measured experimental data. Tests from a Defense Threat Reduction Agency (DTRA) series of experiments were used to develop the model. After successful model development, a separate experiment was used to validate the model. This test is part of an ongoing test program conducted by the Air Force Research Lab (AFRL). This chapter describes the successful modeling results from those tests as well as current model limitations.

4.1 DTRA TESTS

The DTRA internal detonation testing program included two phases. Phase I of the included 16 tests with the 4-room, 1-dimensional configuration shown in Figure 4.1.

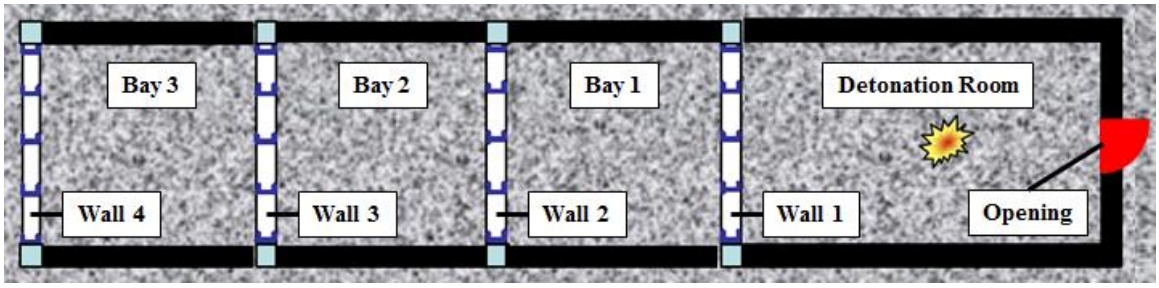

Figure 4.1 DTRA Test 1 Plan View (adapted from DTRA, 2009)

4.1.1 Phase I Description

The first two tests had four test walls as shown in Figure 4.1. In tests three through sixteen, Test Wall 4 was converted to a non-responding wall. The side walls, floor slab, and roof were all constructed of reinforced concrete and considered non-responding surfaces (Wenner and Sheffield, 2011). Figure 4.2 shows an elevation

photograph of the test structure. The additional floor, ceiling, and columns in the front of the photograph in Figure 4.2 were for the construction of additional rooms used in the Phase II test series (Wenner and Sheffield, 2011). See Section 4.1.4 for additional details on Phase II.

Figure 4.2 DTRA Test, Phase I Elevation Photograph (adapted from Kersul, 2014)

Three different wall types were tested in the DTRA tests: steel stud, wood stud, and CMU. Varying explosive charge weights and detonation locations were used in the detonation room. Some of the Phase I tests also examined existing openings, doors, glass panels, and partial-height walls. The tests that were relevant to this research study were tests that included full-height steel-stud test walls with no existing openings or doors in the test walls. By limiting the tests to this configuration, the research is able to focus on the structural response and break-up of steel-stud walls without introducing additional variables. The tests which met this configuration were Test 1, Test 8, and Test 9. Details about the specific test configuration and results of those tests are provided in Sections 4.1.2 and 4.1.3. The overall test setup for all the Phase I tests is presented in this Section.

4.1.1.1 Test Bed Layout

The detonation room has an existing opening centered at the base of the rear wall in the detonation room, as shown in Figure 4.1. This opening allows for some of the gas pressure in the detonation room to be vented. Each bay is separated by a test wall shown in Figure 4.1. The test walls generally span the entire height and width of the rooms they separate and are constructed using common construction practices for the given wall material (DTRA, 2009; Sheffield et al, 2009; Wenner and Sheffield 2011). Additional details about the steel-stud wall construction are provided in Section 4.1.1.3.

4.1.1.2 Instrumentation

The instrumentation used in the DTRA tests included pressure gauges and high-speed video. The pressure gauges were used to measure the total overpressure in the room, including both the shock overpressure and gas overpressure. High-speed cameras were used to capture the test wall response.

4.1.1.3 Steel-Stud Wall Details

The steel-stud walls used in the DTRA tests were constructed using typical construction details with the studs spaced 16 in. on center. The studs were attached to the track using one #8 screw on each stud flange. Two rows of 2-in. metal straps were installed on both wall faces. When straps are used for lateral bracing, metal blocks must be installed at each end of a wall, and spaced 8 ft. on center (SSMA, 2013; ClarkDietrich, 2015). These blocks were installed accordingly. The top and bottom track were attached to the ceiling and floor slabs, respectfully, each with powder actuated fasteners. Half-inch thick gypsum board was installed on each face of the wall (Sheffield et al., 2009).

4.1.2 DTRA Test 1

The DTRA Test 1 was the primary test used to develop the model for the research study outlined in this dissertation. It was chosen as the primary test because it included full-height steel-stud walls with a small explosive charge placed in the center of the detonation room. This configuration was considered to be a baseline case relative to the other tests in the research program.

4.1.2.1 DTRA Test 1 Details and Observations

Test 1 used a small explosive charge placed in the center of the detonation room (Kersul, 2014). The test included four test walls as described in Section 4.1.1, and all four walls failed during the test.

4.1.2.2 DTRA Test 1 Model Inputs

Test 1 is simulated and run in the model developed for the research study, but first, the inputs used in the model must be described. The model includes five rooms: the detonation room, Bay 1, Bay 2, Bay 3, and a large outside air room. There are four test walls assumed to be the entire width and height of the bays. The volume of the outside air is nearly 10^6 times larger than the volume of an individual bay as recommended in Section 3.3.1.2. The weight of a wall must be converted to mass by dividing by the gravitational acceleration shown in Equation (4-1).

$$m = \frac{W}{g} \tag{4-1}$$

where $m =$ mass

$W =$ Weight

$g =$ gravitational acceleration = 32.174 ft/s^2

There are no existing openings in any of the test walls. The existing opening in the detonation room is included in the BlastX load calculation. The initial air in all rooms is assumed to be at atmospheric pressure and at 68 degrees Fahrenheit, which gives an initial energy, e_0, equal to 70365 (ft·lbf)/lbm and an initial density, ρ_0, equal to 0.0752 lbm/ft^3. These inputs are all entered into the Mathcad sheet developed for the research study.

The input loading for DTRA Test 1 is computed using BlastX as described in Section 3.3.2. The detonation room and outside air room are input into BlastX. The existing opening in the detonation room is placed between the two rooms. The explosive charge type and weight is placed in the center of the detonation room. On the test wall, targets are placed every 0.5 ft. Targets are not placed on the edges of the test wall. The BlastX simulation is run for a duration of 0.4 second, and the pressure-time output is formatted into equal time intervals of 0.00001 second. The output pressure is given in psi, and these are the units used as the input into the Mathcad sheet as described in Section 3.3.5. The BlastX-generated input load plot is shown in Figure 4.3 compared to an actual detonation room pressure gauge reading. The magnitudes of the pressure and impulse curves are not included, but the overall shape of the predicted versus actual detonation room loading can be observed. Peak pressures are underestimated, but the impulse matches fairly well, with the maximum impulse overestimated by 18%. These acceptable loading differences are due to the simplifications discussed in Section 3.3.2. Further discussion on the loading limitations is presented in Section 4.4.1.

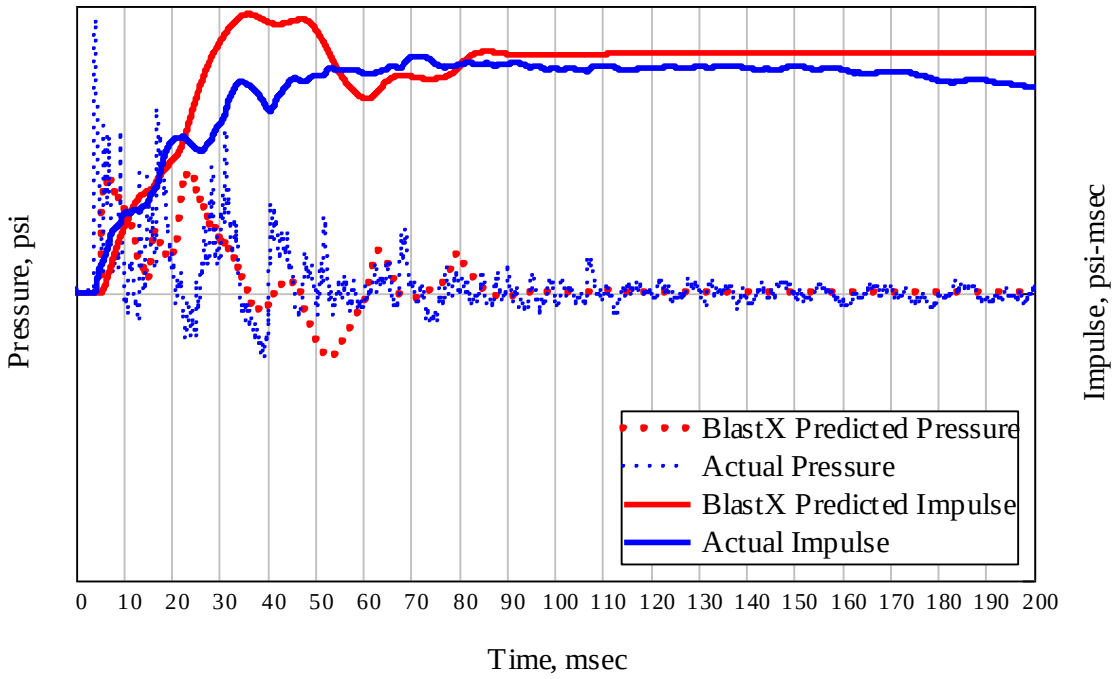

Figure 4.3 DTRA Test 1 BlastX Predicted Load versus Actual Pressure Gauge Data in Detonation Room

The wall resistance is computed using the SAP2000 pushover analysis as described in Section 3.3.3.3. The stud is modeled using the section properties provided by the SSMA Product Technical Guide (2013). The material yield strength is increased by the DIF and SIF. Local buckling controls for the stud used in the DTRA test walls, and the yield moment is calculated using Equation (3-7). The yield rotation is computed using Equation (3-8). The resulting yield moment and yield rotation values are used in defining the hinges.

The shear and tension link properties used to simulate the connections are computed according to Section 3.3.3.3. The fasteners used to connect the track to the floor and ceiling are assumed to be RAMSET 1510SD powder-actuated fasteners. These were the fasteners used in DTRA Test 5 (Wenner and Sheffield, 2011), and no further specifics were given on the fasteners used in Test 1. The strength of the fasteners was obtained

from the RAMSET Technical Manual (2011). Based on this assumption, the shear connection behavior is controlled by a track bearing failure at the track-to floor and track-to-ceiling connections. The calculated shear failure force is 220 lbs. per stud. Some plasticity is expected in this type of failure, and although this is not typically calculated, the displacement before the wail completely fails and the energy absorbed from this plasticity is important. Based on observed failures of this type in DTRA Test 1, and a computation of the displacement from a track bearing failure, the displacement at failure is estimated to be one in. A bilinear force-displacement model is used in the force-displacement relationship for the shear link. To avoid slopes of infinity (perfectly rigid) or zero (perfectly plastic), the yield displacement is 0.1 times the failure displacement, and the yield force is 0.95 times the shear failure force. Figure 4.4 shows the shear link used in the DTRA Test 1 SAP2000 Pushover Analysis.

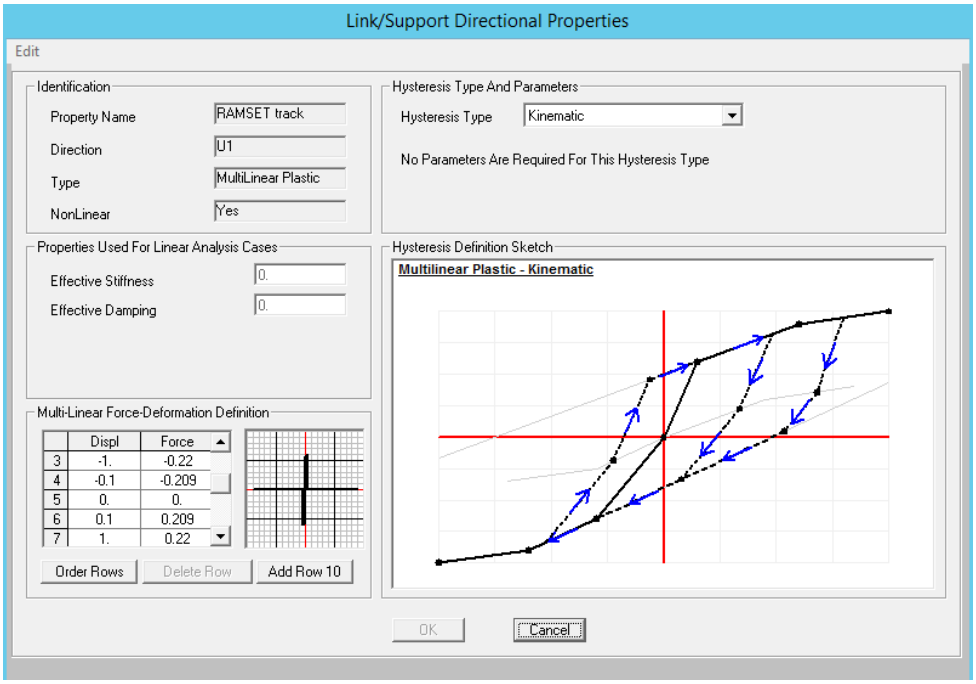

Figure 4.4 Shear Link used in DTRA Test 1 SAP2000 v15 Pushover Analysis

The tension connection behavior is controlled by the tension pull-out strength of the powder-actuated fastener. The tension failure force is 314 lbs. per stud. No plastic behavior is assumed when the powder-actuated fastener pulls out of the concrete, so the tension link has no plasticity. A small quantity of elasticity is given to the tension link in the force-displacement relationship; a failure displacement of 0.1 in. is used with a failure force of 314 lbs.

The SAP2000 pushover analysis of the stud from DTRA Test 1 produces the resistance curve shown in Figure 4.5. The results of the hinges and links in SAP2000 can be checked, and these results show the shear failure of the connections control the overall resistance curve. The observed dynamic failure of the test walls for DTRA Test 1 is a shear-type failure of the powder-actuated fasteners, which is consistent with what was computed in the SAP2000 pushover analysis. The resistance curve is approximated as a bilinear function to be input into the Mathcad sheet. The yield force is 418 lbs., the yield

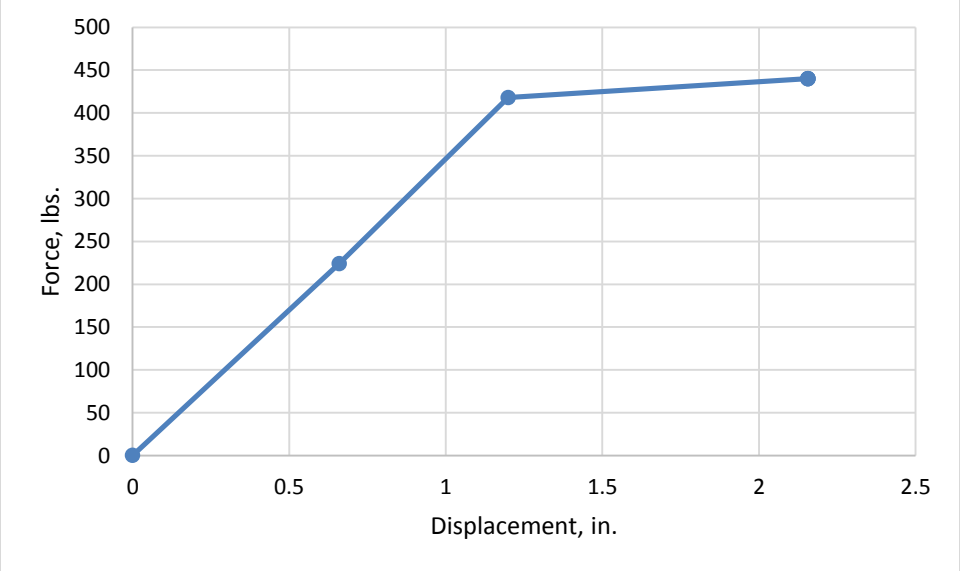

Figure 4.5 DTRA Test 1 Resistance Curve Produced from SAP2000 Pushover Analysis

displacement is 1.20 in., the ultimate force is 440 lbs., and the ultimate displacement is 2.16 in. The Mathcad sheet inputs for the resistance function variables, $\sigma_{yspring}$, δ_y, σ_u, and δ_u, must be converted to psf and ft. This conversion is accomplished by the forces being divided by the stud spacing (16 in.) and height to get psf, and the displacements and stud spacing are divided by 12 in./ft to convert to ft.

The inputs for the wall break-up model are automatically computed within the Mathcad sheet based on the wall properties and computed loading.

4.1.2.3 DTRA Test 1 Analysis and Results

After all the inputs are computed and entered into the Mathcad sheet, the model was run. The model outputs pressure-time data for Bay 1, Bay 2, and Bay 3. The model's predicted results are compared with the actual data from two pressure gauges in each Bay. The pressure-time plots of the model prediction and actual pressure gauges for Bay 1 are shown in Figure 4.6. Bay 2 results are shown in Figure 4.7, and Bay 3 results are shown in Figure 4.8. The pressure and impulse values are divided by an arbitrary value "P". This is done to present numerical values of the pressure and impulse without providing specific results from limited distribution tests.

For all three bays, the overall shape of the predicted pressure and impulse curves match the actual data well. The maximum predicted values are compared to the maximum gauge values for pressure and impulse in Table 4.1. The maximum of the two gauges in each room is used for comparisons because this would indicate the most severe case in each room. In Table 4.1, negative values for the difference and percent error from the maximum terms represent an under-prediction, whereas positive values are an over-prediction. In Bay 1, the peak pressure is not predicted accurately. The predicted peak

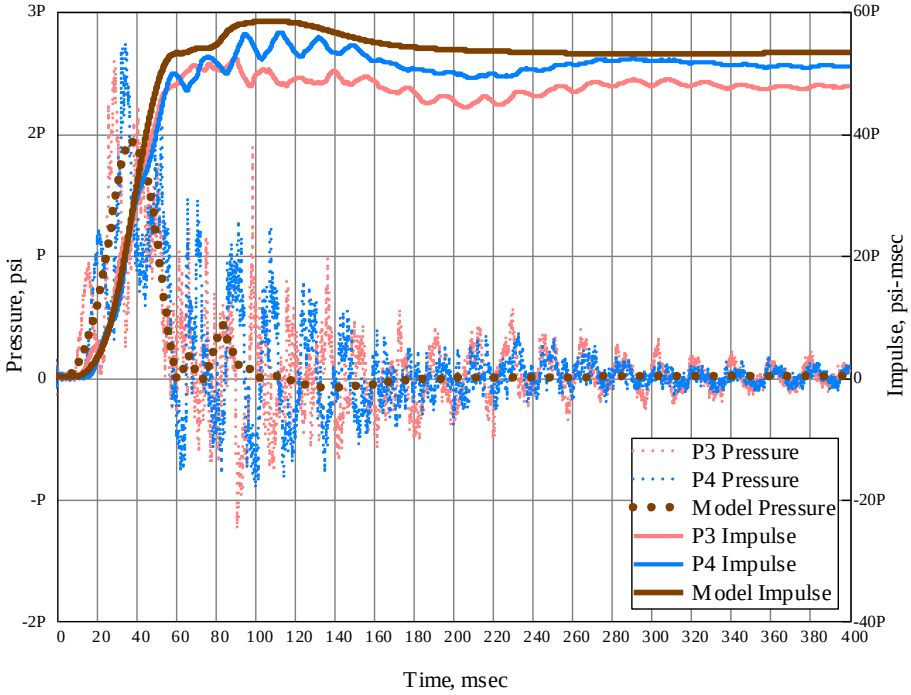

Figure 4.6 DTRA Test 1 Bay 1 Model Prediction versus Pressure Gauge Data: Gauge Data from DTRA (2010a)

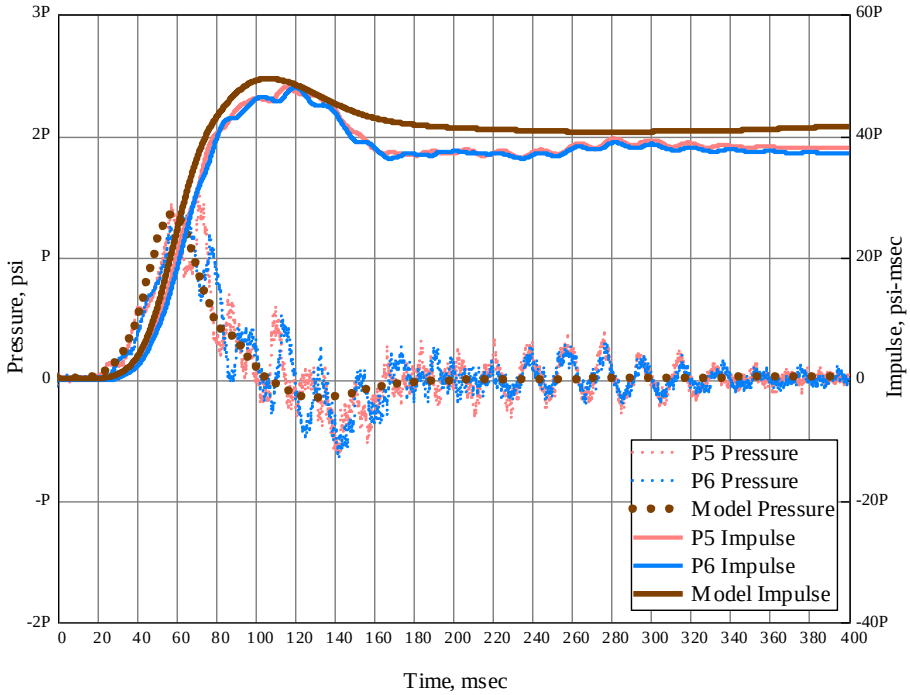

Figure 4.7 DTRA Test 1 Bay 2 Model Prediction versus Pressure Gauge Data: Gauge Data from DTRA (2010a)

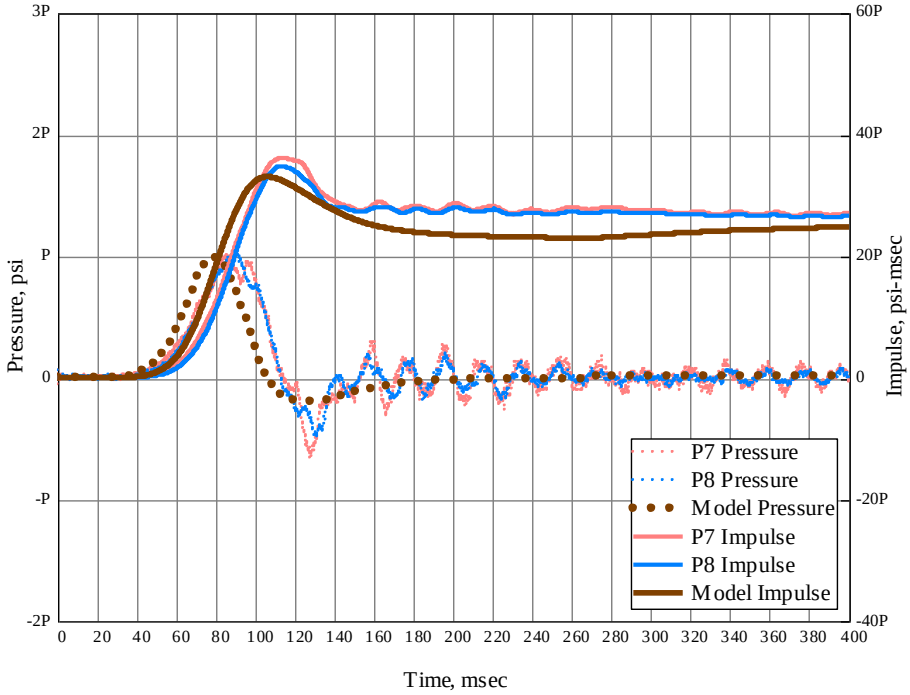

Figure 4.8 DTRA Test 1 Bay 3 Model Prediction versus Pressure Gauge Data: Gauge Data from DTRA (2010a)

pressure is 29.4% below the maximum gauge pressure. However, this result is expected in rooms close to the detonation room because of the complex behavior of shock waves. Even though the model does not capture the peak pressures in Bay 1, it is able to capture the impulse. The maximum predicted impulse in Bay 1 is only 3.0% higher than the maximum gauge impulse. As stated by Ohrt et al. (2013), the impulse is believed to be a particularly important load parameter in regards to wall response. Therefore, accurately predicting the impulse is more important than predicting the peak pressure when the goal is to predict blast load propagation. This may not be the case if the goal is to evaluate a different parameter, such as occupant health and safety in a particular room, where peak overpressure and debris are important factors.

The peak pressures in Bays 2 and 3 are more accurately predicted than in Bay 1. The maximum predicted pressures are under-predicted compared to the maximum gauge

pressures by 10.2% and 4.0%, respectfully. The maximum impulses in Bays 2 and 3 are also predicted well, and are within 3.0% and 8.5% of the maximum gauge values, respectively. Due to the complexity of blast load prediction, predicted impulses for all three rooms within 10% of the actual impulses is considered a successful prediction.

Table 4.1 DTRA Test 1 Predicted Results versus Maximum Pressure Gauge Data: Pressure values, P_{max}, are in psi and Impulse values, I_{max}, are in psi-msec Gauge Data from DTRA (2010a)

	DTRA Test 1					
	Bay 1		Bay 2		Bay 3	
	P_{max}	I_{max}	P_{max}	I_{max}	P_{max}	I_{max}
Predicted Value	1.94P	58.3P	1.35P	49.4P	0.98P	33.1P
Max Gauge Value	2.75P	56.6P	1.50P	47.9P	1.02P	36.1P
Difference	-0.81P	1.7P	-0.15P	1.5P	-0.04P	-3.1P
% Error from Max	**-29.4%**	**3.0%**	**-10.2%**	**3.0%**	**-4.0%**	**-8.5%**
R^2 from Max	0.53	0.96	0.80	0.95	0.68	0.88

Predicting the timing of the pressure histories for a room is also important. The duration of the pressure waves will impact the total impulse in a room. The timing affects not only the magnitude of the impulse but also when walls fail and when air mass flow occurs. There are no adjustments made to the time in the model. The results seen in Figure 4.6, Figure 4.7, and Figure 4.8 show the timing of the predicted curves closely matches the measured data. Predicted pressures versus the gauge pressures generally rise and fall at similar times, and predicted peak impulses versus gauge peak impulses are also reached at similar times. In Bay 2, the predicted pressure waves initiate slightly earlier than the gauge pressure waves. An error in the timing will likely propagate and be even more noticeable in later rooms. This can be seen in Bay 3 as the predicted pressure wave occurs earlier than Bay 2 when compared to the gauge pressure waves in each

respective room. The predicted pressure wave in Bay 3 is approximately 10 msec early, but still an acceptable prediction.

To get a better comparison of the success of the predicted results versus the actual data, a coefficient of determination, or R^2 value, is desired to place a numerical value on how well the predicted pressure and impulse curves match the data over the entire duration of the test. The pressure gauge data contains significant noise that can especially be seen from the gauges in Bay 1 shown in Figure 4.6. Evaluating a coefficient of determination for how well the predicted pressure matches the noisy pressure gauge data would not provide meaningful results because of the exaggerated differences between the noisy peaks of the gauge data and the smooth predicted curves. To alleviate the extremes of the gauge data, some of the noise is filtered out. To do this, a fast Fourier transform (FFT) is performed on the pressure gauge data. Any frequency greater than 100 hertz is filtered out, and then an inverse fast Fourier transform is performed to return the data to a pressure-time format. The resulting pressure and impulse curves for the filtered data are shown in Figure 4.9.

It is difficult to discern which extremes in the gauge pressure data are actual maximums and minimums or simply noise. This filtered data is not to be substituted as a more accurate representation of the actual pressure history, but it is simply a tool to provide a curve that allows a meaningful numerical evaluation of the accuracy of the predicted model. The coefficient of determination, R^2, is then calculated comparing the predicted pressure to the filtered gauge data for each pressure gauge. This coefficient represents the summation of the squares of the difference between the filtered and computed value each time step. These R^2 values are presented in the last row of Table 4.1 for the maximum pressure and impulse gauge data sets in each bay. The impulse curves have a higher R^2 value and, in general, are a better prediction than the pressure curves.

The R^2 value for the impulse in Bay 3 is slightly lower than the values for the other two bays. This outcome can partially be attributed to the timing error in Bay 3 discussed previously. The R^2 value can evaluate the effectiveness of the model's ability to predict both magnitudes of the pressure and impulse histories and the timing of these curves.

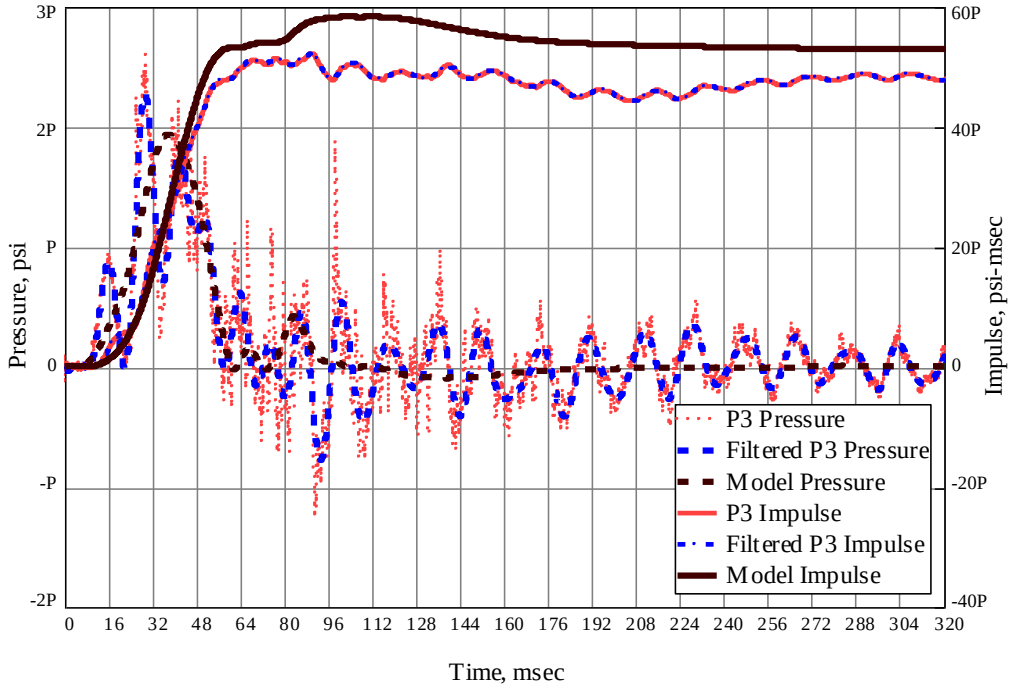

Figure 4.9 DTRA Test 1 Bay 1 Filtered Pressure Data for Gauge P3 for Use in R^2 Computation: Gauge Data from DTRA (2010a)

The model outlined in this dissertation successfully implemented a mechanics-based method to predict blast load propagation without the need for empirically derived inputs. The model also produces improved results compared to the original WAI model. The WAI model pressure and impulse results from DTRA Test 1 are presented in Figure 4.10 for Bay 1, Figure 4.11 for Bay 2, and Figure 4.12 for Bay 3. Visual observation of the plots in those figures shows the model outlined in this dissertation does a better job of predicting the peak pressures and impulses.

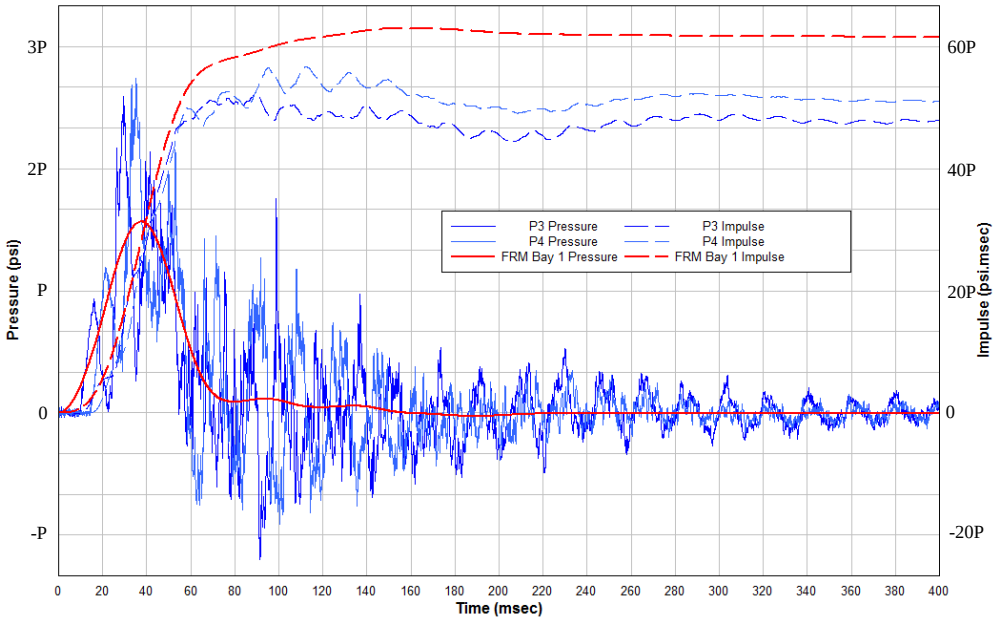

Figure 4.10 WAI Model Results for DTRA Test 1, Bay 1 (Tennant et al., 2011)

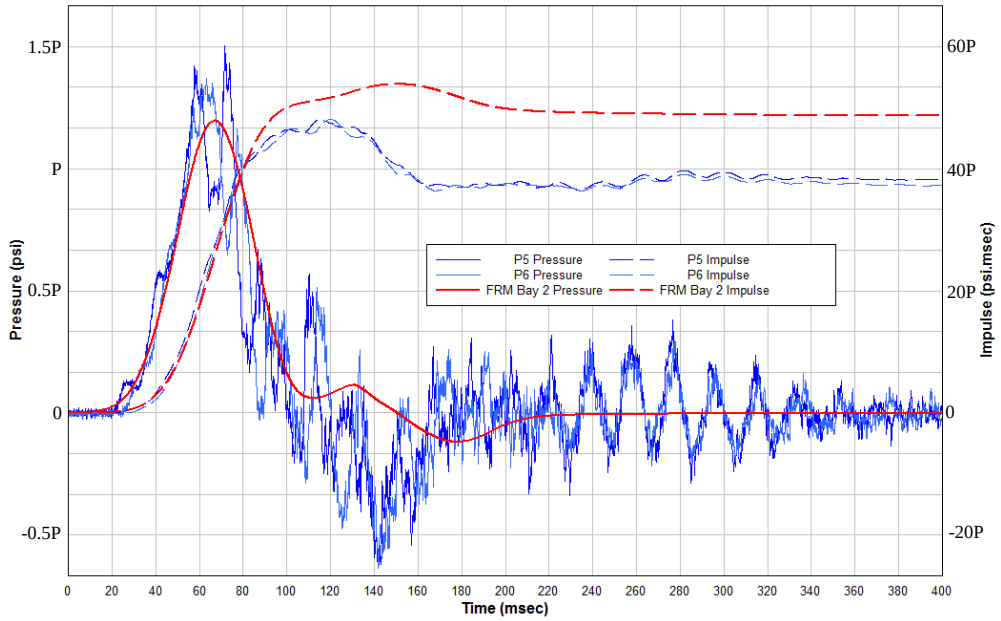

Figure 4.11 WAI Model Results for DTRA Test 1, Bay 2 (Tennant et al., 2011)

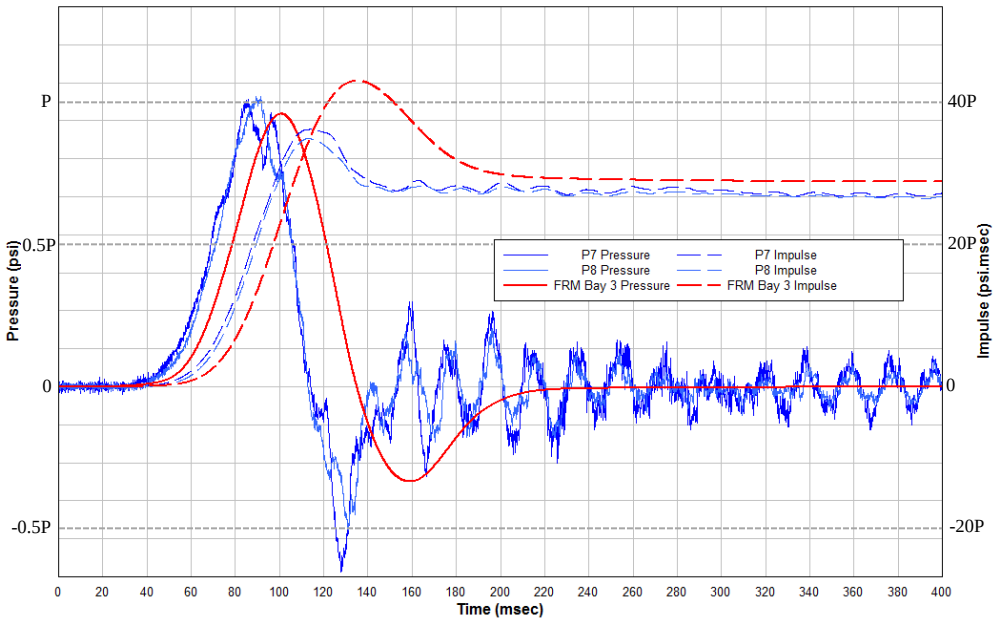

Figure 4.12 WAI Model Results for DTRA Test 1, Bay 3 (Tennant et al., 2011)

Table 4.2 Comparison of Current Research Study Model Results to WAI Model Results: Pressure values, P_{max}, are in psi and Impulse values, I_{max}, are in psi-msec Gauge Data from DTRA (2010a)

	DTRA Test 1					
	Bay 1		Bay 2		Bay 3	
	P_{max}	I_{max}	P_{max}	I_{max}	P_{max}	I_{max}
Max Gauge Value	2.75P	56.6P	1.50P	47.9P	1.02P	36.1P
Current Model	1.94P	58.3P	1.35P	49.4P	0.98P	33.1P
% Error from Max	**-29.4%**	**3.0%**	**-10.2%**	**3.0%**	**-4.0%**	**-8.5%**
WAI Model	1.57P	62.7P	1.20P	53.3P	0.97P	43.3P
% Error from Max	**-75.2%**	**9.6%**	**-25.1%**	**10.1%**	**-6.0%**	**16.5%**

The approximate maximums for pressure and impulse are interpreted from the WAI pressure and impulse plots, and a comparison of the results of the current research study model to the results of the WAI model is given in Table 4.2. The current research study model clearly improves the blast load propagation predictions.

4.1.3 DTRA Test 8 and Test 9

DTRA Test 8 and Test 9 were the other two tests in the DTRA Phase I test series that included full-height steel-stud walls with no existing openings. They each included a larger charge weight than Test 1, with one placed near the first test wall to examine the effect of a close-in charge and the other placed at the same location as Test 1. The other change from Test 1 was the removal of Test Wall 4. In its place, as described in Section 4.1.1.1, was a non-responding wall with an existing opening centered at the base of the wall. Overall, the wall failures were more destructive in Test 8 and Test 9 due to the larger charge weight used. Originally, Test 8 and Test 9 were intended to be used to validate the model developed in the research study described herein. The wall failure modes associated with a larger charge, however, were not appropriately captured in the original wall break-up model. Therefore, Test 8 and Test 9 were both used to complete the development of the wall break-up model described previously in Section 3.3.4. The details and results of these two Phase I tests are included in the following sections.

4.1.3.2 DTRA Test 9 Details and Observations

DTRA Test 9 is considered before Test 8 because only the charge weight is increased compared to Test 1, which only changes one main variable in the loading computation. Test 8 uses a larger charge weight than Test 1 and also places the charge closer to the test wall than Test 1, changing two main variables. In DTRA Test 9, the increased explosive charge is placed in the center of the detonation room as it was in Test

1. Overall, all three test walls in DTRA Test 9 failed drastically. The gypsum board was blown off the studs on all faces of all three test walls (Wenner et al., 2011a).

4.1.3.3 DTRA Test 9 Model Inputs

Most of the model inputs for DTRA Test 9 test remain the same as the inputs for Test 1. Unless otherwise stated, the input for Test 9 is the same as the Test 1 input described in Section 4.1.2.2. The test walls used in Test 9 were constructed in the same manner as Test 1. Therefore, all model inputs for Test Walls 1 through 3 are the same as for DTRA Test 1. Even though Test Wall 4 is non-responding, it must still be included in the model because it separates Bay 3 from the outside air. The dimensions of the wall remain the same as in Test 1, but the opening must be specified in the existing opening variable. The wall resistance and mass must also be increased so that the wall does not respond. To accomplish this, the wall yield stress, $\sigma_{yspring}$, ultimate stress, σ_u, and mass, m, are all proportionally increased by one order of magnitude until the displacement of Test Wall 4 is less than 0.1 in.

The DTRA Test 9 loading computation in BlastX is similar to that of Test 1; only the charge weight is increased. This increased charge weight is input into BlastX, and the detonation room loading is computed.

4.1.3.4 DTRA Test 9 Analysis and Results

The DTRA Test 9 model inputs were entered into the Mathcad sheet, and the model predicted the pressure and impulse curves for all three bays. The predicted results are compared to the actual pressure gauge data in Figure 4.13 for Bay 1, Figure 4.14 for Bay 2, and Figure 4.15 for Bay 3. Overall, the results show good agreement. Again, the peak pressures are not well predicted in the bays close to the detonation room, but the impulses in all three bays are acceptably accurate.

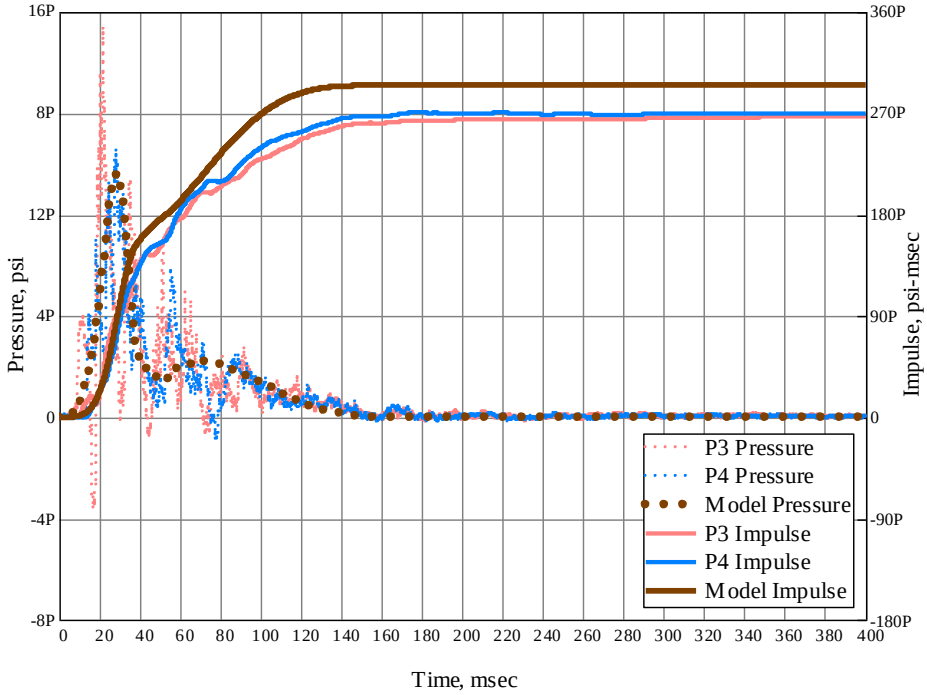

Figure 4.13 DTRA Test 9 Bay 1 Model Prediction versus Pressure Gauge Data: Gauge Data from DTRA (2013b)

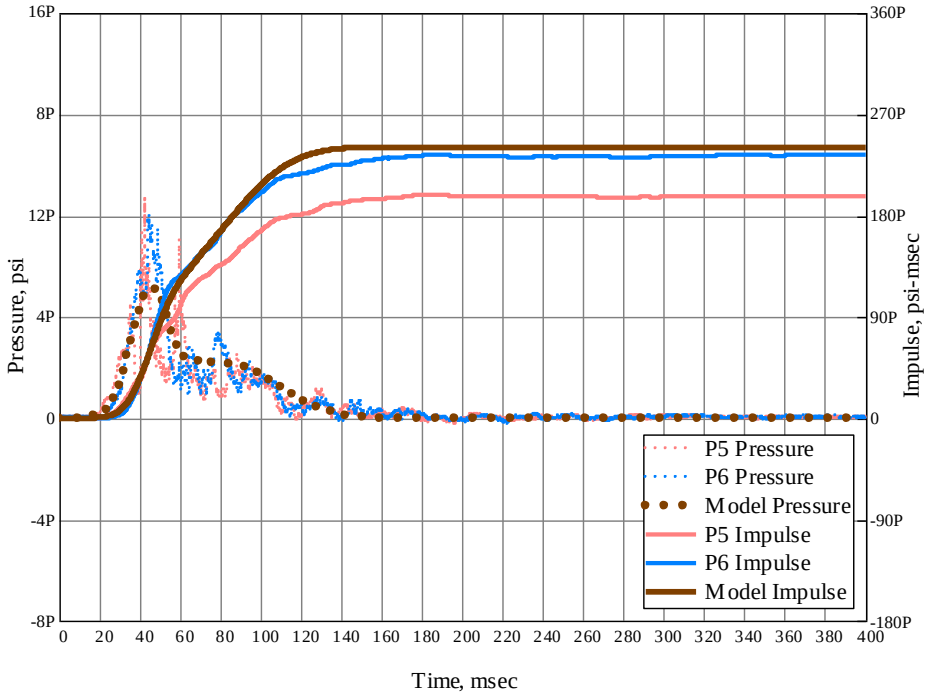

Figure 4.14 DTRA Test 9 Bay 2 Model Prediction versus Pressure Gauge Data: Gauge Data from DTRA (2013b)

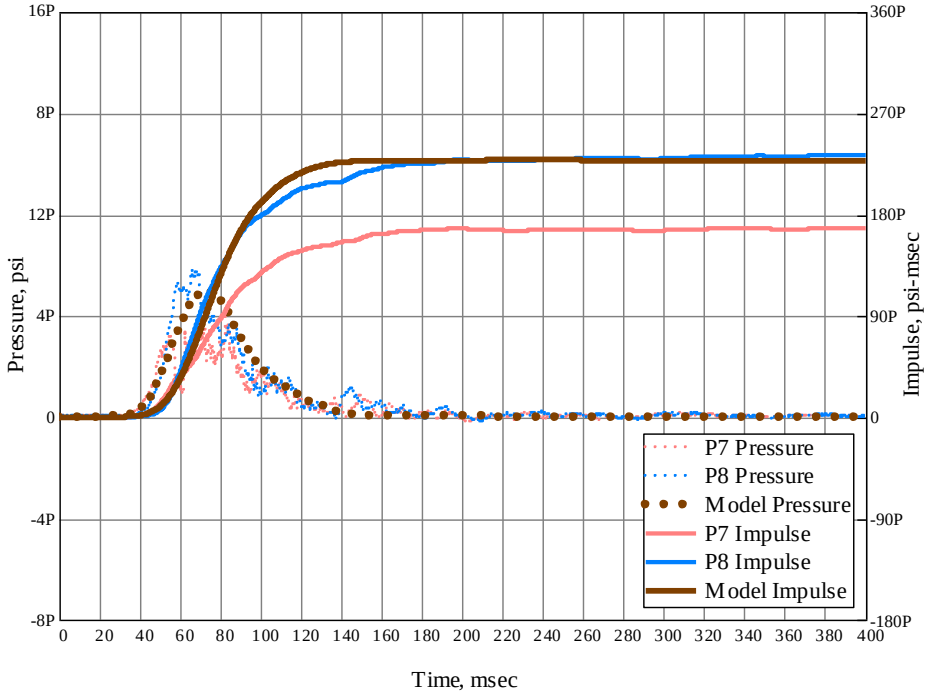

Figure 4.15 DTRA Test 9 Bay 3 Model Prediction versus Pressure Gauge Data: Gauge Data from DTRA (2013b)

Table 4.3 DTRA Test 9 Predicted Results versus Maximum Pressure Gauge Data: Pressure values, P_{max}, are in psi and Impulse values, I_{max}, are in psi-msec Gauge Data from DTRA (2013b)

	DTRA Test 9					
	Bay 1		Bay 2		Bay 3	
	P_{max}	I_{max}	P_{max}	I_{max}	P_{max}	I_{max}
Predicted Value	9.58P	294.6P	5.10P	240.3P	4.96P	228.2P
Max Gauge Value	15.5P	270.5P	8.69P	324.1P	5.86P	233.8P
Difference	-5.87P	24.1P	-3.59P	6.2P	-0.90P	-5.6P
% Error from Max	**-38.0%**	**8.9%**	**-41.3%**	**2.6%**	**-15.4%**	**-2.4%**
R^2 from Max	0.49	0.92	0.81	0.99	0.90	0.99

Table 4.3 provides a comparison of the predicted maximum pressures and impulses to the maximum gauge data. It also provides the R^2 values to show how well the

overall pressure and impulse curves match the curves from the maximum gauge data. As with DTRA Test 1, the predicted peak impulse in all three bays is within 10% of the actual impulse, and the R^2 values for the Bay 2 and Bay 3 impulses are better than anticipated at a value of 0.99.

4.1.3.5 DTRA Test 8 Details and Observations

The DTRA Test 8 setup is nearly identical to Test 9. The only difference is the placement of the explosive charge. For Test 8, the explosive charge is placed 1.35 ft. from the first test wall, while in Test 9, it is placed in the center of the detonation room. Similarly to DTRA Test 9, all three test walls failed drastically. Again the gypsum board was blown off the studs on all faces of all three test walls (Wenner et al., 2011a).

4.1.3.6 DTRA Test 8 Model Inputs

The BlastX detonation room loading computation is the only change for the DTRA Test 8 inputs compared to the Test 9 inputs. The location of the explosive charge is changed to 1.35 ft. from the first test wall.

4.1.3.7 DTRA Test 8 Analysis and Results

The model was run for the DTRA Test 8 simulation. The results are presented in the same manner as for Test 1 and Test 9. Figure 4.16 shows the results for Bay 1, Figure 4.17 shows Bay 2, and Figure 4.18 shows Bay 3. The comparison to the maximum gauge data and R^2 values are presented in Table 4.4. Again, the results demonstrate that the model does a good job predicting the actual data. The predicted maximum impulse is within 10% of the maximum gauge data for Bays 1 and 3, and it is at 10.3% for Bay 2. The R^2 value for the predicted impulse curve is at or above 0.95 for each bay.

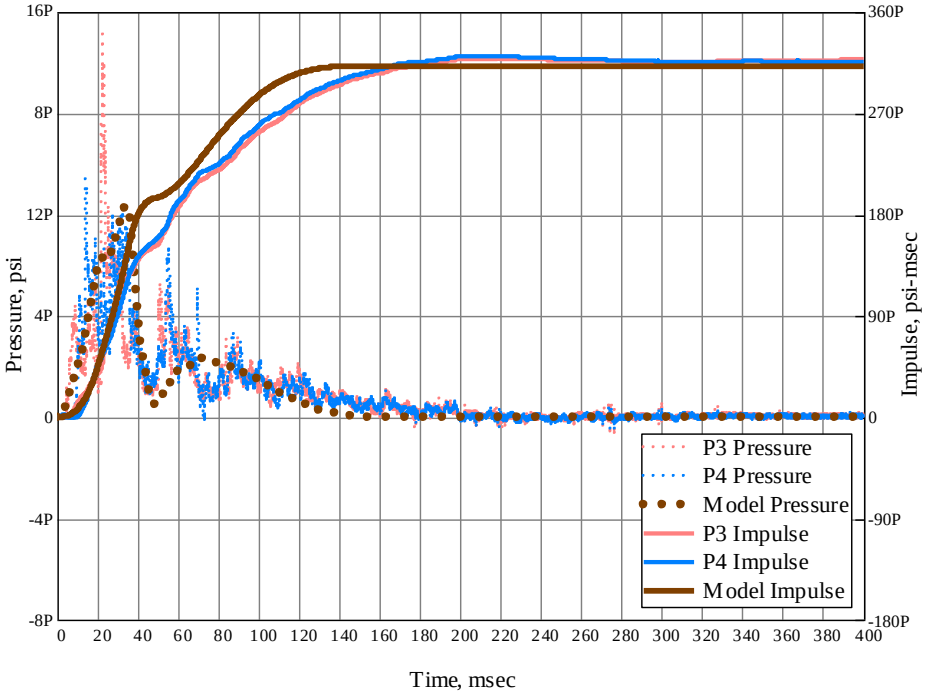

Figure 4.16 DTRA Test 8 Bay 1 Model Prediction versus Pressure Gauge Data: Gauge Data from DTRA (2013a)

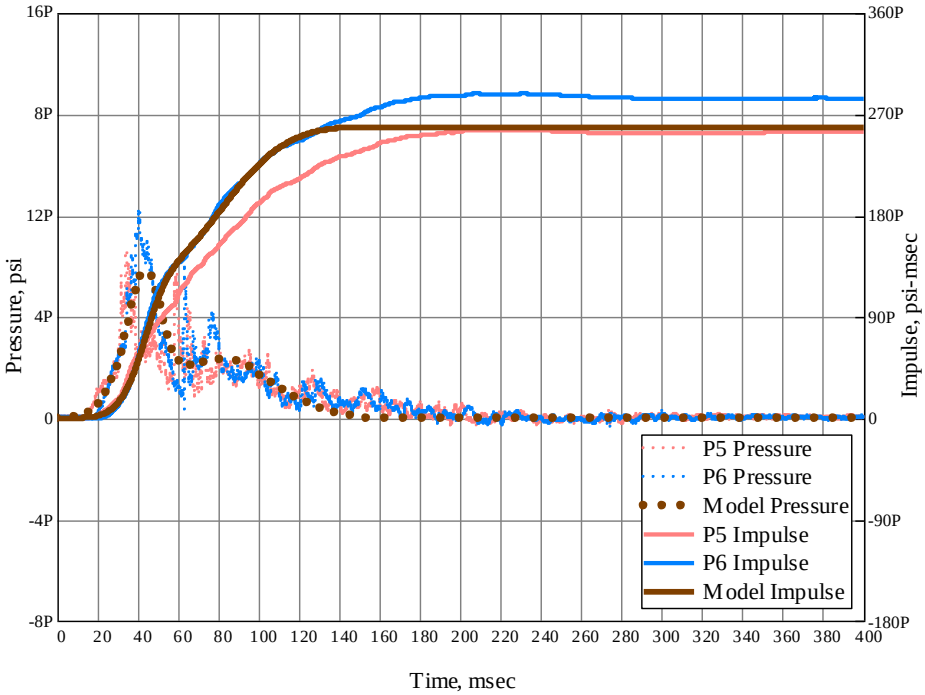

Figure 4.17 DTRA Test 8 Bay 2 Model Prediction versus Pressure Gauge Data: Gauge Data from DTRA (2013a)

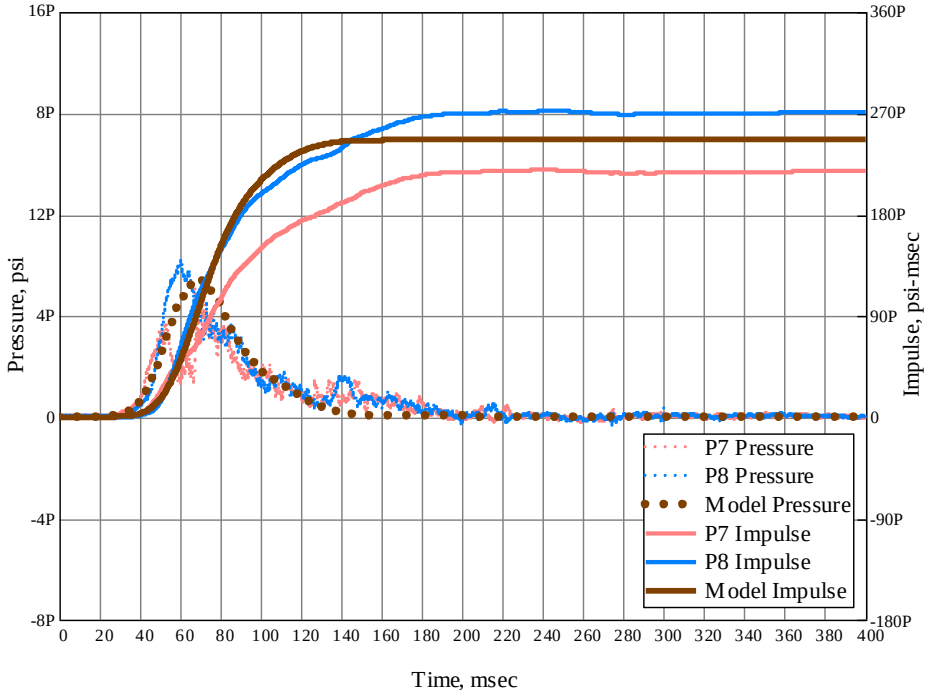

Figure 4.18 DTRA Test 8 Bay 3 Model Prediction versus Pressure Gauge Data: Gauge Data from DTRA (2013a)

Table 4.4 DTRA Test 8 Predicted Results versus Maximum Pressure Gauge Data: Pressure values, P_{max}, are in psi and Impulse values, I_{max}, are in psi-msec Gauge Data from DTRA (2013a)

	DTRA Test 8					
	Bay 1		Bay 2		Bay 3	
	P_{max}	I_{max}	P_{max}	I_{max}	P_{max}	I_{max}
Predicted Value	8.30P	312.1P	5.78P	258.5P	5.40P	246.6P
Max Gauge Value	15.08P	320.5P	8.30P	288.2P	6.15P	272.0P
Difference	-6.78P	-8.4P	-2.52P	-29.7P	-0.75P	-25.4P
% Error from Max	**-44.9%**	**-2.6%**	**-30.4%**	**-10.3%**	**-12.2%**	**-9.4%**
R^2 from Max	0.71	0.97	0.90	0.95	0.88	0.97

4.1.4 DTRA Test Phase II

The DTRA Phase II test series consisted of nine additional tests with an additional row of rooms. Figure 4.19 shows and example layout from the Phase II test series. For this research, however, a 6-room configuration of all full-height steel-stud walls was not conducted. Additional variables such as partial-height stud walls, CMU walls and steel-stud walls in the same test configuration, hallways, existing openings, and doors were added in all of the tests with steel-stud walls (Kersul, 2014). These configurations all add complexity and variables that are not yet included in the current model. Therefore, these tests were not used to validate the model or to examine multi-dimensional blast propagation through steel-stud walls.

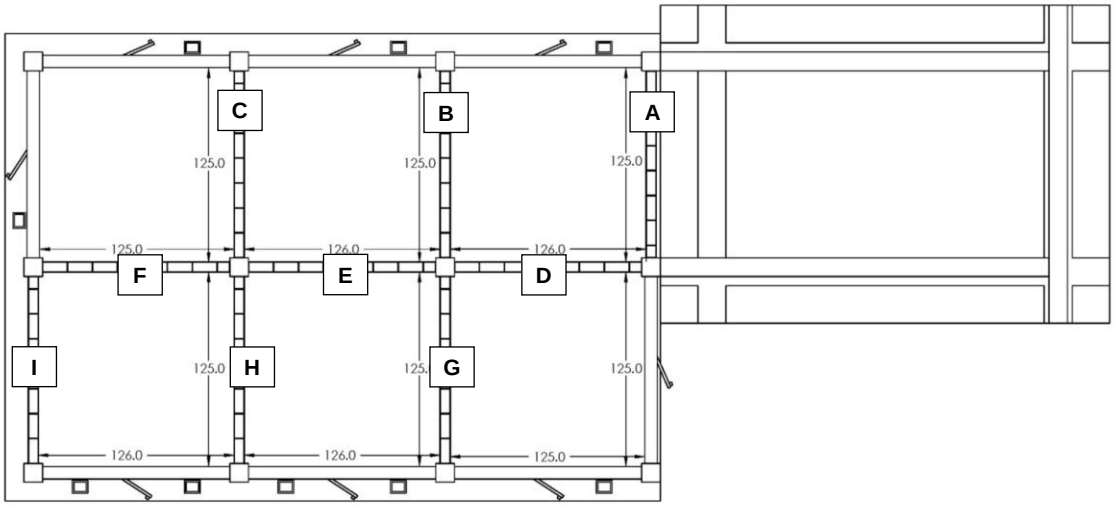

Figure 4.19 DTRA PHASE II Example Layout (Kersul, 2014)

4.1.5 Overall Performance of Predictive Model for DTRA Tests

Overall, the simplified model developed for this research study does a good job predicting the blast load propagation in the DTRA Phase I tests. Test 1, Test 8 and Test 9 provide a wide range of wall responses and threat scenarios. Test 1 included a small

charge placed in the center of the detonation room, and the wall failures included rigid body failures where the gypsum board was blown off the first test wall and remained intact on the other three test walls. Test 9 included a larger charge than Test 1, still placed in the center of the detonation room, and the wall failures were all rigid body failures with all the gypsum board being blown off. Test 8 included the same size charge as Test 9, but placed close-in to the first test wall. The gypsum board on the first test wall was pulverized, the gypsum board fractured before rigid body failure on the second test wall, and the third test wall failed as a rigid body with the gypsum board being blown off. The model was able to accurately predict results for all the different charges and wall break-up modes observed in the three DTRA tests.

The model predicts the impulse in each bay extremely well, with the peak impulse prediction never being greater than 10.3% error from the maximum measured impulse. This prediction level is quite accurate, especially when considering the variability of the measured data in a given bay. The difference between the maximum impulses from the two pressure gauges in the same bay varied by as much as 28% in the actual DTRA tests, and the predicted results are well within that level of variability. The R^2 value for the impulse curves is also never less than 0.88 for all bays in all three tests. Overall, the shape of the pressure curve is also represented well. The peak pressures are not captured well in the room closest to the detonation room for Test 1, and in the two rooms closest to the detonation room in Test 8 and 9. However, the impulse is still predicted well in these rooms, and the peak pressures in Bay 3 are predicted well. In general, the timing of the curves is also well predicted by the model. Tennant et al. (2011) present the WAI model predictions for DTRA Test 1, and comparing the results to those from the model outlined in this dissertation, one can conclude the current research study model has made significant improvements.

4.2 AFRL TESTS AND MODEL VALIDATION

Predicted results from the three DTRA tests are expected to match the actual test results well as the model was developed using data from those three tests. To validate the model developed herein, a different test simulation must be run, and the accuracy of the predicted results must be evaluated against measured test data. The test chosen for model validation is an ongoing test program performed by the Air Force Research Lab. Two of the tests included a steel-stud test wall with gypsum board and were used to validate the model (Watts et al., 2013). The test setup details, observations, and results have not been authorized for public release and consequently are not included in this section.

4.2.1 AFRL Tests Analysis and Results

For these two AFRL tests, the inputs for the model are calculated in accordance with Section 3.3 and in the same manner described in DTRA Test 1 in Section 4.1.2.2. Again, details of these inputs are not authorized for public release.

Both tests were simulated in the model. The resulting predicted pressure and impulse curves are compared to the measured pressure and impulse curves from the average of all pressure gauges in a room. Pressure and impulse values are not presented, but a percent error for each test prediction, as well as the R^2 values for the predicted curves versus the filtered curves, as described in Section 4.1.2.3, are shown in Table 4.5.

The predicted pressure and impulse match the actual test data well. As described previously, the peak pressure is often significantly under-predicted, and this result is expected. In addition, the maximum impulse matches well. The predicted maximum impulse is within 10.6% of the maximum impulse of the average of all pressure gauges for AFRL Test 1, and within 2.6% for AFRL Test 2.

Table 4.5 AFRL Tests Predicted Results versus Maximum Pressure Gauge Data: Data from Staubs et al. (2014a)

	AFRL Test 1		AFRL Test 2	
	Pressure	Impulse	Pressure	Impulse
% Error	-27.2%	-10.6%	-46.0%	-2.6%
R^2	-0.30	0.69	0.74	0.98

In AFRL Test 1, the shape of the pressure curve does not match the test data as well as it did in the DTRA tests. This is because of a large negative pressure phase in the BlastX detonation room loading computation. This large negative phase in the detonation room loading does not exist in the actual test data. The resulting R^2 values for AFRL Test 1 reflect the differences in the shape of the pressure and impulse curves. However, even with the errors in the computed detonation room load and the misrepresentation of the pressure curve shape, the maximum impulse is well predicted in the receiving room. AFRL Test 2 does not contain the same error in the detonation room loading with the negative pressure prediction as found in the AFRL Test 1 loading computation, and therefore, the results match the test data much more closely. The resulting R^2 value of 0.98 for the impulse curve reflects the significantly better prediction for AFRL Test 2.

Overall, the model does an excellent job predicting the impulse for the AFRL tests, and impulse is the most important load parameter affecting structural response and load propagation in an internal detonation scenario involving steel-stud walls.

4.2.2 Model Validation

The model was used to predict the blast propagation in the AFRL tests, and it successfully predicted the peak impulses. The overall shape of the pressure curves matched the test data well, or could be explained by examining the computed detonation

room loading versus the actual detonation room loading. The successful implementation of the model to predict and match the data from an internal blast test validates it can be used to reasonably predict blast load propagation in structures with steel-stud walls subjected to an internal blast.

4.3 PREDICTIVE APPLICATIONS

The model developed within the research study outlined in this dissertation can be used as a limited predictive tool. Currently, it is limited to one-dimensional room arrangements with non- responding floors and ceilings. The responding walls must be constructed using steel studs and cannot have existing openings. The detonation room computation can compute loads for any charge type and weight within the limits of BlastX. The overall successful timing of predicted results in the DTRA tests show that the wall resistance and wall break-up model are a good representation of wall behavior and would handle a load smaller than seen in DTRA Test 1 where walls would not fail. The tests with charge weights larger than DTRA Test 1 also showed the model could handle loads that pulverize the gypsum board; because the model accurately captures impulses, the author believes the model can handle charge weights even larger than that used in the tests examined in the current research.

If an internal blast scenario meets these criteria, this model can be used to predict the blast load propagation. From an offensive weapons perspective, blast loads in adjacent rooms can be predicted to assess lethality or collateral damage. If test wall construction details are not known, reasonable assumptions can be made based off common U.S. construction details presented within this research. From a protective design perspective, a user can analyze several charge weights and locations and predict damage and danger to personnel and equipment. Also, the user can predict the increased

level of protection achieved by increasing overall wall strength, such as improving connection strength.

Although still limited, the model can be a powerful tool for the practicing engineer. The model can quickly predict accurate blast load propagation results and damage estimates from an internal blast. The user can also make adjustments and quickly see how changes to either blast load or wall resistance can affect a blast load experienced several rooms away from a detonation.

4.4 LIMITATIONS

This research focused on one-dimensional, full-height, steel-stud walls subjected to internal blast loads. The motivation was to thoroughly investigate and develop a model involving the response and break-up of a steel-stud wall and to study the effects of wall failure on internal blast load propagation. By narrowing in so tightly on one aspect of the internal blast problem, a strong foundation for a complete simplified blast load propagation model was developed. This narrow focus, however, also leads to some limitations in the model that are acknowledged and described in this section.

4.4.1 Detonation Room Loading Non-responding Walls

In the model developed herein, an uncoupled approach is used to determine the detonation room loading as it is calculated in BlastX by modeling the room with all non-responding walls. This simplification allows for a predictive load to be computed for any given detonation room geometry and charge within the capabilities of BlastX. Failing interior walls, however, significantly affect the loading in the detonation room (Ohrt et al., 2013). In general, the presence of a failing wall in the detonation room will lower the detonation room impulse compared to the impulse in a detonation room with all non-responding walls.

In the previously presented DTRA and AFRL tests involving steel-stud walls, however, this over-prediction of the detonation room loading did not have a significant negative impact on the predicted results. Figure 4.20, Figure 4.21, show the over-prediction from DTRA Test 1 and DTRA Test 9, respectively. The maximum impulse is significantly overestimated in each case, ranging between 17% and 18% for those two tests, yet the predicted blast propagation impulses remain within 10% of the measured test data for all rooms in those tests.

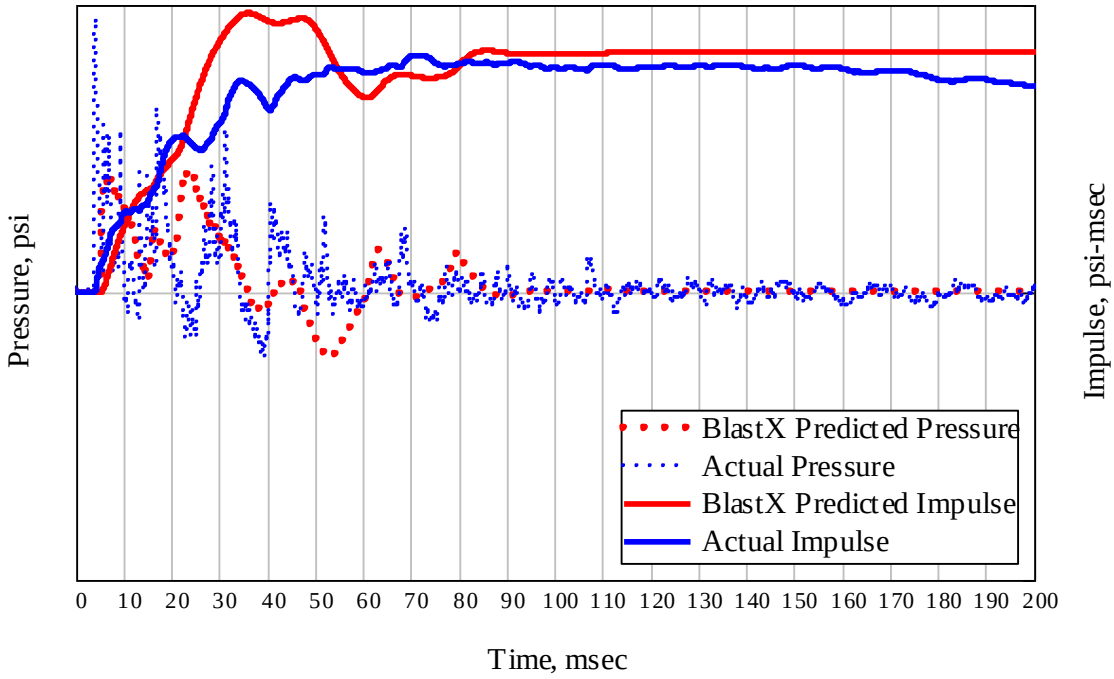

Figure 4.20 DTRA Test 1 BlastX Computed Detonation Room Loading versus Actual Pressure Gauge Data

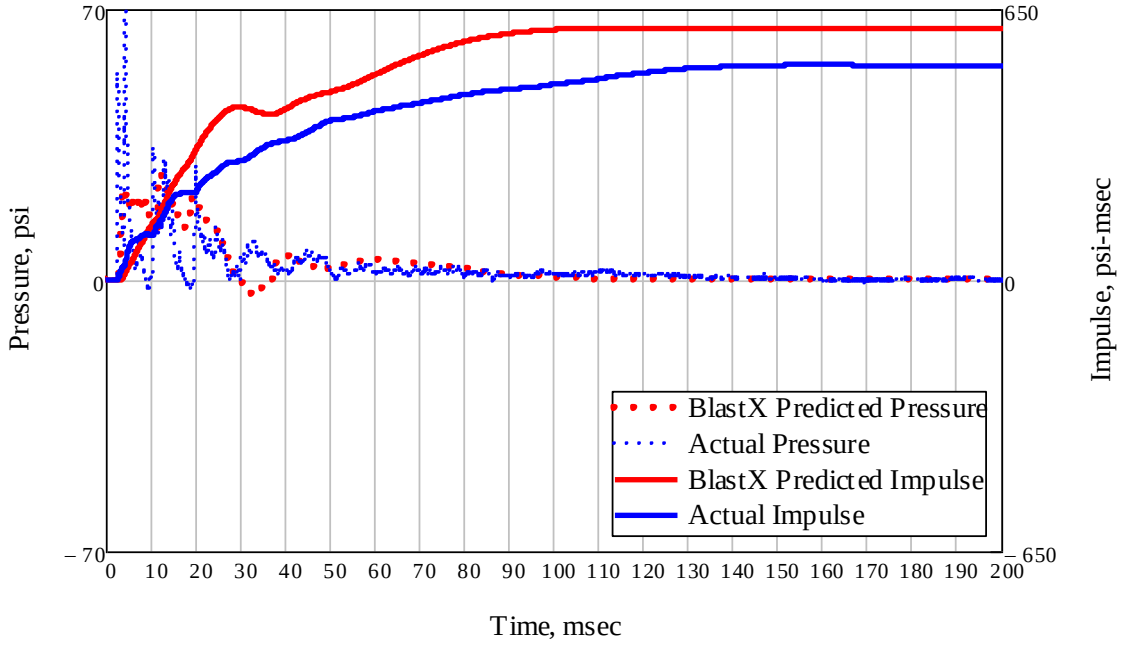

Figure 4.21 DTRA Test 9 BlastX Computed Detonation Room Loading versus Actual Pressure Gauge Data

This limitation can potentially be addressed two ways. First, when modeling a given threat, an engineer can make simplifying assumptions that leads to a smaller detonation room loading than what is currently implemented in the model. Second, a reduction factor could be developed based on charge density, wall strength, and wall mass where the calculated load from BlastX would be slightly reduced. A reduction factor, however, should only be applied after the initial peak pressure and impulse when the wall type begins to affect the detonation room load. More analysis would need to be done on existing test data and possibly additional testing performed to see if a reduction factor could be developed.

4.4.2 Sheathing Material

The current model was developed for typical interior wall construction with steel studs and 0.5-in. gypsum board sheathing on each side. Two main limitations exist if the sheathing material is changed. First, the structural resistance of the sheathing material is currently ignored. Second, the wall break-up model would change for different sheathing materials.

In the calculation of the wall resistance, the strength of the gypsum board is ignored, and only the resistance of the steel studs is used. This method produced the best results for the brittle, relatively weak gypsum board as explained in Section 3.3.3.4. Other common sheathing materials, including oriented strand board (OSB), plywood, or sheet steel would provide considerable strength to a steel-stud wall system. In these cases, using the method of calculating a series of uncoupled SDOF component responses could be used, as described in Section 2.3.1.1, to develop the wall's resistance function.

The wall break-up model was also developed to work for typical interior wall construction with 0.5-in. thick gypsum board on each side of the wall. The wall break-up model accounts for the break-up of the wall after the steel stud frame has failed, so the wall opening is highly dependent on the sheathing material. Other sheathing materials require further investigation, which may necessitate modifications to the current wall break-up model to accurately compute response. Nonetheless, based on a review of all currently available data, the overall break-up modes are adequately captured with the current break-up model. Thus, it is assumed this same method could be used to model other sheathing materials, but further research and investigation is needed.

4.4.3 Load-mass Factor and Flexural Response

The load-mass factor is used to create an equivalent SDOF system as described in Section 2.3.1.1. Because it can reasonably predict the maximum displacement of a blast-

loaded structural component, this simplified approach is favored in practice. For the research study described herein, however, the load-mass factor used was always 1.0 because connection failure dominated the response of the test walls, and the displaced shape was close to rigid body motion as shown in Figure 3.9.

For a steel-stud wall with stronger connections than found in typical construction details, the structural response would be dominated by flexure. The load-mass factor could be computed using the displaced shapes associated with the different phases of response (i.e., elastic, elastic-plastic, plastic) in the SAP2000 static pushover analysis. No test data exist, however, for internal explosions with steel-stud walls responding in flexurally dominated modes, so further research is needed to determine how well the model can accommodate flexural response.

4.4.4 Debris Load

The debris load from failing walls is ignored in the model developed for this research. Examining the times of wall failures and high speed video, it is believed that for the tests examined within this research, adjacent wall failures occurred from the overpressure experienced within a room before the debris of a previously failed wall impacted the adjacent wall. This will not always be the case. A wall with a stronger resistance than those examined in this research may not fail due to the overpressure alone, and it would experience an increased load from flying debris. This debris can cause significant loads and damage to other walls, as well as pose a lethal threat to occupants.

4.5 SUMMARY

The model outlined in this dissertation was developed using three experimental tests involving full-height steel-stud walls in the DTRA test series. The model computes

the blast load propagation accurately for these tests, as the predicted impulses in each room are all within 10.3% of the maximum measured impulses. The model was then validated by accurately predicting blast load propagation in a separate experimental test series involving full-height steel-stud walls. The predicted impulses for these tests in performed by AFRL were all within 10.6% of the measured impulses.

Due to the focused approach of the research study, the model is currently limited to one-dimensional room configurations involving typically constructed, full-height steel-stud walls with gypsum board sheathing and no existing openings. Limitations of the model are acknowledged, and additional testing and research are needed to address these limitations and improve the model. Future research opportunities are presented in the next chapter.

Chapter 5

Summary and Conclusions

5.1 Motivation and Objectives

Since the end of the Cold War era, the world has seen a significant escalation in international terrorism (Krauthammer, 2005). The United States has taken particular interest in the terrorist threat because a number of attacks occurred within its borders during this time, including the attacks on the World Trade Center and the Pentagon on September 11, 2001. The preferred weapon of terrorists through this time has been explosive devices, with 57% and 54% of the total terrorist attacks occurring in 2013 and 2014, respectively, involving explosives (National Consortium for the Study of Terrorism and Responses to Terrorism, 2015). These explosives include suicide vests, backpack bombs, and other small devices that could be detonated inside a building. The targets of terrorist attacks are often non-military and likely involve buildings constructed with typical details. The top four target categories of terrorist attacks in 2014 included private citizens and property, police, government, and business, and they accounted for 75% of the total attacks.

The way in which the U.S. military currently trains and fights has also shifted in recent years from a conventional warfare focus during the Cold War to a focus on military operations in urban terrain (MOUT). MOUT operations pose unique challenges to military commanders, including the employment of military munitions in an urban environment. Military munitions are often used to defeat hardened targets, and when used against buildings constructed with typical details in an urban setting, they can potentially cause excessive collateral damage.

Most of the past research involving blast effects on structures has primarily involved external detonations or internal detonations on hardened facilities. The current terrorist threat and increase in military operations in urban terrain have created a need to analyze internal detonations in buildings constructed with typical details. Typical buildings contain multiple lightly constructed interior walls that may experience violent failure when subjected to blast loads. A key component of predicting the damage and survivability of these urban buildings is the ability to quantify the blast loads that propagate through failing walls (Ohrt et al., 2013). This analysis is important from both a protective design perspective and a munitions employment perspective. From a protective design standpoint, engineers need the ability to assess a building's capacity to survive a given internal explosive threat. In regards to munitions employment, the military needs the ability to assess damage form a munition used on an urban target.

The goal of the research study outlined in this dissertation is to develop an engineering-level model to predict damage and blast load propagation in a typically constructed building resulting from an internal detonation. The research focuses on full-height steel-stud walls and develops a mechanics-based predictive model rather than an empirically-derived model.

5.2 PROPOSED MODEL FOR CURRENT RESEARCH STUDY

The model developed in the research study described herein extends the capabilities of a model developed by Weidlinger Associates, Inc. (WAI) (Tennant et al., 2011; Vaughan et al., 2013). A description of the WAI model is provided in Section 2.4.2. The model for the current study includes the structural response of the walls utilizing equivalent SDOF systems for each wall, and it couples this wall response with the air mass flow through openings.

In general, the model developed for the research study described herein uses a simplified method to simulate blast propagation throughout a building by computing the pressure in each room, which is affected by the wall response and the flow of air mass through openings. Some of the main assumptions and simplifications of the model are:

- Non-responding floor and ceiling: The floor and ceiling are considered rigid.
- No debris or fragment load: Additional impulse due to debris and fragments impacting walls is ignored.
- One-dimensional: Side walls in each room are rigid and non-responding.

The model calculates the pressure history in all rooms except the detonation room. A pressure history from the detonation room is generated from a BlastX simulation of the charge exploding in the detonation room. This loading acts on the first responding wall that separates the detonation room from the first room in the direction of blast load propagation. The pressure in each additional room can change at each time step due to the coupled structural response and flow of air mass through openings. Each wall is modeled by two phases that occur in series. The first phase is the structural response, which is modeled as an SDOF system with a nonlinear resistance, and the dynamic response is computed numerically. After the wall structurally fails, the second phase of the wall breaking up is defined by the break-up model. The wall continues to move dynamically with no resistance until it reaches a specified maximum displacement, and the wall no longer interacts with the air. When a wall reaches its maximum displacement, the wall no longer exists, and the pressures of the two rooms equalize.

The greatest contribution of this new proposed model is its ability to be used in a predictive sense. The WAI model has several components that are empirically derived, and overall it relies on experimental test data. The model developed herein includes

mechanics-based parameters and three main improvements to the WAI model. First, the detonation room loading is simulated using the computer program BlastX. The ability of BlastX to predict loads has been validated through several experimental tests involving internal and external detonations (Britt et al., 2001). It can be used for many different detonation room geometries, charge types, charge weights, and charge locations. This improved loading method is discussed further in Section 3.3.2. The second improvement is the method to determine the structural resistance of a wall for the SDOF systems. The model developed for the research study uses the actual properties of a wall and its connection details to perform a static pushover analysis in SAP2000. This SAP2000 analysis results is a nonlinear resistance function that can capture the interaction of multiple static failure modes, material and geometric nonlinearities, and potential tension membrane action. Complete details of the structural resistance development are described in Section 3.3.3. The final improvement involves the wall break-up model. This break-up model includes all possible break-up modes encountered in the current research in a single model. The parameters of the displacement-dependent component are dependent on a wall's physical properties and loading.

5.3 RESULTS AND VALIDATION

The model presented in this dissertation was developed using a series of experiments performed by DTRA. Three tests, DTRA Test 1, DTRA Test 8, and DTRA Test 9, from this series included full-height steel-stud walls and were used for the research study (DTRA, 2010a; 2013a; 2013b). All three tests included a detonation room and three additional rooms, all separated by a full-height steel-stud test wall with 1/2-in. gypsum board on each face. The side walls, floor, and ceiling were all reinforced concrete, non-responding surfaces. DTRA Test 1 used a small explosive charge placed in

the center of the detonation room, and DTRA Test 8 and Test 9 used a charge weight larger than Test 1. The charge in Test 8 was placed close-in to the first test wall, and the charge in Test 9 was positioned in the center of the detonation room. Details of the test setups and model inputs are included in Section 4.1.

The DTRA tests were analyzed with the model, and accurate blast load propagation was computed for each room. The peak pressures in the room adjacent to the detonation room were not well predicted due to the complexities of shock wave behavior. The impulse, however, in each room was accurately predicted. For DTRA Test 1, the predicted impulse in each room was within 8.5% of the measured maximum impulse. These predictions are each at least 6% better than the WAI model predictions for each room in DTRA Test 1. The predicted impulses for DTRA Test 8 were all within 10.3% of the measured maximum impulses, and in DTRA Test 9, predicted impulses were all within 8.9%. For typical blast analysis scenarios, a prediction within 10% of measured results is considered accurate due to inherent uncertainties of the problem, such as unknown charge weight and location, or ambiguous construction details. Also, the difference of the measured impulse between two pressure gauges in a single room varied by as much as 28%, so a predicted impulse within 10% of the maximum measured impulse is entirely acceptable. Complete analysis of the DTRA tests is provided in Section 4.1.

To validate the model, a predictive analysis was performed on a separate test case that was not used to develop the model. This validation test case was an ongoing experimental test series done by AFRL (Staubs et al., 2014a; 2014b). The test series included two tests with a steel-stud test wall. The model successfully predicted the impulse for both tests. As expected, the peak pressures were significantly underestimated. The predicted impulse, though, was within 10.6% of the average measured impulse for

AFRL Test 1, and within 2.6% of the average measured impulse for AFRL Test 2. The successful prediction of the impulses in the receiving room for these two tests validated the model's predictive capability.

5.4 CONCLUSION

In the WAI model, Tennant et al. (2011) demonstrated that using SDOF systems for the structural response of interior walls coupled with air mass flow computations works well to model internal detonations and the resulting blast load propagation. The research study outlined in this dissertation uses the framework of the WAI model and demonstrates these concepts can be incorporated into an engineering-level model for steel-stud walls where the components of the model are mechanically based rather than empirically derived. The model developed for the research study described herein can simulate an internal detonation and predict blast load propagation through failing steel-stud walls by computing detonation room loading using BlastX, analyzing the structural response of the walls using equivalent SDOF systems with resistance functions developed from a SAP2000 pushover analysis, accounting for the break-up of walls using a break-up model dependent on a wall's physical properties and loading, and computing air mass flow through openings.

5.5 RECOMMENDATIONS FOR FUTURE RESEARCH

The methodology of isolating a specific part of the internal detonation scenario used to develop the model for the research study described herein can be used to further improve the model and expand it to incorporate more possible scenarios and other wall types. Additional experimental testing and analysis is needed to isolate additional variables and scenarios such as connections stronger than typical construction details, stronger steel studs than those used in the DTRA and AFRL tests, sheathing material

other than gypsum board, existing openings in the steel-stud walls, two-dimensional room configurations, ceiling response, and including debris loads. Several limitations of the current model are described in Section 4.4, and these limitations are the basis for the recommendations for future research.

The current model overestimates the loading in the detonation room because it is computed with all non-responding walls as explained in Section 4.4.1. Further investigation is needed to determine how a more accurate detonation room loading can be predicted that accounts for the response of walls in the detonation room. Two potential options should be examined. First, an overall reduction factor can be developed and applied to the current detonation room loading computation. This reduction factor would depend on the responding wall type and strength, and possibly the load magnitude. The second option is to compute a coupled detonation room loading where the loading depends on the structural response of the walls in the detonation room. This method requires the structural response and wall break-up methodologies of the current model to be incorporated into an existing blast load computation program that includes shock wave reflections, such as BlastX.

The experimental tests used in the research study only included 1/2-in. gypsum board sheathing. Different sheathing materials used with steel-stud walls, such as plywood, OSB, and sheet steel, will affect the structural resistance of a wall and the wall break-up. It is believed that a series of uncoupled SDOF component responses including the resistance of these additional sheathing materials could be used, as described in Section 2.3.1.1, to develop a wall's resistance function. It is also believed that for these additional sheathing materials, parameters can be developed for a wall break-up model similar to the one developed for steel-stud walls with gypsum board. Further

experimental testing is needed, however, to analyze these sheathing materials used in an internal detonation scenario.

The SAP2000 static pushover analysis method to determine the steel-stud wall resistance function has the capability to account for significant plastic flexural response and tension membrane action. This type of response was not observed in any of the experimental tests used in the research study because of the relatively weak connections found in typical construction details. As described in Section 4.4.3, further experimental tests involving connections stronger than typical construction details in an internal detonation scenario are needed to investigate if the current model can accurately predict blast load propagation when this type of wall flexural response is realized.

In the tests observed for the research study, it is believed that all walls failed due to overpressure before debris from the previously failed wall impacted them. If walls are built to be stronger than typical construction, this may not always be the case. Again, additional experimental tests are needed with connections and studs stronger than typical construction details to investigate how debris load affects wall failures and blast load propagation.

The current model has only been developed and validated for a one-dimensional scenario. Most actual internal detonation scenarios will include side walls and ceilings or even floors that can respond and fail due to blast loads. Existing experimental data for steel-stud walls only existed in a one-dimensional setup. It is recommended that additional experimental tests first be conducted with full-height steel-stud walls with no existing openings in a two-dimensional setup. Then, further experimental tests should be conducted to include the response and failure of ceilings. Such a series of tests would allow for the isolated analysis of additional variables. First, the current model could be evaluated in a two-dimensional scenario, with the additional dimension as the only

variable being evaluated. Second, additional variables, such as a third dimension with a responding ceiling, could be added.

Finally, the mechanics-based method of developing the engineering-level model described herein can be applied to different wall types. It is believed that the resistance function development and wall break-up model methodologies used in the current model could be applied to wood-stud walls, CMU walls, and any other type of common interior wall. The research presented in this dissertation has created a predictive blast load propagation model for internal detonations for one specific scenario involving full-height steel-stud walls in a one-dimensional room configuration. This model can continue to be improved to encompass a broader spectrum of scenarios and become an extremely useful engineering-level tool for protective design and munitions employment.

DISCLAIMER: The author can provide additional information on the limited distribution material within this research to personnel with proper authorization. Please contact the author for access to this information.

References

ABS Consulting. (2014). "CE 384T Project High Speed Video, Team 3" *2014-04-22_UT_T03_45deg*. 22 Apr 2014; San Antonio, TX

American Concrete Institute (ACI). (2015). *Committee Home: 370 – Blast and Impact Load Effects*. <https://www.concrete.org/committees/directoryofcommittees/acommitteehome.aasp?committee_code=0000370-00>. Accessed on July 23, 2015.

American Institute of Steel Construction (AISC). (2010). "Specification for Structural Steel Buildings." *ANSI/AISC 360-10*. Chicago, IL.

American Iron and Steel Institute (AISI). (2007). "North American Specification for the Design of Cold-Formed Steel Structural Members." *AISI S100-2007*; Washington, DC

American Society of Civil Engineers (ASCE). (2010). *Design of Blast-Resistant Buildings in Petrochemical Facilities, 2nd Edition*. Task Committee on Blast Resistant Design; Reston, VA.

American Society of Civil Engineers (ASCE). (2011). "Blast Protection of Buildings." *ASCE/SEI 59-11*; Reston, VA.

American Society of Civil Engineers (ASCE). (2014). "Seismic Evaluation and Retrofit of Existing Buildings." *ASCE/SEI 41-13*; Reston, VA.

American Society of Civil Engineers (ASCE). (2015). *SEI Blast, Shock and Impact*. <http://www.asce.org/templates/membership-communities-committee-detail.aspx?committeeid=000000885403>. Accessed on July 23, 2015.

ANSYS. (2015). *ANSYS AUTODYN*. <http://www.ansys.com/Products/Simulation+Technology/Structural+Analysis/Explici+Dynamics/ANSYS+Autodyn>. Accessed on June 16, 2015.

Applied Research Associates Inc. (2014). *Computational Physics: Capabilities*. <http://www.ara.com/Capabilities/c_computational_physics.htm>. Accessed June 16, 2015.

ASTM International (ASTM). (2013). "Standard Specification for Sheet Steel, Zinc-Coated (Galvanized) or Zinc-Iron Alloy-Coated (Galvannealed) by the Hot-Dip Process." *ASTM A653/A653M – 13*; West Conshohocken, PA.

Ayhan, D. and Schafer, B. W. (2012). "Moment-Rotation Characterization of Cold-Formed Steel Beams." *CFS-NEES-RR02*. National Science Foundation: NEESR-CR: Enabling Performance-Based Seismic Design of Multi-Story Cold-Formed Steel Structures; Baltimore, MD.

Bewick, B., O'Laughlin, C., and Williamson, E. (2011). "Simplified Methods for Improving the Blast Resistance of Cold-Formed Steel Walls." *Applied Mechanics and Materials*, 82, 515-520.

Bewick, B. T., O'Laughlin, C. G., and Williamson, E. B. (2013). "Evaluation of Conventional Construction Techniques for Enhancing the Blast Resistance of Steel Stud Walls." *J. Struct. Eng.*, 139(Nov), 1992-2002.

Biggs, J. M. (1964). *Introduction to Structural Dynamics*. McGraw-Hill; New York, NY.

Bondok, D. H., Salim, H. A., and Agee, B. M. (2015). "Improved Static Resistance and Failure Mechanisms of Conventional Cold-Formed Steel Stud Walls." *J. Perform. Constr. Facil.*, 29(3).

Bondok, D. H., and Salim, H. A. (2014). "Numerical Modeling of Conventional Steel Stud Walls' Static Resistance for Blast Response Predictions." *J. Struct. Eng.*, 140(7).

Britt, J. R., Conklin, B. K., Frank, S. M., Smith, B. C., and A. P. Ohrt. (2010). "Modeling Improvements in the Airblast Diffraction and Clearing Models in BlastX." *Proceedings of the 79th SAVIAC Conference*; Orlando, FL. (Limited Distribution)

Britt, J. R., Joachim, C. E., and McMahon, G. W. (2002). "Blast Model Improvements in BlastX Code." *73rd Shock and Vibration Symposium*; Newport, RI. (Limited Distribution)

Britt, J. R., Ranta, D. E., and C. E. Joachim. (2001). "BlastX Code, Version 4.2, User's Manual." *ERDC/GSL TR-01-2*, U.S. Army Engineer Research and Development Center (ERDC); Vicksburg, MS. (Limited Distribution)

Chopra, A. K. (2007). *Dynamics of Structures: Theory and Applications to Earthquake Engineering, 3rd Edition*. Pearson Education; Upper Saddle River, NJ.

ClarkDietrich Building Systems (ClarkDietrich). (2015). *Blocking/Strapping: Commonly Used Bracing for Wall Studs Deeper Than 6"*. <http://www.clarkdietrich.com/products/bridging-bracing/blocking-strapping>. Accessed on Aug 5, 2015.

Cold-Formed Steel Engineers Institute (CFSEI). (2008). "Design Aids and Examples for Distortional Buckling." *Technical Note G100-08*; Washington, D.C.

Computers and Structures Inc. (CSI). (2011a). *CSI Analysis Reference Manual: For SAP2000, ETABS, SAFE, and CSiBridge*; Berkeley, CA.

Computers and Structures Inc. (CSI). (2011b). *SAP2000*. Version 15; Berkeley, CA. <www.csiamerica.com/products/SAP2000>

Defense Threat Reduction Agency (DTRA). (2009). (Limited Distribution)

Defense Threat Reduction Agency (DTRA). (2010a). (Limited Distribution)

Defense Threat Reduction Agency (DTRA). (2010b). (Limited Distribution)

Defense Threat Reduction Agency (DTRA). (2013a). (Limited Distribution)

Defense Threat Reduction Agency (DTRA). (2013b). (Limited Distribution)

Department of the Army, (1994). "Facility and Component Explosive Damage Assessment Program: Theory Manual, Version 1.2." *Technical Report 92-2*. Protective Design, Mandatory Center of Expertise, Department of the Army Corps of Engineers; Omaha, NE.

Department of Defense. (DoD). (2002). "Design and Analysis of Hardened Structures to Conventional Weapons Effects." *Unified Facilities Criteria Document UFC 3-340-01*; Washington D.C. (Limited Distribution)

Department of Defense. (DoD). (2008). "Structures to Resist the Effects of Accidental Explosions." *Unified Facilities Criteria Document UFC 3-340-02*; Washington, D.C.

Department of State (DoS). (2015). *Country Reports on Terrorism 2014*. Washington, D.C.

Desch, Michael, C., ed. (2001). *Soldiers in Cities: Military Operations on Urban Terrain*, Strategic Studies Institute, U.S. Army War College; Carlisle, PA

Federal Emergency Management Agency (FEMA). (2000). "Prestandard and Commentary for the Seismic Rehabilitation of Buildings." *FEMA 365*. Prepared by American Society of Civil Engineers; Washington D.C.

Feldgun, V. R., Karinski, Y. S., Edri, I., Tsemakh, D., and Yankelevsky, D. Z. (2012). "On Blast Pressure Analysis Due to a partially Confined Explosion: II. Numerical Studies." *J. of Protective Structures*, 3(1), 61-79.

Fisher Fixings UK Ltd (Fisher). (2013). "Frame Fixings / Stand-off Installation." *Section 3*; Wallingford, Great Britain

Gypsum Association. (2010). "Gypsum Board Typical Mechanical and Physical Properties." *GA-235-10*. Hyattsville, MD.

Joint Chiefs of Staff (JCS). (2013). "Joint Urban Operations." *Joint Publication 3-06*. Washington, D.C.

Kersul, A. (2014). "Internal Detonation Experiments" *International Physical Security Forum*; Tel Aviv, Israel

Knauf. (2011). "W11 Knauf Metal Stud Partitions." *W11/engl./D/05.11/FB/D-English Translation*; Iphofen, Germany

Krauthammer, T. (2005). "ASCE Design Guide for Physical Security." *Proceedings of the 2005 Structures Congress*, SEI, New York, NY.

Krauthammer, T. (2008). *Modern Protective Structures*. CRC Press; Boca Raton, Fl.

Li, Z., Williams, S., Tian, D., Strecker, A. M., (2014). "CE 384T: Blast-Resistant Design Term Project Report." Department of Civil, Architectural, and Environmental Engineering. University of Texas at Austin.

Light Gauge Steel Engineers Association (LGSEA). (2001). "Powder-Actuated Fasteners in Cold-Formed Steel Construction." *Technical Note 562*; Washington, D.C.

Livermore Software Technology Corporation (LSTC). (2011). *LS-DYNA*. <http://www.lstc.com/products/ls-dyna>. Accessed June 16, 2015.

National Consortium for the Study of Terrorism and Responses to Terrorism (START). (2015). "Annex of Statistical Information." *Country Reports on Terrorism 2014*. U.S. Department of State; Washington, D.C.

Ngo, T., Mendis, P., Gupta, A., Ramsay, J. (2007). "Blast Loading and Blast Effects on Structures – An Overview." Elec. J. Struct. Eng., 7 (Special Issue: Loading on Structures – 2007), 76-91.

Ohrt, A. P. (2012). "Residual Airblast in a Two-Dimensional Array of Failing Walls." *Proceedings of the 13th Joint Classified Bombs/Warheads & Ballistics Symposium*; Monterey, CA. (Limited Distribution)

Ohrt, A. P. and Ehlers, R.Z. (2010). "Preliminary Investigation of Airblast Propagation through Failing Surfaces." *Proceedings of the 11th Joint Classified Bombs/Warheads & Ballistics Symposium*; Monterey, CA. (Limited Distribution)

Ohrt, A. P., Watts, D. and Staubs, E. (2013). "Residual Airblast Through MOUT Walls—Preliminary Results and Analysis." *Proceedings of the 15th International Symposium on the Interaction of the Effects of Munitions with Structures (ISIMS)*; Potsdam, Germany. (Limited Distribution)

Parametric Technology Corporation (PTC). (2012). *Mathcad*. Version 15.0; Needham, MA. <http://www.ptc.com/product/mathcad>

Precast/Prestressed Concrete Institute (PCI). (2015). *Blast Resistance and Structural Integrity*. <http://committees.pci.org/Committees/committeehome.asp?committee_code=BI>. Accessed on July 23, 2015.

RAMSET. (2011). *Technical Manual*; Glendale Heights, IL.

Salim, H., Dinan, R., and Townsend, P. T. (2005a). "Analysis and Experimental Evaluation of In-Fill Steel-Stud Wall Systems under Blast Loading." *J. Struct. Eng.*, 131(8), 1216-1225.

Salim, H., Muller, P., and Dinan, R. (2005b). "Response of Conventional Steel Stud Wall Systems under Static and Dynamic Pressure." *J. Perform. Constr. Facil.*, 19(4), 267-276.

Sammarco, E. L., (2014). "Development of Simplified Dynamic Response Models for Blast-Loaded Bridge Components." *Doctoral Dissertation*, The University of Texas at Austin; Austin, TX.

Sandia National Laboratories. (2014). *CTH Capabilities*. <http://www.sandia.gov/CTH/Capabilities-leftnav-level1_js.html>. Accessed June 16, 2015.

Sheffield, C. S., Torres, L. M. and Morrill, K.B. (2009). Defense Threat Reduction Agency; Kirtland AFB, NM. (Limited Distribution)

Simpson Strong-Tie Company Inc. (2015). "Connectors for Cold-Formed Steel Construction." *C-CFS-15*; Pleasanton, CA.

Staubs, E., Watts, D. and Ohrt, A. (2014a). Air Force Research Lab Munitions Directorate; Eglin AFB, FL. (Limited Distribution)

Staubs, E., Watts, D. and Ohrt, A. (2014b). Air Force Research Lab Munitions Directorate; Eglin AFB, FL. (Limited Distribution)

Steel Stud Manufacturers Association (SSMA). (2013). "Product Technical Guide." *ICC ES ESR #3064P*; Chicago, IL.

Sun, M. and Packer, J. A. (2014). "High Strain Rate Behaviour of Cold-Formed Rectangular Hollow Sections." *Eng. Struct.*, 62-63(Mar), 181-192.

Tennant, D., McClennan, S., Bogosian, D., Vaughan, D., Salari, R., Mould, J., and Lawver, D. (2011). "Engineering Models for Damage to Structural Components Subjected to Internal Blast Loading." *Phase II SBIR Final Report FR2011-06*. Defense Threat Reduction Agency; Kirtland AFB, NM. (Limited Distribution)

Tennant, D., Mould, J., Lawver, D., McClennan, S., Vaughan, D., Bogosian, D. (2009). "Engineering Models for Damage to Structural Components Subjected to Internal Blast Loading." *Phase I SBIR Final Report DTRA-TR-09-03*. Defense Threat Reduction Agency; Ft. Belvoir, VA. (Limited Distribution)

U.S. Army Corps of Engineers (USACE). (2008). "Single Degree of Freedom Structural Response Limits for Antiterrorism Design." *PDC-TR 06-08 Rev. 1*. Protective Design Center; Omaha, NE.

U.S. Army Corps of Engineers (USACE). (2011). "BlastX – Version 7.0.1.0." U.S. Army Engineer Research and Development Center (ERDC); Vicksburg, MS and Air Force Research Laboratory (AFRL); Eglin AFB, FL. (Limited Distribution)

Vaughan, D., Mould, J., Levine, H., and Tennant, D. (2013). "Simulating Explosive Detonations within Multiroom Buildings." *Proceedings of the ASME 2013 Pressure Vessels and Piping Conference*; Paris, France.

Watts, D., Ohrt, A.P. and Staubs, E. (2013). "Residual Airblast Thru MOUT Walls – Test Description." *Proceedings of the 15th International Symposium on the Interaction of the Effects of Munitions with Structures (ISIMS)*; Potsdam, Germany. (Limited Distribution)

Weidlinger Associates, Inc. (WAI). (2011). *NLFlex.* <http://www.wai.com/nlflex.aspx?print=true>. Accessed on June 22, 2015.

Wenner, S. and Sheffield C.S. (2011). Defense Threat Reduction Agency; Kirtland AFB, NM. (Limited Distribution)

Wenner, S., Finch, J. and Sheffield C.S. (2011a). Defense Threat Reduction Agency; Kirtland AFB, NM. (Limited Distribution)

Wenner, S., Finch, J. and Sheffield C.S. (2011b). Defense Threat Reduction Agency; Kirtland AFB, NM. (Limited Distribution)

Wenner, S., Finch, J. and Sheffield C.S. (2011c). Defense Threat Reduction Agency; Kirtland AFB, NM. (Limited Distribution)

Williams, G. D., (2009). "Analysis and response Mechanisms of Blast-Loaded Reinforced Concrete Columns." *Doctoral Dissertation*, The University of Texas at Austin; Austin, TX.

Williamson, E. B. (2014). *Course Notes from CE 384T: Blast-Resistant Structural Design*. Department of Civil, Architectural, and Environmental Engineering. University of Texas at Austin.

Williamson, E. B., Bayrak, O., Williams, G. D., Davis, C. E., Marchand, K. A., McKay, A. E., Kulicki, J., and Wassef, W. (2010). "Blast-Resistant Highway Bridges: Design and Detailing Guidelines." *NCHRP Report 645*. National Cooperative Highway Research Program, Transportation Research Board; Washington, D.C.

Yu, W.W. and LaBoube, R.A. (2010). *Cold-Formed Steel Design, 4th Edition*. John Wiley & Sons, Inc.; Hoboken, NJ.